Effect of stratification due to suspended sediment on velocity and concentration distribution in turbulent flows

by

Julie Marine Herrmann

Submitted to the Department of Civil and Environmental Engineering
in partial fulfillment of the requirements for the degree of

Master of Science in Civil and Environmental Engineering

at the

MASSACHUSETTS INSTITUTE OF TECHNOLOGY

February 2004

Author .....
Department of Civil and Environmental Engineering
December 12, 2003

Certified by .....
Ole S Madsen
Professor of Civil and Environmental Engineering
Thesis Supervisor

Accepted by .....
Heidi Nepf
Chairperson, Department Committee on Graduate Students

Effect of stratification due to suspended sediment on velocity and concentration distribution in turbulent flows

by

Julie Marine Herrmann

Submitted to the Department of Civil and Environmental Engineering
on December 12, 2003, in partial fulfillment of the
requirements for the degree of
Master of Science in Civil and Environmental Engineering

Abstract

Sediment-induced stratification effects on velocity profiles and sediment concentration distribution in a steady, uniform turbulent flow are examined in this thesis. The early work concerning sediment stratification relates this to von Karman's constant's variability. Subsequent attempts to account for stratification were based on the stratified flow analogy, introducing the parameters α and β, whose values were assumed to be those obtained for thermally stratified flows. Following these investigators, we assume stratification effects to be expressed through these parameters. We solve the governing equations for velocity and sediment concentration for a parabolic, a simplified linear-constant and an extremely simplified linear neutral eddy viscosity model. Analytically closed form solutions are obtained. The parabolic and linear-constant models' formulae require numerical evaluation of integrals. The linear model provides excellent estimates of velocity and concentration and does not require numerical computation. We run our model against experimental data to obtain the optimal set $[\alpha, \beta]$. For neutral conditions, $\beta = 0$ by definition, and we obtain $\alpha = 1$. For stratified conditions the optimal values are $\alpha = 0.8$ and $\beta = 4.0$. Accounting for stratification slightly improves the prediction of velocity and concentration in comparison with the case where we do not account for it. For predictive purposes, we need to know the movable bed roughness and the reference concentration. Analyses of experimental data sets provide predictive relationships for reference concentration and movable bed roughness in terms of sediment and flow parameters. An examination of the effects of uncertainty in the predictive capability of our model reveals that this overshadows the slight improvement resulting from accounting for stratification. Finally, our stratification model appears to be nearly equivalent to making von Karman's constant a variable as done in the earliest attempts to account for stratification in sediment-laden flows.

Thesis Supervisor: Ole S Madsen
Title: Professor of Civil and Environmental Engineering

Acknowledgments

The writing of this thesis has been a challenging but most rewarding experience. I would first like to express my deepest gratitude to Professor Ole Madsen for his invaluable guidance and advice. His constant enthusiasm and energy, his encouragement and his sense of humour have helped me brave the rough times when things did not seem to go in the right direction.

I would like to thank the generous financial and intellectual support of the MIT Civil and Environmental Engineering Department and of the MIT Sea Grant Program.

I gratefully aknowledge the professors and students of MIT Parsons Laboratory, thanks to whom I have discovered various fascinating aspects of environmental studies.

I would like to thank my labmates, particularly Amy and Homero, for their friendship, warmth and cheerfulness. I am also deeply grateful to all my friends from MIT who made this place a great place to live.

Most of all, I would like to thanks my parents and my sister for their wholehearted love and support. They have encouraged and trusted me throughout the years, and have given me the strength and courage to pursue my dreams, wherevere they may lead me.

And last, but certainly not least, I thank Alexis for being who he is.

Contents

Introduction

The understanding of many coastal oceanographic problems requires a comprehensive knowledge of the structure of the bottom boundary layer on the continental shelf. This layer is a region of turbulent mixing of mass, momentum and heat, and of frictional dissipation of energy. It is also an interface between seabed and overlying water column, where exchanges of particles, chemicals, and organisms occur. Several processes influence the bottom boundary layer structure: surface waves, low frequency currents, moveable bed effects, bioturbation, planetary rotation, temperature and salinity stratification, internal waves, bottom topography effects and stratification due to suspended sediments. This last process is investigated here.

Sediment transport in the continental shelf bottom boundary layer governs a wide range of processes, such as pollutant transport or near-bottom flows and mixing of biological communities, and is of practical concern for many engineering applications. Many models for sediment transport processes have already been developed. Most of these models do not account for stratification due to concentration of suspended sediment. Exceptions to this are studies by Vanoni (1975), Smith and McLean (1977), followed by Glenn and Grant (1987) and Glenn and Styles (2000). Vanoni (1975) [1] relates stratification to von Karman's constant's variability. Later, most attempts to model the effects due to sediment in suspension in a turbulent flow have been based on the stratified flow analogy (Smith and McLean (1977) [24], Glenn and Grant (1987) [10], Styles and Glenn (2000) [28]. In particular, these investigators introduced two empirical constants α and β to express the effects of strafication due to sediment in suspension. Their values were considered the same as those obtained from thermally stratified atmospheric boundary layers (Businger et al., 1971). However, this analogy

between thermally stratified boundary layers and sediment-induced stratification was not justified in these procedures and the validity of the theoretical framework for this application is open to question and must be established experimentally. Only Villaret and Trowbridge (1991) [30]) used data obtained from experiments with suspended sediments to determine α and β. However, their study did not lead to a definitive determination of α and β. Therefore, it would be of great environmental interest to investigate the effects of stratification on sediment transport. If the influence of stratification proved to be important, it would be interesting to develop a rigorous analytical model for the tranport of sediment in a stratified environment and to incorporate this in existing bottom boudary layer hydrodynamic models.

The effects of stratification due to suspended sediments are investigated here. First, the early works on the effects of sediment stratification are reviewed, and the physical processes which affect the transport of sediments are presented. In contrast to previous studies, a closed-form analytical solution is developed and a model is established for velocity and concentration profiles. This model is calibrated and validated through comparison with available experimental velocity and concentration measurements for flows carrying sediment in suspension. From comparisons with experimental data estimates of the values of stratification parameters appropriate for use when the stratification is caused by suspended sediments are obtained. Since a limited subset of the data used were obtained for flows over movable beds, rather than fixed beds, formulae for the reference concentration and the bed roughness are obtained. Finally, the improvement of velocity, concentration and transport rate predictions when stratification is taken into account is assessed by example computations.

Chapter 1

Model for a stratified sediment laden flow over a plane sloping bed

1.1 The continental shelf boundary layer

Two distinct boundary layers develop in the near bottom flow field on the continental shelf: one associated with the current and one associated with the wave. This is illustrated in Figure 1-1. The thickness of the current boundary layer is limited by water depth or Ekman layer height. For a fully rough turbulent flow, the current boundary layer can be divided into a near-bottom, constant stress or logarithmic region, and an outer log deficit region. The wave boundary layer has a typical thickness of 2 to 20 centimeters, and is nested within the current boundary layer. It can also be divided into a constant stress region, and an outer log deficit region. In our study, we concentrate on the near bottom current boundary layer, and we consider a flow without waves.

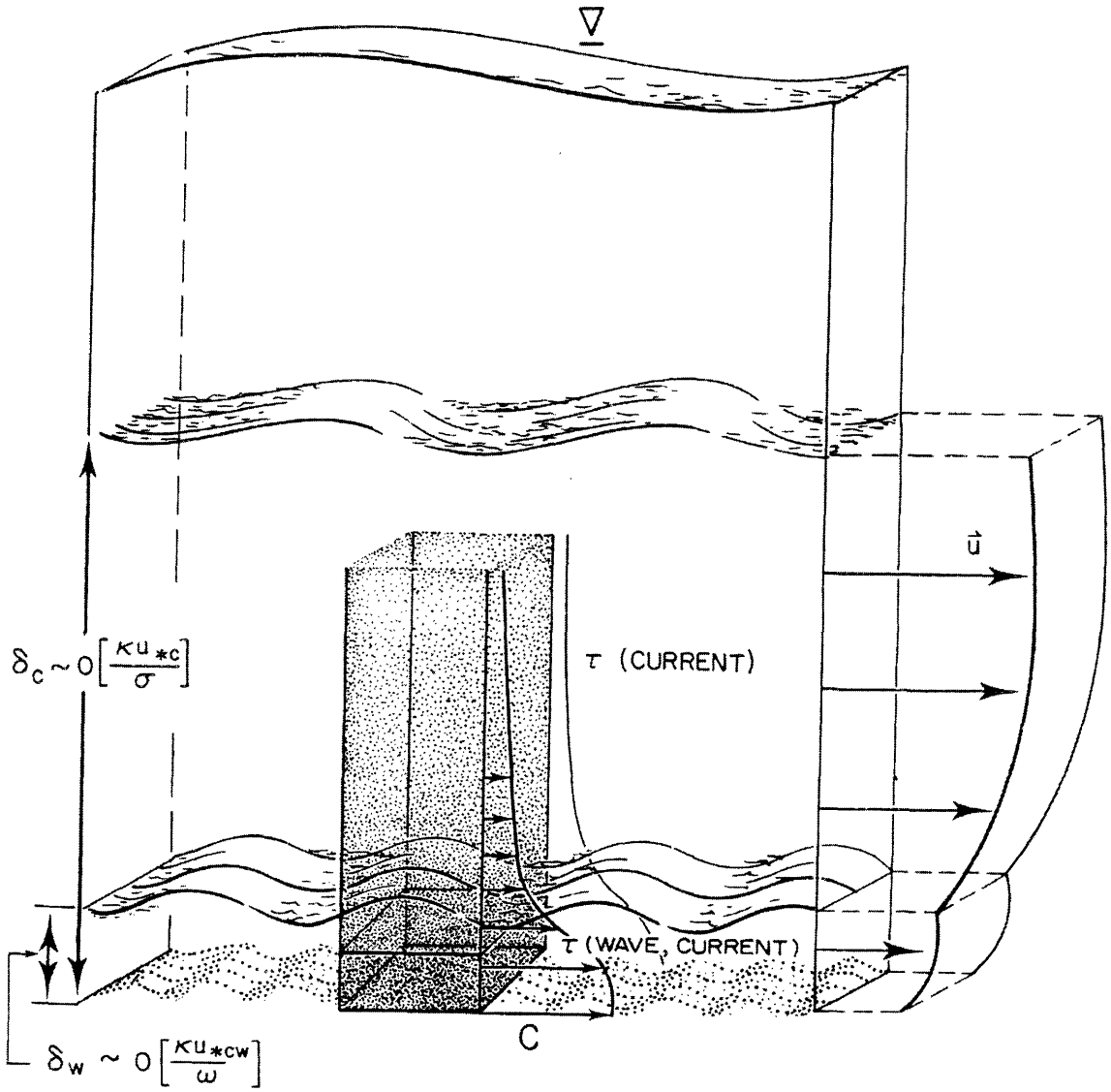

Figure 1-1: Skematic of the continental shelf bottom boundary layer illustrating the nested wave and current boundary layer structure (Glenn, 1986 [9])

1.2 Self-induced stratification due to suspended sediment

In the bottom boundary layer, stratification can be induced by vertical gradients of temperature, salinity or suspended sediment concentration. If the shear stress layer is large enough, significant amounts of sediment can be in suspension in the water column. The upward turbulent diffusion of sediment is balanced by the tendency of the sediment to fall out of suspension. The sediment concentration therefore decreases with height, resulting in a vertical concentration gradient: the flow is stably stratified.

Stable stratification inhibits the vertical turbulent transport of mass and momentum, by decreasing the correlation between the vertical and horizontal turbulent fluctuations. Less low momentum fluid is transported upward from the bottom through the water column since the upward fluctuations are associated with negative buoyancy in a stably stratified fluid. Thus the shear in the velocity profiles increases in comparison with the non-stratified neutral flow with the same boundary shear stress.

If the sediment settling velocity is very large, all the particles tend to be in the vicinity of the bottom. On the contrary, if the settling velocity is very small, all the particles tend to stay in suspension. In both cases, this does not result in a significant sediment concentration gradient through the water column. However, if the settling velocity belongs to an intermediate range, a significant concentration gradient can exist in the water column. Since the density of the fluid-sediment suspension also decreases with height, this significant gradient can stably stratify the flow. Turbulent fluctuations will be different from those in a non-stratified neutral flow and this will influence vertical turbulence diffusion if there is a significant density difference over the momentum transporting scale. Therefore, stratification is expected to occur only in some regions of the water column. Indeed, in the higher region of the water column, the sediment concentration is too small to result in any significant density difference. In the lower region, the momentum transporting eddies are very small, therefore the density difference over the eddy length scale is too small. We therefore

expect stratification effects to be most pronounced in an intermediate layer.

1.3 The Richardson number and the Monin Obukov length as a measure of stratification

1.3.1 The stratified flow analogy

Most past attempts to model the effects due to sediment in suspension in a turbulent flow have been based on the stratified flow analogy: the effects of stratification of suspended sediment are similar to those of a downward heat flux in the stably stratified atmospheric surface layer. The turbulence closures used in the sediment stratification context are similar to those used to study thermally stratified flows. In particular, the empirical constants have been assumed to have the same values (Smith and McLean (1977) [24], Glenn and Grant (1987) [10], Styles and Glenn (2000) [28]).
In heat convection theory, for geophysical flows such as those in the atmosphere and in the ocean, the flux Richardson Number is defined as the ratio of the buoyancy term of the turbulence kinetic energy budget equation and the negative of the shear terms of that same equation (Kundu and Cohen (2002) [15]).

$$R_f = \frac{g\alpha\overline{w'T'}}{\overline{u'w'}\frac{dU}{dz} + \overline{v'w'}\frac{dV}{dz}} \tag{1.1}$$

where T is the temperature, g is the acceleration due to gravity, z is the direction normal to the wall, U and V are the horizontal wind component, u', v' and w' are the components of the turbulent velocity fluctuations, T' is the turbulent temperature fluctuation α is the thermal expansion coefficient.
The Monin-Obukov length is then defined as the height at which the Richardson number (which parameterizes if convection is free or forced) equals 1:

$$L = \frac{z}{R_f} \tag{1.2}$$

By analogy with heat flow theory, following Stull (1988) [27], the flux Richardson number for a continuously sediment-stratified flow is defined as (Styles and Glenn (2000) [28])

$$R_f = -\frac{\frac{g}{\overline{\rho_T}}\overline{\rho'_T w'}}{\overline{u'w'}\frac{\partial \overline{U}}{\partial z}} \tag{1.3}$$

where g is the acceleration due to gravity, $\overline{\rho_T}$ is the mean density of the fluid-sediment suspension, ρ'_T is the turbulent density fluctuation, $\overline{U}$ and is the horizontal component of the Reynolds averaged velocity , u' is the horizontal component of the turbulent velocity fluctuations, w' is vertical component of the turbulent velocity fluctuations. The x-axis is chosen parallel to the flow. Similarly, for sediment stratification problems, the Monin Obukov length scale is defined as:

$$L = \frac{z}{R_f} \tag{1.4}$$

and z/L is referred to as the stability parameter. The Miles theorem (1961) [18], whose proof was elegantly presented by Howard (1961) [13], states that if the Richardson Number R_f is greater than 0.25 everywhere, then the stratified flow is stable. This suggests that the Richardson Number may be used as a measure of stratification: it measures the importance of flow stratification in inhibiting turbulent transfer of momentum and mass, with $R_{f,critical} = 0.25$ being the critical value above which turbulence production is being completely eliminated.

1.3.2 Early work concerning sediment stratification

The early work concerning sediment stratification relates stratification with von Karman's constant's variability. For a two-dimensional, steady, uniform flow in an open channel, Vanoni (1975) [1], the local shear stress can be expressed as

$$\tau = \rho g S(h - z) \tag{1.5}$$

where z is the distance above the bottom, h is the depth of flow, ρ is the fluid density and S is the bottom slope of the channel. Setting $z = 0$, the bottom shear stress τ_o

can be expressed by

$$\tau_o = \rho g h S \tag{1.6}$$

The local shear stress τ can then be expressed in terms of the bottom shear stress τ_o by

$$\tau = \tau_o \left(\frac{h - z}{h} \right) \tag{1.7}$$

The local shear stress may also be written

$$\tau = \nu_T \frac{d(\rho U)}{dz} \tag{1.8}$$

where ν_T is the momentum transfer coefficient, generally referred to as the turbulent eddy viscosity.

For a two-dimensional, steady, uniform flow in an open channel, Vanoni (1975) [1] uses the Prandtl - von Karman velocity defect law:

$$\frac{U - U_{max}}{\sqrt{\frac{\tau_o}{\rho}}} = \frac{2.3}{\kappa} log \frac{z}{h} \tag{1.9}$$

where U_{max} is the maximum horizontal velocity over the depth, i.e. the surface velocity, h is the depth of the flow, $U(z)$ is the horizontal velocity, κ is the von Karman's constant, and τ_o is the bottom shear stress. Vanoni analysis measurements obtained by the United States Army Corps of Engineer (1951), where τ_o and h are maintained constant: the log profile of velocity measurements is fitted by a straight line, whose slope N is

$$N = \frac{\kappa}{2.3\sqrt{\frac{\tau_o}{\rho}}} \tag{1.10}$$

Using equation (1.6) to compute τ_o, Vanoni obtains values of κ from equation (1.10). Plotting κ against $\overline{C}$, the mean concentration over the depth, and using equations (1.7) and (1.8), he then concludes that a decrease in κ corresponds to an increase in the mean concentration $\overline{C}$ and in a decrease in the momentum transfer coefficient ν_T (also called eddy viscosity). He deduces that the effect of suspended sediment in a flow is to reduce the value of the von Karman's constant κ below its value for

clear fluids. To explain the observed decrease in κ and the corresponding decrease in the momentum transfer coefficient when sediment is in suspension, he hypothesizes that the turbulence is damped by the sediment. According to Vanoni (1975) [1], the sediment is actually kept in suspension by the vertical velocity and the energy to do this must therefore come from the turbulence. The power to hold a grain of sand in suspension is the submerged weight of the grain times the fall velocity of the grain, thus the power to support the sediment of a given size or settling velocity w_s in a column of fluid of cross-sectional area and height equal to the depth h is

$$P_s = (s-1)\rho w_s g \overline{C} h \tag{1.11}$$

where ρ_s is the sediment density and $\overline{C}$ is the mean sediment concentration over the water column. The power to overcome the friction on the column of water is (Vanoni, 1975 [1])

$$P_f = \rho g h \overline{U} S = \tau_o \overline{U} \tag{1.12}$$

where $\overline{U}$ is the mean horizontal velocity over the water column. The ratio P_s/P_f, equal to the ratio of the energy required to support the sediment in the column of water to the energy required to overcome the friction, is

$$\frac{P_s}{P_f} = (s-1)\frac{w_s \overline{C}}{\overline{U} S} \tag{1.13}$$

Einstein and Chien (1952,1955) [1] have correlated κ against P_s/P_f using data of several investigators (see Figure 1-2).

More fundamental analysis have been carried out by Smith and McLean (1977) [24], Glenn and Grant (1987) [10] and Styles and Glenn (2000) [28]. These studies are not based on the variability of von Karman's constant κ, which is kept constant.

Smith and McLean (1977) [24] examine the effects of suspended sediment-induced stable stratification and present procedures to compute the associated reduction in eddy diffusivity based on the standard atmospheric boundary layer methods. They

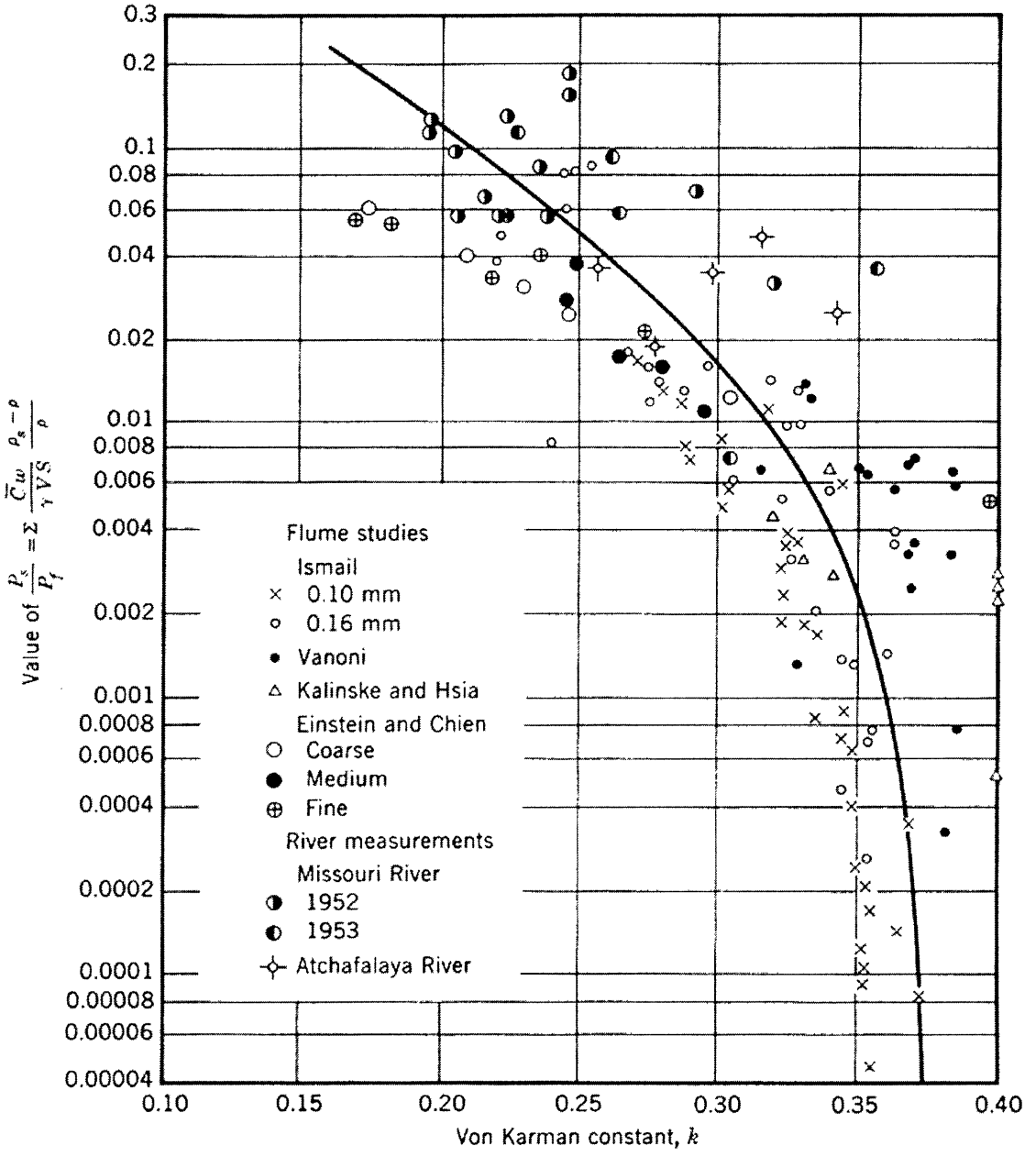

Figure 1-2: Variation of von Karman's constant κ with Suspended-Sediment Concentration, Einstein and Chien (1955) [1]

introduce an eddy viscosity of the form

$$\nu_T = \frac{\nu_{To}}{\alpha}(1 - \beta R_f)$$

where ν_{To} is the neutral eddy viscosity, α is the ratio of the eddy diffusivity of mass to that of momentum, and β is a constant derived from the atmospheric boundary layer theory and found to be 4.7 ± 0.5 by Businger et al. (1971). In their study, they assume α to be unity.

Glenn and Grant (1987) [10], and Styles and Glenn (2000) [28], assume that the effects of vertical stratification on the momentum balance are expressed through a modification to the neutral eddy viscosity

$$\nu_T = \frac{\nu_{To}}{(1 + \beta R_f)} \tag{1.14}$$

and to the eddy diffusivity

$$\nu_S = \frac{\nu_{To}}{(\gamma + \beta R_f)} \tag{1.15}$$

where β and γ are constants. The values of γ and β are obtained from thermally stratified atmospheric boundary layer theory (Businger et al.,1971): $\beta = 4.7$ and $\gamma = 0.74$. The ratio between eddy viscosity and eddy diffusivity is

$$\frac{\nu_T}{\nu_S} = \frac{1 + \beta R_f}{\gamma + \beta R_f} > 1 \tag{1.16}$$

for the values of $\gamma = 0.74$ and $\beta = 4.7$ and a Flux Richardson Number $R_f > 0$. These authors then develop iterative procedures in order to compute concentration and velocity profiles.

However, the analogy between thermally stratified boundary layer and sediment-induced stratification was not justified in these procedures and the validity of the theoretical framework for this application is open to question and must be established experimentally.

Villaret and Trowbridge (1991) [30] analyse velocity profiles obtained from labora-

tory measurements of ensemble-averaged velocity and ensemble-averaged particle concentration, in order to test the applicability of the stratified flow analogy to dilute suspensions of sand in turbulent flows of water. They examine the difference between velocity profiles in neutral and stratified flows, assuming, following Smith and McLean (1977) [24], that the eddy viscosity and the eddy diffusivity are expressible in the following form:

$$\nu_T = \nu_{To}(1 - \beta_1 R_f)$$

and

$$\nu_S = \frac{\nu_{To}}{\alpha}(1 - \beta_2 R_f)$$

where α, β_1 and β_2 are constants. They assume β_1 and β_2 to be equal ($\beta_1 = \beta_2 = \beta$) in their analysis. They qualitatively observe effects of stratification on velocity profiles, but are not able to obtain definitive results regarding β and α. Moreover, in their analysis, the bottom roughness for a given sediment size is considered constant, and the difference between velocity profiles in stratified and neutral flow is solely attributed to the stratification effect, i.e. to α, β and R_f.

1.4 General Governing Equations

Following Glenn and Grant (1987) [10], the volumetric sediment concentrations are expected to be at most of order $10^{-3} cm^3/cm^3$, except in the immediate vicinity of the bed. We can therefore neglect particle-particle interactions, and develop the governing equations assuming sediment concentrations are small, and treat the fluid-sediment suspension as a continuum. The sediment size and density are considered to be uniform. As explained by Glenn (1983) [9], if the particle diameter and response time are much smaller than the turbulent length and time scales, respectively, the conservation of momentum for a single particle in a turbulent flow reduces to:

$$\vec{u_s} = \vec{u} \tag{1.17}$$

$$w_s = w - w_s$$

where $\vec{u_s}$ and w_s are the horizontal and vertical particle velocities, $\vec{u}$ and w are the horizontal and vertical fluid velocities, and w_s is the particle settling (or fall) velocity. The particle settling velocity can be found experimentally by balancing the weight of the submerged particle with the fluid drag force on the particle. Formulae have been proposed to compute the settling velocity of natural sands, and will be presented later in Section 3.1.2.

Conservation equations can be written for sediment mass,

$$\frac{\partial c_s}{\partial t} + \vec{\nabla} \cdot (c_s \vec{u_s}) + \frac{\partial}{\partial z}(c_s w_s) = 0 \tag{1.18}$$

for fluid mass,

$$\frac{\partial c}{\partial t} + \vec{\nabla} \cdot (c \vec{u}) + \frac{\partial}{\partial z}(cw) = 0 \tag{1.19}$$

and for fluid momentum

$$\frac{D \vec{u}}{Dt} + 2w_v \vec{k} \times \vec{u} + 2 \vec{w_H} \times w \vec{k} = -\frac{\vec{\nabla} p}{\rho} + \nu(\vec{\nabla^2} \vec{u} + \frac{\partial^2 \vec{u}}{\partial z^2}) \tag{1.20}$$

where x, y, z are the components of a Cartesian coordinate system with z measured positive upward from the bottom, t is the time, $\vec{w_H}$ and w_v are the horizontal and vertical components of the Earth's angular velocity, $\vec{k}$ is the vertical unit vector, p is the pressure, ν is the kinematic viscosity, $c_s(x, y, z, t)$ is the volumetric concentration of sediment and $c(x, y, z, t)$ is the volumetric concentration of fluid. These concentrations are related by

$$c_s + c = 1 \tag{1.21}$$

Using (1.17) in (1.18) leads to

$$\frac{\partial c_s}{\partial t} + \vec{\nabla} \cdot (c_s \vec{u}) + \frac{\partial}{\partial z}(c_s w) - w_s \frac{\partial c_s}{\partial z} = 0 \tag{1.22}$$

Adding (1.18) and(1.19) and using (1.21) and(1.17) leads to

$$\vec{\nabla} \cdot \vec{u} + \frac{\partial w}{\partial z} - w_s \frac{\partial c_s}{\partial z} = 0 \tag{1.23}$$

The fluid velocity, concentration and pressure as well as the sediment concentration and velocity can be partitioned into mean and turbulent components

$$\begin{aligned}
\vec{u}\ (x,y,z,t) &= \vec{U}\ (x,y,z) + \vec{u'}\ (x,y,z,t) \\
w(x,y,z,t) &= W(x,y,z) + w'(x,y,z,t) \\
p(x,y,z,t) &= P(x,y,z) + p'(x,y,z,t) \\
\vec{u_s}\ (x,y,z,t) &= \vec{U_s}\ (x,y,z) + \vec{u_s'}\ (x,y,z,t) \\
w_s(x,y,z,t) &= W_s(x,y,z) + w_s'(x,y,z,t) \\
c_s(x,y,z,t) &= C_s(x,y,z) + c_s'(x,y,z,t)
\end{aligned} \tag{1.24}$$

where the capital letter denotes the mean variable associated with the current and the prime denotes the turbulent fluctuation, and the mean concentration, pressure and velocity are assumed to be quasi-steady. From the expression of sediment velocity (1.17), it follows that

$$w_s(x,y,z,t) = W(x,y,z) - w_s + w'(x,y,z,t)$$

therefore

$$\begin{aligned}
W_s(x,y,z) &= W(x,y,z) - w_s \\
w_s' &= w'
\end{aligned} \tag{1.25}$$

We substitute the partitioned variables in the governing equations, and take the Reynolds average of the equations over a time that is long compared to the turbulent scale. The equations are then simplified introducing the following scaling arguments, presented by Grant and Madsen (1986) [12]: (i) Coriolis acceleration has a negligible

effect near the bottom and is neglected in the model described here; (ii) mean concentration and velocity are assumed to be horizontally nearly homogeneous; (iii) viscous stresses are neglected compared to Reynolds stresses since rough turbulent flow is expected; (iv) horizontal derivatives of turbulent fluxes can be neglected compared to those in the vertical and (v) in the momentum equation, the nonlinear convective accelerations can be neglected compared to the local acceleration. The resulting equations governing the near bottom flow are

$$0 = -\frac{\vec{\nabla} P}{\rho} + \frac{\partial}{\partial z}(-\overrightarrow{\overline{u' w'}}) \tag{1.26}$$

$$-w_s \frac{\partial C_s}{\partial z} + \frac{\partial \overline{c_s' w'}}{\partial z} = 0 \tag{1.27}$$

where the overbar represents the Reynolds average.

1.5 Turbulent closure scheme

The turbulent closure scheme developed in the eddy viscosity model used by Glenn (1983) [9] is used here to solve (1.26) and (1.27). The closure scheme assumes that the vertical turbulent fluxes can be written as an eddy diffusivity multiplied by the vertical gradient of the appropriate Reynolds averaged quantity.

$$-\overrightarrow{\overline{u' w'}} = \nu_T \frac{\partial \vec{U}}{\partial z} \tag{1.28}$$

$$-\overline{c_s' w_s'} = \nu_{Ts} \frac{\partial C_s}{\partial z} \tag{1.29}$$

$$-\overline{c' w'} = \nu_{Tf} \frac{\partial C_f}{\partial z} \tag{1.30}$$

where ν_T, ν_{Ts} and ν_{Tf} are the eddy diffusivities of momentum, sediment mass and fluid mass. Substituting the relations (1.25) and (1.21) in (1.29) and (1.30), it follows that the eddy diffusivity of sediment mass ν_{Ts} and the eddy diffusivity of fluid mass ν_{Tf} are equal. We therefore define the mass eddy diffusivity $\nu_S = \nu_{Ts} = \nu_{Tf}$.

1.6 Governing equation for the concentration

Substituting (1.29) in the governing equation (1.27), we obtain

$$w_s \frac{\partial C_s}{\partial z} + \frac{\partial \left(\nu_S \frac{C_s}{\partial z}\right)}{\partial z} = 0 \tag{1.31}$$

The sediment flux at the surface of the water column is equal to zero, and the sediment concentration goes to zero. Therefore, by integrating (1.31) with respect to z, it follows that

$$w_s C_s + \nu_S \frac{\partial C_s}{\partial z} = 0 \tag{1.32}$$

The Reynolds averaged sediment mean concentration C_s depends on the elevation z.

1.7 Governing equation for the velocity

The characteristic shear velocity of the turbulent fluctuations is defined as

$$u_* = \sqrt{\frac{|\tau_o|}{\rho}} \tag{1.33}$$

where τ_o is the bottom shear stress. Following Grant and Madsen (1986) [12] we make the assumption of a linearly varying shear stress

$$\tau = \tau_o \left(1 - \frac{z}{h}\right) = \rho u_*^2 \left(1 - \frac{z}{h}\right) \tag{1.34}$$

where h is the height of the water column and ρ is the fluid density.
Substituting (1.28) in (1.26) leads to

$$0 = -\frac{\vec{\nabla} P}{\rho} + \frac{\partial}{\partial z}\left(\nu_T \frac{\partial \vec{U}}{\partial z}\right) \tag{1.35}$$

Near the bottom, the stress divergence in (1.35) is approximately zero. The turbulent stress in parenthesis is equal to the time-averaged shear stress associated with the

current. Therefore, with x-axis aligned with the flow,

$$\nu_T \frac{\partial U}{\partial z} = \rho u_*^2 \left(1 - \frac{z}{h}\right) \tag{1.36}$$

1.8 Formulation of the problem

1.8.1 Governing equations

From here on, for the sake of simplicity $C(z) = C_s(z)$. We consider a gravity-driven flow of water with a free surface carrying a dilute suspension of solid particles over a plane sloping bottom (see Figure 1-3). The ensemble-averaged motion is independent of streamwise position x, cross-stream position y and time t. All particles are assumed to have the same size and density. The bottom stress and depth are given, and the problem is to determine the ensemble-averaged velocity and particle concentration fields, $U(z)$ and $C(z)$.

For the ensemble-averaged particle concentration $C(z)$, the governing equation for the concentration (1.32) becomes

$$w_s C + \nu_S \frac{dC}{dz} = 0 \tag{1.37}$$

Similarly, the governing equation for the velocity (1.36) may be written

$$\frac{dU}{dz} = \frac{u_*^2}{\nu_T} \left(1 - \frac{z}{h}\right) \tag{1.38}$$

We also assume, following Smith and McLean (1977) [24], that the eddy viscosity and eddy diffusivity are expressible in the following form:

$$\nu_T = \nu_{TN} \left(1 - \beta_u R_f\right) \tag{1.39}$$

$$\nu_S = \nu_{SN} \left(1 - \beta_c R_f\right) \tag{1.40}$$

$$\nu_{SN} = \frac{\nu_{TN}}{\alpha} \tag{1.41}$$

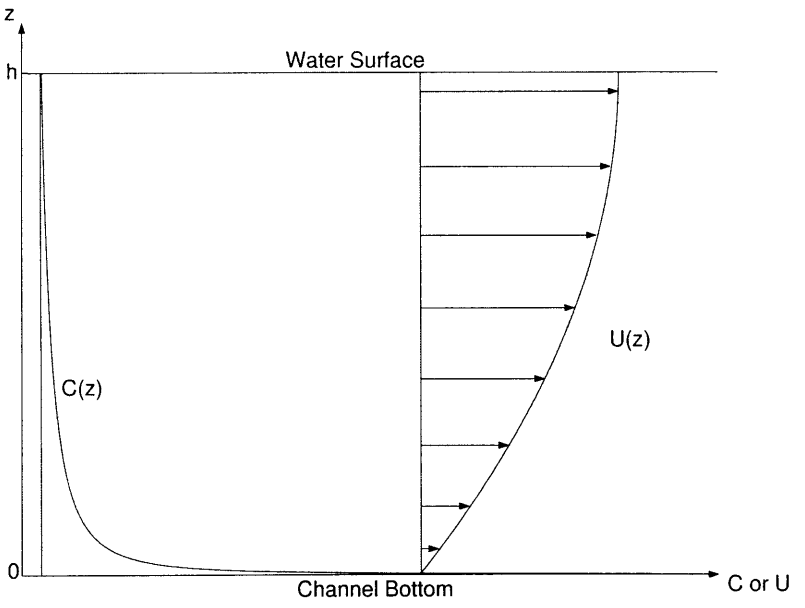

Figure 1-3: Definition sketch of mean concentration of suspended sediment $C(z)$ and mean velocity parallel the bottom $U(z)$

where R_f is the flux Richardson number, ν_{TN} is the neutral eddy viscosity, ν_{SN} is the neutral eddy diffusivity, β_u and β_c are positive constants and α is a constant, the turbulent Schmidt Number for solid particles under neutral conditions. Here, we make the assumption that $\beta_u = \beta_c = \beta$. From equations (1.39), (1.40) and (1.41), we get

$$\nu_S = \frac{\nu_T}{\alpha} \tag{1.42}$$

So the governing equation (1.37) becomes:

$$\frac{dC}{dz} = \frac{-w_s \alpha}{\nu_T} C \tag{1.43}$$

Physically, the eddy viscosity ν_T and the concentration C should be positive, therefore equations (1.38) and (1.43) imply $\frac{dU}{dz} \geq 0$ and $\frac{dC}{dz} \leq 0$.

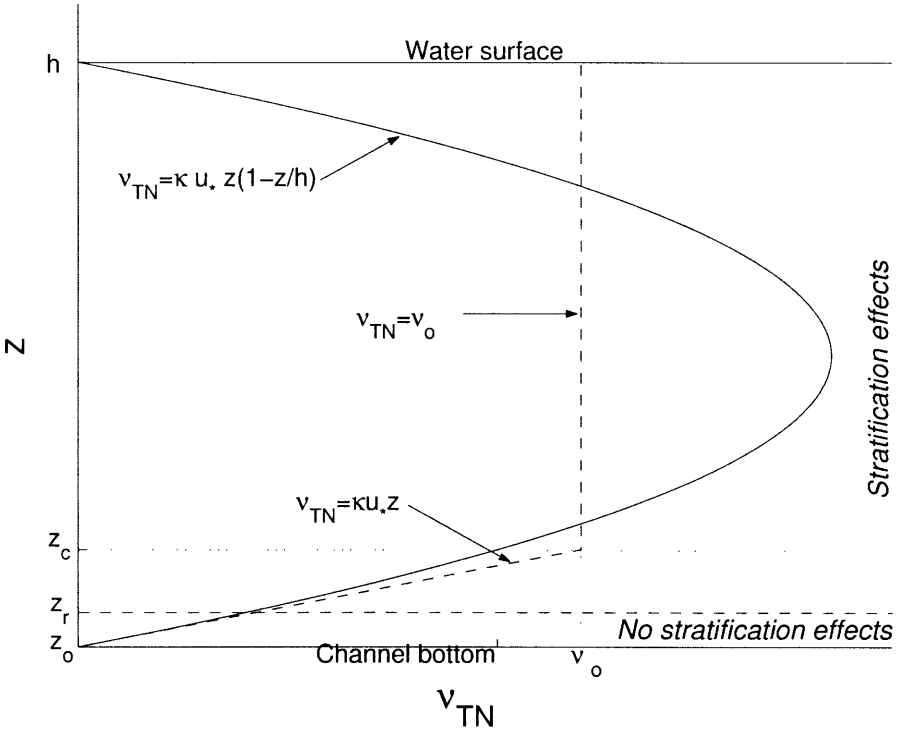

Figure 1-4: Model for the neutral eddy viscosity ν_{TN} and for the stratification effects

1.8.2 Eddy viscosity closure scheme

In agreement with previous studies, e.g. Styles and Glenn (2000) [28], we adopt the model presented in Figure 1-4. From z_o to a reference depth, z_r, which depends on the grain size d, stratification is assumed to have no effect on velocity and concentration. In fact, $z_o < z < z_r$ may be regarded as the thickness of the bedload layer. Above z_r, stratification influences the velocity and the concentration.

Between $z_o(\leq z_r)$ and the surface, the neutral viscosity is assumed to be parabolic: $\nu_{TN} = \kappa u_* z \left(1 - \frac{z}{h}\right) \approx \kappa u_* z$ for $z << h$. A simplified model of the parabolic neutral eddy viscosity model is the following. Between $z_o(\leq z_r)$ and $z_c = h/6$, the neutral viscosity is assumed to be linear: $\nu_{TN} = \kappa u_* z$, and the approximation $z << h$ is made. Between z_c and the surface, the neutral viscosity is assumed to be constant: $\nu_{TN} = \nu_o = \kappa u_* z_c$.

In the following study, we therefore solve the governing equations (1.38) and (1.43) for those two cases. Combining these results enables us to build a model for sediment

concentration and velocity in a stratified sediment-laden flow over a plane sloping bed.

Chapter 2

Solution for velocity and sediment concentration

2.1 Richardson Number

The Flux Richardson Number has previously been defined in equation (1.3). Following Glenn (1983) [9], the total density of the fluid-sediment suspension is defined as

$$\rho_T = \rho\,[1 + (s-1)C] \tag{2.1}$$

where ρ is the water density, s is the ratio

$$s = \frac{\rho_s}{\rho} \tag{2.2}$$

and ρ_s is the sediment density. Substituting partitioned variables for $\rho_T = \overline{\rho_T} + \rho'_T$ and c_s, it is found that after Reynolds-averaging

$$\overline{\rho_T} = \rho(1 + (s-1)C) \approx \rho \tag{2.3}$$

and

$$\rho'_T = \rho(s-1)c'_s \tag{2.4}$$

From Monin and Yaglom (1971) [19], using the closure equations (1.28) and (1.30) as well as equations (1.21), (2.3) and (2.4), the flux Richardson number defined in equation (1.3) can be expressed as

$$R_f = -\frac{\frac{g}{\overline{\rho_T}}\overline{\rho'_T w'}}{\overline{u'w'}\frac{\partial \overline{U}}{\partial z}} = -\frac{\frac{g}{\rho}\overline{\rho(s-1)c'_s w'}}{\overline{u'w'}\frac{\partial \overline{U}}{\partial z}} = -\frac{g(s-1)\overline{c'_s w'}}{\overline{u'w'}\frac{\partial \overline{U}}{\partial z}} = \frac{-g\nu_S\,(s-1)\,\frac{dC}{dz}}{\nu_T\left(\frac{dU}{dz}\right)^2} \tag{2.5}$$

Using (1.38), (1.39) and (1.43), we obtain after some simple algebraic manipulations

$$R_f = \frac{g\,(s-1)\,w_s C \nu_{TN}}{u_*^4\left(1-\frac{z}{h}\right)^2\left(1+\frac{\beta g(s-1)w_s\nu_{TN}}{u_*^4\left(1-\frac{z}{h}\right)^2}C\right)} \tag{2.6}$$

2.2 Solution for the parabolic neutral eddy viscosity

The neutral eddy viscosity is parabolic for $z_o \leq z \leq h$

$$\nu_{TN} = \kappa u_* z\left(1-\frac{z}{h}\right) \tag{2.7}$$

2.2.1 Neutral Profiles

For the neutral case, using the governing equation (1.38) leads to

$$\frac{dU_N}{dz} = \frac{u_*}{\kappa z} \tag{2.8}$$

Therefore the neutral velocity follows the logarithmic law of the wall :

$$U_N\,(z) = \frac{u_*}{\kappa} ln\left(\frac{z}{z_o}\right) \tag{2.9}$$

where z_o is the bottom roughness defined by

$$U_N\,(z_o) = 0 \tag{2.10}$$

The reference level for C_r, the reference concentration, is $z = z_r$, i.e.

$$C_N(z_r) = C_r \tag{2.11}$$

Using the governing equation (1.43) and introducing the constant

$$q = \frac{w_s \alpha}{\kappa u_*} \tag{2.12}$$

known as the Rouse parameter, the equation for the neutral concentration is

$$\frac{dC_N}{dz} + \frac{q}{z\left(1 - \frac{z}{h}\right)} C_N = 0$$

or

$$\frac{C_N'(z)}{C_N(z)} + \frac{q}{z\left(1 - \frac{z}{h}\right)} = 0$$

Integrating and using the boundary condition (2.11), we obtain for the neutral concentration

$$C_N(z) = C_r \left(\frac{(h - z) z_r}{(h - z_r) z} \right)^q \tag{2.13}$$

Through the water column $z_o \leq z < h$, therefore $C_N(z)$ and $U_N(z) > 0$, as they should be.

2.2.2 Stratified Profiles

Using the equations (2.6) and (2.7), we obtain for the Flux Richardson Number

$$R_f = \frac{azC}{1 - \frac{z}{h} + \beta azC} \tag{2.14}$$

with a being a constant given by

$$a = \frac{g(s-1) w_s \kappa}{u_*^3} = L^{-1}/C \tag{2.15}$$

where L is the Monin-Obukov length (Styles and Glenn (2000) [28]).Therefore,

$$1 - \beta R_f = \frac{1 - \frac{z}{h}}{1 - \frac{z}{h} + \beta a z C}$$

and we obtain the stratified eddy viscosity for $z_r < z < h$

$$\nu_T = \kappa u_* z \left(1 - \frac{z}{h}\right)(1 - \beta R_f) = \frac{\kappa u_* z \left(1 - \frac{z}{h}\right)^2}{1 - \frac{z}{h} + \beta a z C} \tag{2.16}$$

Concentration Distribution

The governing equations for the stratified concentration are valid above the reference elevation z_r. The governing equation (1.43) for the concentration becomes

$$\frac{dC}{dz} + \frac{w_s \alpha}{\nu_T} C = 0 \tag{2.17}$$

Using (2.16) this may be written

$$\frac{dC}{dz} + \frac{w_s \alpha}{\kappa u_*} \frac{1 - \frac{z}{h} + \beta a z C}{z \left(1 - \frac{z}{h}\right)^2} C = 0$$

or

$$\frac{dC}{dz} + \frac{w_s \alpha}{\kappa u_*} \frac{C}{z \left(1 - \frac{z}{h}\right)} + \frac{w_s \alpha \beta a}{\kappa u_*} \frac{C^2}{\left(1 - \frac{z}{h}\right)^2} = 0$$

This equation may formally be written

$$C'(z) + P(z) C + Q(z) C^2 = 0 \tag{2.18}$$

with

$$P(z) = \frac{q}{z \left(1 - \frac{z}{h}\right)} \tag{2.19}$$

and

$$Q(z) = \frac{\beta a q}{\left(1 - \frac{z}{h}\right)^2} \tag{2.20}$$

with q defined by (2.12). In (2.18) we recognize Ricatti's equation (see Appendix A), which can be solved introducing $f(z)$ such that

$$C(z) = \frac{f'(z)}{Q(z) f(z)} \tag{2.21}$$

Then, equation (2.18) is equivalent to :

$$f'' + \left(P - \frac{Q'}{Q}\right) f' = 0$$

or

$$\frac{f''}{f'} = -P + \frac{Q'}{Q}$$

Integrating once,

$$ln|f'| = ln|Q| + ln\left|\frac{z}{h-z}\right|^{-q} + constant$$

from which

$$f' = AQ\left(\frac{h-z}{z}\right)^q = A_1 \frac{(h-z)^{q-2}}{z^q} \tag{2.22}$$

with A and A_1 constant and $A_1 = q\beta aA$.

Then, integrating equation (2.22) between z_r and z,

$$f = A_2 + A_1 \int_{z_r}^{z} \frac{(h-z')^{q-2}}{z'^q} dz' \tag{2.23}$$

where A_2 is a constant. Hence, using (2.21), the concentration can be expressed as :

$$C(z) = \frac{(h-z)^q}{h^2 q\beta a z^q \left(\int_{z_r}^{z} \frac{(h-z')^{q-2}}{z'^q} dz' + A'\right)}$$

where $A' = \frac{A_2}{A_1}$ is a constant. We introduce $Z_r(z) = \int_{z_r}^{z} \frac{(h-z')^{q-2}}{z'^q} dz'$. $Z_r(z_r) = 0$ and $Z_r(z) > 0$ for $z_r < z < h$.

Introducing the variable $y = \frac{h}{z'}$,

$$Z_r(z) = \int_{h/z}^{h/z_r} \frac{(y-1)^{q-2}}{h} dy$$

Integrating the right hand side of this equation leads to :

$$Z_r(z) = \frac{1}{h(q-1)}\left[\left(\frac{h}{z_r}-1\right)^{q-1} - \left(\frac{h}{z}-1\right)^{q-1}\right], q \neq 1 \tag{2.24}$$

$$Z_r(z) = \frac{1}{h} ln\left(\left|\frac{h/z_r - 1}{h/z - 1}\right|\right) = \frac{1}{h} ln\left(\frac{z(h-z_r)}{z_r(h-z)}\right), q = 1 \tag{2.25}$$

Using (2.11), we finally obtain for the constant A'

$$A' = \frac{(h-z_r)^q}{h^2 q \beta a C_r z_r^q} \tag{2.26}$$

and for the concentration with a quadratic neutral eddy viscosity

$$C(z) = \frac{(h-z)^q}{h^2 q \beta a z^q \left(Z_r(z) + \frac{(h-z_r)^q}{h^2 q \beta a C_r z_r^q}\right)} \tag{2.27}$$

with $Z_r(z)$ given above by (2.24) and (2.25). All the terms in $C(z)$ are strictly positive for $z_r < z < h$, therefore the concentration is positive for $z_r \leq z < h$.
Moreover, we have from equation (2.27) and making use of the expression for the neutral concentration distribution given by (2.13)

$$C(z) = \frac{(h-z)^q}{h^2 q \beta a z^q Z_r(z) + \frac{(h-z_r)^q z^q}{C_r z_r^q})} = C_r \left(\frac{z_r(h-z)}{z(h-z_r)}\right)^q \frac{1}{1 + \frac{h^2 q \beta a z_r^q C_r Z_r(z)}{(h-z_r)^q}}$$

$$= C_N(z) \frac{1}{1 + \frac{h^2 q \beta a z_r^q C_r Z_r(z)}{(h-z_r)^q}} \tag{2.28}$$

Therefore, $C(z) < C_N(z)$ for $z_r < z < h$. Stratification results in a decrease in concentration compared with a neutral non-stratified flow. In equation(2.28),when $\beta \to 0$, i.e. the stratification effects disappear, this reduces to the neutral case: $C(z) \to C_N(z)$.

Velocity Profile

Below z_r, stratification has no effect on the velocity and $U(z) = U_N(z) = \frac{u_*}{\kappa} ln\left(\frac{z}{z_o}\right)$ for $z_o < z < z_r$. Between z_r and h, using the governing equation (1.38) and equation

(2.16) for the stratified eddy viscosity, we obtain

$$\frac{dU}{dz} = \frac{u_* \left(1 - \frac{z}{h} + \beta a z C\right)}{\kappa z \left(1 - \frac{z}{h}\right)}$$

and therefore

$$\frac{dU}{dz} = \frac{u_*}{\kappa z} + \frac{u_* \beta a C}{\kappa \left(1 - \frac{z}{h}\right)} = \frac{dU_N}{dz} + \frac{dU_S}{dz} \tag{2.29}$$

where $\frac{dU_S}{dz} = \frac{u_* \beta a C}{\kappa\left(1-\frac{z}{h}\right)}$. Therefore, integrating (2.29) once and using the boundary condition (2.10), we obtain for the velocity:

$$U(z) = \frac{u_*}{\kappa} ln\left(\frac{z}{z_o}\right) + \frac{u_* \beta a}{\kappa} \int_{z_r}^{z} \frac{C(z')}{1 - \frac{z'}{h}} dz' = U_N(z) + U_S(z), z_r \leq z < h \tag{2.30}$$

Since the concentration is positive for $z_r < z < h$, the term $\frac{u_* \beta a C}{\kappa\left(1-\frac{z}{h}\right)}$ is positive, and as we integrate it between z_r and $z \geq z_r$, U_S is strictly positive, i.e. $U(z) > U_N(z)$ for $z > z_r$. Stratification result in an increase in velocity compared to a neutral non-stratified flow. When $\beta \to 0$ in equation(2.30), i.e. the effects of stratification disappear, $U(z) \to U_N(z)$.

The integral in $U_S(z)$ with $C(z')$ given by (2.28) can be evaluated numerically. However, an explicit analytical solution may be derived under the assumption $z << h$.

In the case where $z << h$, and $q \neq 1$, we can approximate (2.24)

$$Z_r(z) \approx \frac{1}{h(q-1)} \left[\left(\frac{h}{z_r}\right)^{q-1} - \left(\frac{h}{z}\right)^{q-1}\right]$$

and equation (2.27) for the concentration becomes

$$C(z) \approx \frac{q-1}{q\beta a \left[z_r \left(\frac{z}{z_r}\right)^q - z + \frac{q-1}{q\beta a C_r} \left(\frac{z}{z_r}\right)^q\right]} = \frac{1-q}{q\beta a \left[z + \left(\frac{z}{z_r}\right)^q \left(\frac{1-q}{q\beta a C_r} - z_r\right)\right]} \tag{2.31}$$

Similarly, when $z << h$ and $q \neq 1$ equation (2.20) gives $Q(z) \approx \beta a q$ and equation (2.30) becomes

$$U(z) \approx U_N(z) + \frac{u_* \beta a}{\kappa} \int_{z_r}^{z} C(z')\, dz'$$

Therefore

$$U_S(z) \approx \frac{u_* \beta a}{\kappa} \int_{z_r}^{z} \frac{f'(z')}{Q(z') f(z')} dz' \approx \frac{u_*}{\kappa q} \int_{z_r}^{z} \frac{f'(z')}{f(z')} dz' = \frac{u_*}{\kappa q} ln \left| \frac{f(z)}{f(z_r)} \right|$$

From (2.23) and (2.26)

$$f(z) = A_2 + A_1 \int_{z_r}^{z} \frac{(h - z')^{q-2}}{z'^q} dz' \approx A_2 + A_1 \int_{z_r}^{z} \frac{h^{q-2}}{z'^q} dz'$$

$$\approx A_2 + A_1 \frac{h^{q-2}}{1-q} \left[z^{1-q} - z_r^{1-q} \right] \approx A_1 \left(A' + \frac{h^{q-2}}{1-q} \left[z^{1-q} - z_r^{1-q} \right] \right)$$

$$= A_1 \left(\frac{(h - z_r)^q}{h^2 q \beta a C_r z_r^q} + \frac{h^{q-2}}{1-q} \left[z^{1-q} - z_r^{1-q} \right] \right)$$

$$\approx \frac{A_1 h^{q-2}}{1-q} \left(\frac{1-q}{q \beta a C_r z_r^q} + z^{1-q} - z_r^{1-q} \right)$$

Finally, for $q \neq 1$, when $z << h$, the stratified velocity can be expressed as

$$U(z) \approx U_N(z) + \frac{u_*}{\kappa q} ln \left| 1 + \frac{q \beta a C_r z_r^q}{1-q} \left(z^{1-q} - z_r^{1-q} \right) \right| \tag{2.32}$$

for $z \geq z_r$. For $z_o < z \leq z_r$, $U(z) = U_N(z)$.

In the case where $z << h$, and $q = 1$, we can approximate (2.25)

$$Z_r(z) \approx \frac{1}{h} ln \left(\frac{z}{z_r} \right)$$

and equation (2.27) becomes

$$C(z) \approx \frac{h}{\beta a h^2 z \left[\frac{1}{h} ln\left(\frac{z}{z_r}\right) + \frac{h}{h^2 \beta a C_r z_r}\right]} = \frac{1}{\beta a z \left[ln\left(\frac{z}{z_r}\right) + \frac{1}{\beta a C_r z_r}\right]} \tag{2.33}$$

When $z << h$ and $q = 1$, equation (2.20) gives $Q(z) \approx \beta a$ and using equation (2.21), equation (2.30) becomes

$$U(z) \approx U_N(z) + \frac{u_*}{\kappa} \int_{z_r}^{z} \frac{f'(z)}{f(z)} dz' = U_N(z) + \frac{u_*}{\kappa} ln \left|\frac{f(z)}{f(z_r)}\right|$$

Moreover, we have from (2.23)

$$f(z) = A_2 + A_1 \int_{z_r}^{z} \frac{(h - z')^{-1}}{z'^q} dz' \approx A_2 + A_1 \int_{z_r}^{z} \frac{(h)^{-1}}{z'^q} dz' = A_2 + \frac{A_1}{h} ln \left|\frac{z}{z_r}\right|$$

$$= A_2 \left(1 + \frac{A_1}{A_2 h} ln \left|\frac{z}{z_r}\right|\right) = A_2 \left(1 + \frac{1}{A' h} ln \left|\frac{z}{z_r}\right|\right) = A_2 \left(1 + \beta a C_r z_r ln \left|\frac{z}{z_r}\right|\right)$$

Therefore, when $q = 1$ and $z << h$,the stratified velocity can be expressed as

$$U(z) \approx U_N(z) + \frac{u_*}{\kappa} ln \left|1 + \beta a C_r z_r ln \left|\frac{z}{z_r}\right|\right| \tag{2.34}$$

for $z \geq z_r$. For $z_o < z \leq z_r$, $U(z) = U_N(z)$.

2.3 Solution for the linear-constant neutral eddy viscosity

Between z_o and $z_c = h/6$ (the Inner Layer Region), we approximate the quadratic eddy viscosity by a linear variation, $\nu_{TN} = \kappa u_* z$, and make the assumption $z << h$, therefore keeping only the first-order terms. Between z_c and the surface (the Outer Layer Region), we approximate the neutral eddy viscosity by a constant, $\nu_{TN} = \nu_o = \kappa u_* z_c$. The neutral eddy viscosity is continuous at $z = z_c$ (see Figure 1-4).

2.3.1 The Inner Layer Region

We assume $z << h$ and linearize the governing equations. Doing this, equation (1.38) becomes the law of the wall, i.e.

$$\nu_T \frac{dU}{dz} = u_*^2 \tag{2.35}$$

Neutral Profiles

With the assumption $z << h$, Equation (2.7) becomes

$$\nu_{TN} = \kappa u_* z \tag{2.36}$$

corresponding to a logarithmic neutral velocity profile :

$$U_N(z) = \frac{u_*}{\kappa} ln\left(\frac{z}{z_o}\right) \tag{2.37}$$

Using the governing equation (1.43) the equation for the neutral concentration is :

$$\frac{dC_N}{dz} + \frac{q}{z} C_N = 0$$

or

$$\frac{C_N'(z)}{C_N(z)} + \frac{q}{z} = 0$$

where q is given by (2.12). Integrating and using the boundary condition (2.11), we obtain for the neutral concentration :

$$C_N(z) = C_r \left(\frac{z_r}{z}\right)^q \tag{2.38}$$

Flux Richardson Number

Using equation (2.14) and the assumption $z << h$ leads to

$$R_f = \frac{azC}{1 + \beta azC} \tag{2.39}$$

Stratified concentration in the Inner Layer Region

Combining equations (1.43), (1.40) and (2.39) leads to :

$$\frac{dC}{dz} + P(z)\,C(z) + Q(z)\,C(z)^2 = 0 \tag{2.40}$$

with $P(z) = \frac{\alpha w_s}{u_* \kappa}\frac{1}{z} = \frac{q}{z}$ and $Q(z) = \frac{\alpha w_s \beta a}{u_* \kappa} = q\beta a = constant.$
Introducing f with $C = \frac{f'}{Qf}$, equation (2.40) is equivalent to:

$$f''(z) + \frac{q}{z} f'(z) = 0 \tag{2.41}$$

- First case: $q \neq 1$

  Integrating (2.41) gives $f'(z) = B_1 z^{-q}$, and integrating again

$$f(z) = \frac{B_1}{1-q}\left(z^{1-q} + B\right) \tag{2.42}$$

  where B_1 and B are constants. Therefore,

$$C(z) = \frac{f'}{Qf} = \frac{1-q}{q\beta a\,(z + Bz^q)}$$

  Using $C(z_r) = C_r$, we obtain $B = z_r^{-q}\left(\frac{1-q}{C_r q \beta a} - z_r\right)$ and :

$$C(z) = \frac{f'}{Qf} = \frac{1-q}{q\beta a\left(z + z_r^{-q}\left(\frac{1-q}{C_r q\beta a} - z_r\right) z^q\right)} \tag{2.43}$$

  i.e. we get the same result as obtained from the approximation $z << h$ in equation (2.27), cf. (2.31).

- Second case: $q = 1$

  Integrating (2.41) gives $f'(z) = \frac{B_2}{z}$, and integrating again:

$$f(z) = B_2\,(ln(z) + B_3) \tag{2.44}$$

where B_2 and B_3 are constant. Hence,

$$C(z) = \frac{f'}{Qf} = \frac{1}{\beta a z \left(ln(z) + B_3\right)}$$

Using $C(z_r) = C_r$, we obtain $B_3 = \frac{1}{\beta a z_r} - lnz_r$, and:

$$C(z) = \frac{f'}{Qf} = \frac{1}{\beta a z \left(ln\left(\frac{z}{z_r}\right) + \frac{1}{C_r \beta a z_r}\right)} \tag{2.45}$$

We recognize that equation (2.33) obtained by linearizing equation (2.30), is identical to (2.45)

Stratified velocity in the Inner Layer Region

Using equations (1.39), (2.96) and (2.39) the equation for the velocity for $z_r \leq z \leq z_c$ becomes:

$$\frac{dU}{dz} = \frac{u_*}{\kappa z} + \frac{u_* \beta a}{\kappa} C \tag{2.46}$$

Using $C = \frac{f'}{Qf}$, equation (2.46) becomes

$$\frac{dU}{dz} = \frac{u_*}{\kappa}\left(\frac{1}{z} + \frac{\beta a f'}{Qf}\right) \tag{2.47}$$

Integrating equation(2.47) once,

$$U(z) = \frac{u_*}{\kappa}\left(ln\left(\frac{z}{z_o}\right) + \frac{\beta a}{Q} ln\left|\frac{f(z)}{f(z_r)}\right|\right) \tag{2.48}$$

- $q \neq 1$

  Using (2.48) and (2.42)

$$U(z) = \frac{u_*}{\kappa} ln\left(\frac{z}{z_o}\right) + \frac{u_*}{\kappa q} ln\left|\frac{B + z^{1-q}}{B + z_r^{1-q}}\right| = \frac{u_*}{\kappa} ln\left(\frac{z}{z_o}\right) + \frac{u_*}{\kappa q} ln\left|\frac{z_r^{-q}\left(\frac{1-q}{C_r q \beta a} - z_r\right) + z^{1-q}}{z_r^{-q}\left(\frac{1-q}{C_r q \beta a}\right)}\right|$$

$$= \frac{u_*}{\kappa} ln\left(\frac{z}{z_o}\right) + \frac{u_*}{\kappa q} ln\left|1 + \frac{C_r q \beta a z_r^q}{1-q}(z^{1-q} - z_r^{1-q})\right| \tag{2.49}$$

We have the same result as equation (2.32).

- $q = 1$

  Using (2.48) and (2.44)

$$U(z) = \frac{u_*}{\kappa}\left(ln\left(\frac{z}{z_o}\right) + ln\left|C_r\beta a z_r ln\left(\frac{z}{z_r}\right) + 1\right|\right) \tag{2.50}$$

  which is recognized as equation (2.34).

2.3.2 The Outer Layer Region

Here, we do not assume $z << h$. For $z_c \leq z \leq h$ the neutral eddy viscosity is

$$\nu_{TN} = \nu_o = constant \tag{2.51}$$

Neutral Profiles

Using (1.38), the equation for the neutral velocity becomes

$$\frac{dU_N}{dz} = \frac{u_*^2}{\nu_o}\left(1 - \frac{z}{h}\right) \tag{2.52}$$

and therefore the neutral velocity can be expressed as :

$$U_N(z) = \frac{u_*^2}{\nu_o}\left(z - z_c + \frac{z_c^2 - z^2}{2h}\right) + U_{Nc} \tag{2.53}$$

where U_{Nc} is the neutral velocity at $z = z_c$.

Using (1.43) and introducing

$$p = \frac{w_s \alpha}{\nu_o} \tag{2.54}$$

the equation for the neutral concentration is :

$$\frac{dC_N}{dz} + pC_N = 0 \tag{2.55}$$

Integrating and introducing C_{Nc}, the neutral concentration at $z = z_c$, we obtain the neutral concentration

$$C_N(z) = C_{Nc} e^{-p(z-z_c)} \tag{2.56}$$

Flux Richardson Number

Using (2.6) and (2.51), the Flux Richardson Number can be written

$$R_f = \frac{g(s-1) w_s C \nu_o}{u_*^4 \left(1-\frac{z}{h}\right)^2 \left(1 + \frac{\beta g(s-1) w_s \nu_o}{u_*^4 \left(1-\frac{z}{h}\right)^2} C\right)} \tag{2.57}$$

Introducing

$$b = \frac{g(s-1) w_s \nu_o}{u_*^4} \tag{2.58}$$

this is equivalent to

$$R_f = \frac{bC}{\left(1-\frac{z}{h}\right)^2 + \beta b C} \tag{2.59}$$

and therefore

$$1 - \beta R_f = \frac{\left(1-\frac{z}{h}\right)^2}{\left(1-\frac{z}{h}\right)^2 + \beta b C}$$

Using (1.39), we obtain the stratified eddy viscosity

$$\nu_T = \nu_o \frac{\left(1-\frac{z}{h}\right)^2}{\left(1-\frac{z}{h}\right)^2 + \beta b C} \tag{2.60}$$

Stratified concentration in the Outer Layer Region

From (1.43), the equation for the concentration is:

$$\frac{dC}{dz} + \frac{w_s \alpha}{\nu_o} \left(1 + \frac{\beta b}{\left(1-\frac{z}{h}\right)^2} C\right) C = 0$$

Introducing $Q(z) = \frac{\beta b p}{\left(1-\frac{z}{h}\right)^2}$, this is equivalent to

$$C'(z) + pC + QC^2 = 0 \tag{2.61}$$

We recognize Ricatti's equation, which can be solved by introducing f such that $C = \frac{f'}{Qf}$ (see Appendix A). (2.61) is equivalent to

$$f'' + \left(p - \frac{Q'}{Q}\right) f' = 0$$

or

$$\frac{f''}{f'} = \frac{Q'}{Q} - p$$

Integrating once

$$ln\,|f'| = ln\,|Q| - pz + constant$$

or

$$f' = B_1 \frac{exp\,(-pz)}{\left(1 - \frac{z}{h}\right)^2} \tag{2.62}$$

where B_1 is a constant. Integrating (2.62) between z_c and z, we obtain :

$$f = B_1 \int_{z_c}^{z} \frac{exp\,(-pz')}{\left(1 - \frac{z'}{h}\right)^2} dz' + B_2$$

where B_2 is a constant. Introducing $B = \frac{B_2}{B_1}$, and using $C = \frac{f'}{Qf}$ we finally obtain for the concentration:

$$C\,(z) = \frac{exp\,(-pz)}{\beta bp \left(\int_{z_c}^{z} \frac{exp(-pz')}{\left(1-\frac{z'}{h}\right)^2} dz' + B\right)} \tag{2.63}$$

We introduce the function $W_c\,(z) = \int_{z_c}^{z} \frac{exp(-pz')}{\left(1-\frac{z'}{h}\right)^2} dz'$. Using the variable $x = p\,(h - z')$,

$$W_c\,(z) = h^2 p e^{-ph} \int_{p(z_c-h)}^{p(z-h)} \frac{e^{-x}}{x^2} dx$$

Since $h^2 p e^{-ph} \frac{e^{-x}}{x^2} > 0$ for all x, and $p\,(z-h) > p\,(z_c - h)$ for $z > z_c$, $W_c(z) > 0$ for $z > z_c$. Integrating by parts, we can express $W_c\,(z)$

$$W_c\,(z) = h^2 p e^{-ph} \left[\frac{e^{-p(z_c-h)}}{p\,(z_c-h)} - \frac{-e^{p(z-h)}}{p\,(z-h)} - E_i\,(p\,(z_c-h)) + E_i\,(p\,(z-h))\right] \tag{2.64}$$

where $E_i(z) = \int_z^\infty \frac{e^{-x}}{x} dx$.

Using $C(z_c) = C_c$, we finally obtain for the stratified concentration corresponding to constant neutral eddy viscosity

$$C(z) = \frac{C_c exp(-pz)}{exp(-pz_c) + C_c \beta bpW_c(z)} \tag{2.65}$$

The concentration is strictly positive between z_c and the water surface, $z = h$ and may alternatively be written

$$C(z) = C_c exp(-p(z - z_c)) \frac{1}{1 + C_c \beta bpW_c(z) exp(pz_c)}$$

$$= C_N(z) \frac{C_c}{C_{Nc}} \frac{1}{1 + C_c \beta bpW_c(z) exp(pz_c)} \tag{2.66}$$

where C_c and C_{Nc} are the stratified and neutral concentrations at $z = z_c$, respectively obtained by replacing z by z_c in equations (2.27) and (2.13). Since $C_c < C_{Nc}$ and therefore $C(z) < C_N(z)$ for $z > z_c$, stratification decreases the concentration compared to the neutral case. When $\beta \to 0$ in Equation (2.65), $C(z) \to C_N(z)$.

Stratified velocity in the Outer Layer Region

From (1.38) and (2.60), the equation for the velocity becomes

$$\frac{dU}{dz} = \frac{u_*^2}{\nu_o} \left(1 - \frac{z}{h} + \frac{\beta bC}{1 - \frac{z}{h}}\right) = \frac{dU_N}{dz} + \frac{dU_S}{dz} \tag{2.67}$$

where $\frac{dU_S}{dz} = \frac{u_*^2}{\nu_o} \frac{\beta bC}{1 - \frac{z}{h}}$.

With U_c, the velocity at $z = z_c$, integrating (2.67), we have the stratified velocity for a constant neutral eddy viscosity

$$U(z) = \frac{u_*^2}{\nu_o} \left(z - z_c + \frac{z_c^2 - z^2}{2h} + \int_{z_c}^{z} \frac{\beta bC}{1 - \frac{z'}{h}} dz'\right) + U_c = U_N(z) + U_S(z) \tag{2.68}$$

U_c can be written $U_{Nc} + U_{Sc}$, with U_{Sc} being the value of U_S at $z = z_c$, with U_S detailed in equation (2.30). As the concentration is positive , the term in the integral

is positive, and we integrate between z_c and $z \geq z_c$: $U_S(z)$ is positive, and $U(z) \geq U_N(z)$.

In the case where $z << h$, we can approximate $Q \approx \beta bp$ and therefore $f \approx B_1(B + \frac{e^{-pz_c} - e^{-pz}}{p})$. From $C(z) = \frac{f'(z)}{Q(z)f(z)}$, we therefore obtain for the concentration

$$C(z) \approx \frac{1}{\beta p\left(-1 + e^{-p(z_c - z)} + e^{pz} pB\right)}$$

Using the boundary condition $C(z_c) = C_c$, we obtain for B

$$B = \frac{1}{C_c \beta bpe^{pz_c}}$$

and therefore

$$C(z) \approx \frac{1}{\beta p\left(e^{-p(z_c - z)}\left(1 + \frac{1}{b\beta C_r}\right) - 1\right)} \tag{2.69}$$

In equation (2.68), we have

$$U(z) = \frac{u_*^2}{\nu_o}\left(z - z_c + \int_{z_c}^{z} \frac{\beta bC}{1 - \frac{z'}{h}} dz'\right) + U_c$$

$$= \frac{u_*^2}{\nu_o}\left(z - z_c + \int_{z_c}^{z} \frac{\beta b \frac{f'(z')}{Q(z')f(z')}}{1 - \frac{z'}{h}} dz'\right) + U_c$$

$$\approx \frac{u_*^2}{\nu_o}\left(z - z_c + \int_{z_c}^{z} \beta b \frac{f'(z')}{Q(z')f(z')} dz'\right) + U_c$$

$$\approx \frac{u_*^2}{\nu_o}\left(z - z_c + \int_{z_c}^{z} \beta b \frac{f'(z')}{pb\beta f(z')} dz'\right) + U_c$$

$$= \frac{u_*^2}{\nu_o}\left(z - z_c + \frac{1}{p} ln\left|\frac{f(z)}{f(z_c)}\right|\right) + U_c$$

Since $f(z) \approx B_1\left(B + \frac{e^{-pz_c} - e^{-pz}}{p}\right)$,

$$U(z) \approx \frac{u_*^2}{\nu_o}\left(z - z_c + \frac{1}{p} ln\left|\frac{e^{-pz_c} - e^{-pz} + pB}{pB}\right|\right) + U_c$$

$$U(z) \approx \frac{u_*^2}{\nu_o}\left(z - z_c + \frac{1}{p} ln\left|1 + C_c \beta b\left(1 - e^{-p(z - z_c)}\right)\right|\right) + U_c \tag{2.70}$$

2.4 Velocity profile and concentration distribution formulae over the entire water column

We solved the governing equations for velocity profile and sediment concentration distribution in a sediment-induced stratified flow under parabolic neutral eddy viscosity assumption and linear-constant neutral eddy viscosity assumption.

2.4.1 Parabolic neutral eddy viscosity model

Over the entire water column, the neutral eddy viscosity varies as :

$$\nu_{T_N} = \kappa u_* z \left(1 - \frac{z}{h}\right) \tag{2.71}$$

Neutral Profiles

- **Neutral Concentration Distribution**

Using Equation (2.13) from the previous sections with the boundary condition $C(z_r) = C_r$, the neutral concentration can be explicitly written

$$C_N(z) = C_r \left(\frac{(h-z)\, z_r}{(h-z_r)\, z}\right)^q, z_r < z \leq h \tag{2.72}$$

with q defined by (2.12).

- **Neutral Velocity Profile**

Using Equation (2.9), the boundary condition $U(z_o) = 0$ and $U(z)$ continuous at $z = z_r$, the neutral velocity profile is :

$$U_N(z) = \frac{u_*}{\kappa} ln \left(\frac{z}{z_o}\right), z_o < z \leq h \tag{2.73}$$

Stratified Profiles

- **Concentration Distribution**

Using Equation (2.27) from the previous sections with the boundary conditions $C(z_r) = C_r$, with q, a respectively defined by (2.12), (2.15), and $Z_r(z)$ given by

$$Z_r(z) = \frac{1}{h(q-1)}\left[\left(\frac{h}{z_r}-1\right)^{q-1} - \left(\frac{h}{z}-1\right)^{q-1}\right], q \neq 1$$

$$Z_r(z) = \frac{1}{h} ln\left|\frac{h/z_r - 1}{h/z - 1}\right| = \frac{1}{h} ln \frac{z(h-z_r)}{z_r(h-z)}, q = 1$$

we obtained the concentration distribution

$$C(z_r) = C_r$$

$$C(z) = \frac{(h-z)^q}{h^2 q \beta a z^q \left(Z_r(z) + \frac{(h-z_r)^q}{h^2 q \beta a C_r z_r^q}\right)} \tag{2.74}$$

- **Velocity Profile**

The stratified velocity can always be written as the sum of the neutral velocity and an additional term : $U(z) = U_N(z) + U_S(z)$ with $U_S(z) \geq 0$. Using Equation (2.30), the boundary conditions $U(z_o) = 0$, and $U(z)$ continuous at $z = z_r$, we finally obtained

$$U(z) = \frac{u_*}{\kappa} ln\left(\frac{z}{z_o}\right), z_o < z \leq z_r \tag{2.75}$$

$$U(z_r) = \frac{u_*}{\kappa} ln\left(\frac{z_r}{z_o}\right)$$

$$U(z) = \frac{u_*}{\kappa} ln\left(\frac{z}{z_o}\right) + \frac{u_* \beta a}{\kappa} \int_{z_r}^{z} \frac{C(z')}{1 - \frac{z'}{h}} dz', z_r < z \leq h \tag{2.76}$$

with $C(z)$ given by (2.74).

2.4.2 Linear-constant neutral eddy viscosity model

Over the entire water column, the neutral eddy viscosity varies as :

$$\nu_{T_N} = \kappa u_* z, z_o < z \leq z_c \tag{2.77}$$

$$\nu_{T_N} = \kappa u_* z_c = \nu_o, z_c \leq z \leq h \tag{2.78}$$

With $z_c = h/6 > z_r$.

Neutral Profiles

- **Neutral Concentration Distribution**

Using Equation (2.38) and (2.56) from the previous sections, with the boundary conditions $C(z_r) = C_r$ and $C(z)$ continuous at $z = z_c$, the neutral concentration can be explicitly written

$$C_N(z) = C_r \left(\frac{z_r}{z}\right)^q, z_r < z \leq z_c \tag{2.79}$$

$$C_{Nc} = C_N(z_c) = C_r \left(\frac{z_r}{z_c}\right)^q \tag{2.80}$$

$$C_N(z) = C_{Nc} exp\left(-p\left(z - z_c\right)\right), z_c \leq z \leq h \tag{2.81}$$

with q and p given by (2.12) and (2.54).

- **Neutral Velocity Profile**

Using Equations (2.37) and (2.53), the boundary condition $U(z_o) = 0$ with $z_o < z_c$, and $U(z)$ continuous at $z = z_r$ and $z = z_c$, the neutral velocity profile is :

$$U_N(z) = \frac{u_*}{\kappa} ln\left(\frac{z}{z_o}\right), z_o < z \leq z_c \tag{2.82}$$

$$U_N(z_c) = U_{Nc} = \frac{u_*}{\kappa} ln\left(\frac{z_c}{z_o}\right) \tag{2.83}$$

$$U_N(z) = \frac{u_*^2}{\nu_o}\left(z - z_c + \frac{z_c^2 - z^2}{2h}\right) + U_{Nc}, z_c \leq z \leq h \tag{2.84}$$

Stratified Profiles

- **Concentration Distribution**

Using equations (2.43), (2.45), and (2.65) from the previous sections, with the boundary conditions $C(z_r) = C_r$, $C(z)$ continuous at $z = z_c$, and introducing q, a, p, b defined by (2.12), (2.15), (2.54), (2.58), and $W_c(z)$ given by

$$W_c(z) = h^2 p e^{-ph}\left[\frac{e^{-p(z_c-h)}}{p(z_c-h)} - \frac{-e^{p(z-h)}}{p(z-h)} - E_i(p(z_c-h)) + E_i(p(z-h))\right]$$

where $E_i(z) = \int_z^\infty \frac{e^{-x}}{x}dx$, we finally obtained the concentration distribution

$$C(z_r) = C_r$$

$$C(z) = \frac{1}{\beta a z\left(ln\left(\frac{z}{z_r}\right) + \frac{1}{C_r \beta a z_r}\right)}, z_r \leq z \leq z_c, q = 1 \tag{2.85}$$

$$C(z) = \frac{1-q}{q\beta a\left(z + z_r^{-q}\left(\frac{1-q}{C_r q \beta a} - z_r\right) z^q\right)}, z_r \leq z \leq z_c, q \neq 1 \tag{2.86}$$

$$C(z_c) = \frac{1}{\beta a z_c\left(ln\left(\frac{z_c}{z_r}\right) + \frac{1}{C_r \beta a z_r}\right)} = C_c, q = 1 \tag{2.87}$$

$$C(z_c) = \frac{1-q}{q\beta a\left(z_c + z_r^{-q}\left(\frac{1-q}{C_r q \beta a} - z_r\right) z_c^q\right)} = C_c, q \neq 1 \tag{2.88}$$

$$C(z) = \frac{C_c exp(-pz)}{exp(-pz_c) + C_c \beta b p W_c(z)}, z_c \leq z \leq h \tag{2.89}$$

- **Velocity Profile**

The stratified velocity can always be written as the sum of the neutral velocity and an additional term : $U(z) = U_N(z) + U_S(z)$ with $U_S(z) \geq 0$. Using Equations (2.49), (2.50) and (2.68), the boundary conditions $U(z_o) = 0$ with $z_o < z_c$, and $U(z)$ continuous at $z = z_c$ and $z = z_r$, we finally obtained

$$U(z) = \frac{u_*}{\kappa} ln\left(\frac{z}{z_o}\right), z_o < z \leq z_r \tag{2.90}$$

$$U(z_r) = \frac{u_*}{\kappa} ln\left(\frac{z_r}{z_o}\right)$$

$$U(z) = \frac{u_*}{\kappa}\left(ln\left(\frac{z}{z_o}\right) + ln\left|C_r\beta a z_r ln\left(\frac{z}{z_r}\right) + 1\right|\right), z_r < z \leq z_c, q = 1 \tag{2.91}$$

$$U(z) = \frac{u_*}{\kappa} ln\left(\frac{z}{z_o}\right) + \frac{u_*}{\kappa q} ln\left|1 + \frac{C_r q \beta a z_r^q}{1-q}(z^{1-q} - z_r^{1-q})\right|, z_r < z \leq z_c, q \neq 1 \tag{2.92}$$

$$U(z_c) = \frac{u_*}{\kappa}\left(ln\left(\frac{z_c}{z_o}\right) + ln\left|C_r\beta a z_r ln\left(\frac{z_c}{z_r}\right) + 1\right|\right), q = 1 \tag{2.93}$$

$$U(z_c) = \frac{u_*}{\kappa} ln\left(\frac{z_c}{z_o}\right) + \frac{u_*}{\kappa q} ln\left|1 + \frac{C_r q \beta a z_r^q}{1-q}(z_c^{1-q} - z_r^{1-q})\right| = U_c = U_{Nc} + U_{Sc}, q \neq 1 \tag{2.94}$$

and

$$U(z) = \frac{u_*^2}{\nu_o}\left(z - z_c + \frac{z_c^2 - z^2}{2h} + \int_{z_c}^{z} \frac{\beta b C(z')}{1 - \frac{z'}{h}} dz'\right) + U_c, z_c \leq z \leq h \tag{2.95}$$

with $C(z)$ given by (2.89).

2.5 Bottom Boundary Layer

The formulae for the velocity contain integrals that require numerical evaluation. Explicit formulae can be derived in the bottom boundary layer, corresponding to the Inner Layer Region where $z << h$. We obtained approximate formulae for the velocity and the concentration by assuming $z << h$ and linearizing the exact formulae, in Sections 2.2.2. One should obtain the same formulae by assuming $z << h$ and linearizing the governing equations. Doing this, equation (1.38) becomes the law of the wall, i.e.

$$\nu_T \frac{dU}{dz} = u_*^2 \tag{2.96}$$

For the quadratic neutral eddy viscosity case, the assumption $z << h$ corresponds to the linear neutral eddy viscosity model and has therefore already been derived Section 2.3.1. In the following sections, we derive the approximate formulae for the constant neutral eddy viscosity case.

2.5.1 Neutral Eddy Viscosity

For the constant case, equation (2.51) becomes :

$$\nu_{TN} = \nu_o = \kappa u_* z_c \tag{2.97}$$

corresponding to a linear neutral velocity profile :

$$U_N(z) = \frac{u_*^2}{\kappa}(z - z_c) + U_{Nc} \tag{2.98}$$

2.5.2 Flux Richardson Number

For the constant neutral eddy viscosity case, using equation (2.59) and the assumption $z << h$ leads to:

$$R_f = \frac{bC}{1 + \beta bC} \tag{2.99}$$

2.5.3 Outer Layer Region

Using equations (1.39), (2.96) and (2.99) leads to:

$$\frac{dU}{dz} = \frac{u_*^2}{\nu_o}(1 + \beta bC) \tag{2.100}$$

Combining equations (1.43), (1.40) and (2.99) leads to :

$$\frac{dC}{dz} + P(z)\,C(z) + Q(z)\,C(z)^2 = 0 \tag{2.101}$$

With $P(z) = \frac{w_s \alpha}{\nu_o} = p$ and $Q(z) = \frac{b\beta w_s \alpha}{\nu_o} = b\beta p$. Introducing f with $C = \frac{f'}{Qf}$, equation (2.101) is equivalent to:

$$f''(z) + pf'(z) = 0 \tag{2.102}$$

And equation (2.100) becomes :

$$\frac{dU}{dz} = \frac{u_*^2}{\nu_o}\left(1 + \frac{f'}{pf}\right) \tag{2.103}$$

Integrating (2.102) once: $f'(z) = B_1 e^{-pz}$. Integrating again:

$$f(z) = -\frac{B_1}{p}\left(e^{-pz} + B\right)$$

with B_1 and B constant. Therefore,

$$C(z) = \frac{-1}{b\beta\left(1 + Be^{pz}\right)}$$

Using $C(z_c) = C_c$, we obtain $B = -e^{-pz_c}\left(1 + \frac{1}{b\beta C_c}\right)$ and

$$C(z) = \frac{1}{b\beta\left(e^{p(z-z_c)}\left(1 + \frac{1}{b\beta C_c}\right) - 1\right)} \tag{2.104}$$

This is the same expression as equation (2.69) obtained by linearizing equation (2.63). Integrating (2.103) with the boundary condition $U(z_c) = U_c$

$$\begin{aligned} U(z) &= \frac{u_*^2}{\nu_o}\left(z - z_c + \frac{1}{p} ln\left|\frac{f(z)}{f(z_c)}\right|\right) + U_c \\ &= \frac{u_*^2}{\nu_o}\left(z - z_c + \frac{1}{p} ln\left|\frac{e^{-pz} + B}{e^{-pz_c} + B}\right|\right) + U_c \\ &= \frac{u_*^2}{\nu_o}\left(z - z_c + \frac{1}{p} ln\left|1 + b\beta C_c\left(1 - e^{-p(z-z_c)}\right)\right|\right) + U_c \end{aligned} \tag{2.105}$$

and we obtain the same result as equation (2.70).

2.6 Example profiles

To show the effect of stratification on velocity profile and sediment concentration distribution, we compute a concrete example.

2.6.1 Comparison between neutral and stratified profiles

We first use the formulae with the parabolic neutral eddy viscosity, i.e. (2.74) and (2.75), (2.76) for the stratified concentration distribution and velocity profile, and (2.72) and (2.73) for the neutral concentration distribution and velocity profile. We plot profiles for $U(z)$ and $C(z)$ for stratified and neutral cases, taking for this example $\beta = 4$, $\alpha = 1$, $\kappa = 0.4$, $g = 9.8\ m^2/s$, $s = 2.65$, $h = 16\ cm$, $u_* = 5\ cm/s$, $z_o = 0.01\ mm$, $w_s = 2\ cm/s$, $C_r = 0.01\ cm^3/cm^3$, $z_r = 2\ mm$. The results are shown in Figures 2-1 and 2-2. On Figure 2-1, we also show the stratified concentration distribution and velocity profile obtained when taking $\alpha = 0.8$ instead of $\alpha = 1$. Stratification

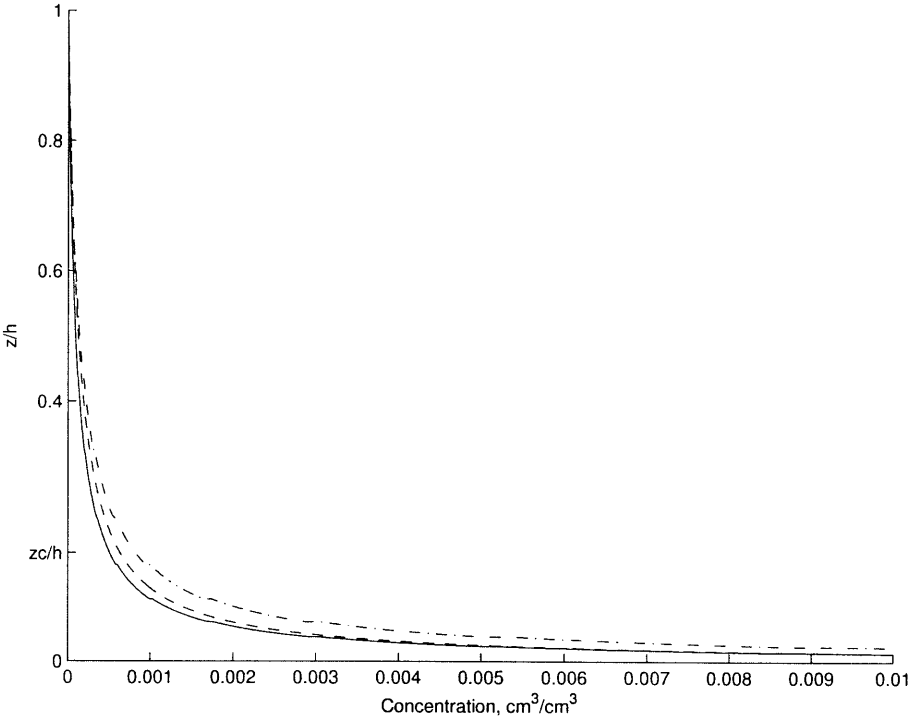

Figure 2-1: Concentration profile for stratified (Equation (2.74)) and neutral (Equation (2.72)) steady uniform sediment laden flows in an open wide channel, with $\beta = 4$, $\kappa = 0.4$, $g = 9.8\ m^2/s$, $s = 2.65$, $h = 16\ cm$, $u_* = 5\ cm/s$, $z_o = 0.01\ mm$, $w_s = 2\ cm/s$, $C_r = 0.01\ cm^3/cm^3$, $z_r = 2\ mm$. Dashed line: neutral with $\alpha = 1$; Plain line: stratified with $\alpha = 1$; Dashed-dotted line: stratified with $\alpha = 0.8$

decreases the eddy diffusivity ν_S compared to the neutral case. This is expressed in equation (1.40), where the Richardson Number R_f and the constant β, both positive, account for stratification. From the governing equation (1.43), everything else being

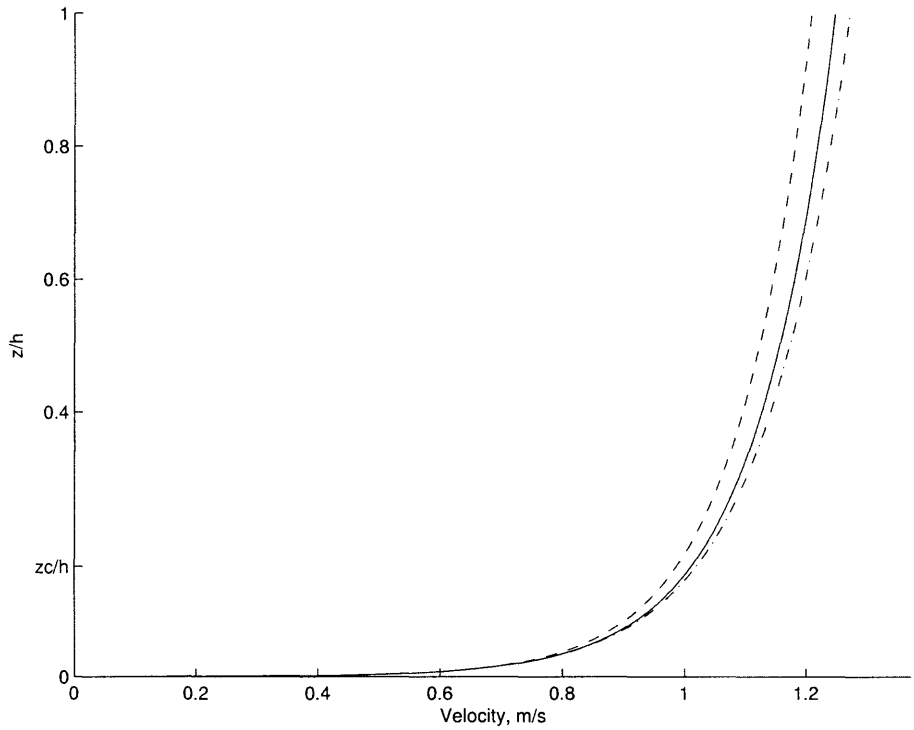

Figure 2-2: Velocity profile for stratified (Equations(2.75) and (2.76)) and neutral (Equation (2.73)) steady uniform sediment laden flows in an open wide channel, with $\beta = 4$, $\kappa = 0.4$, $g = 9.8\ m^2/s$, $s = 2.65$, $h = 16\ cm$, $u_* = 5\ cm/s$, $z_o = 0.01\ mm$, $w_s = 2\ cm/s$, $C_r = 0.01\ cm^3/cm^3$, $z_r = 2\ mm$. Dashed line: neutral with $\alpha = 1$; Plain line: stratified with $\alpha = 1$; Dashed-dotted line: stratified with $\alpha = 0.8$

equal, particularly the roughness z_o and the reference concentration C_r, stratification should therefore result in an decrease of the concentration compared to the neutral case. This effect can be observed in Figure 2-1. Moreover, as assumed when invoking the continuum hypothesis, the concentration is of the order of $10^{-3}cm^3/cm^3$ in most of the boundary layer. However, if there is a difference between α for the neutral case and α for the stratified case (for example $\alpha = 0.8$ for the neutral case and $\alpha = 1$ for the stratified case), everything else being equal, the stratified concentration can be larger than the neutral concentration (Figure 2-1).

Stratification also decreases the eddy viscosity ν_T, which is expressed in equation (1.39), due to the contribution of the Flux Richardson Number and the constant β. From the governing equation (1.38), everything else being equal, stratification should therefore result in an increase of velocity compared to the neutral case. This effect

can be observed in Figure 2-2. We obtain a larger stratified concentration for $\alpha = 0.8$ than for $\alpha = 1$ (Figure 2-1) and hence a smaller eddy viscosity. Thus, a difference between α for the neutral case and α for the stratified case (for example $\alpha = 0.8$ for the neutral case and $\alpha = 1$ for the stratified case), everything else being equal, can therefore result in an even larger difference between the stratified and the neutral velocity profiles, as seen in Figure 2-2.

From Figures 2-1 and 2-2, we can observe that most of the effect due to stratification comes from the near-bottom region, between $z = z_o$ and $z \approx 0.4h$.

2.6.2 Comparison between profiles obtained with parabolic and linear-constant neutral eddy viscosity

In this section, we compare the velocity and concentration profiles obtained with the parabolic neutral eddy viscosity model and with the simplified linear-constant neutral eddy viscosity model between the channel bottom and $z = 0.4h$. For the stratified velocity profiles, we use respectively the formulae with the parabolic neutral eddy viscosity (Equations (2.75), (2.76)) and the formulae with the constant-linear eddy viscosity (Equations (2.90), (2.91), (2.92), (2.93), (2.94) and (2.95)). For the stratified concentration distribution, we use respectively the formula with the parabolic neutral eddy viscosity model (Equation (2.74)) and the formulae with the constant-linear eddy viscosity model (Equations (2.85), (2.86), (2.87), (2.88) and (2.89)). For the neutral velocity profiles, we use respectively the formula with the parabolic neutral eddy viscosity model (Equation (2.73))and the formulae with the constant-linear eddy viscosity model (Equations (2.82), (2.83) and (2.84)). For the neutral concentration distribution, we use respectively the formula with the parabolic neutral eddy viscosity (Equation (2.72)) and the formulae with the constant-linear eddy viscosity (Equations (2.79), (2.80) and (2.81)). The results are presented in Figures 2-3, 2-4, 2-5 and 2-6.

For the concentration, the difference between the simplified and parabolic model looks

negligible (see Figures 2-3 and 2-4). However, since we obtained a closed-form equation (2.74) for the parabolic neutral eddy viscosity model, using the simplified model rather than the parabolic model does not really have an advantage. For the velocity, the difference between the parabolic model and the simplified model is extremely small between the $z = z_o$ and $z = z_c$, but becomes larger above $z = z_c$ (see Figures 2-5 and 2-6). However, the simplified model is less computer-time consuming than the parabolic model since in the Inner Layer region, formulae (2.91), (2.92), (2.93) and (2.94) do not require numerical computation contrary to formulae (2.76). Therefore, using the simplified model for the velocity in the Inner Layer Region provides a good estimate of the velocity and has a computer-time advantage. However, using the simplified model above $z = z_c$ does not provide a very accurate estimate of the velocity.

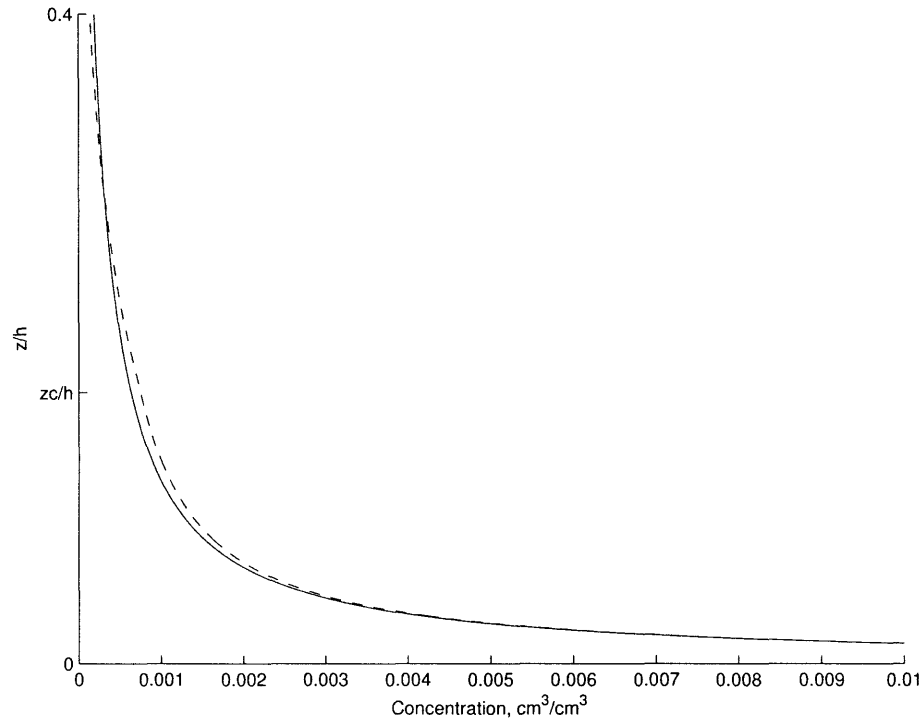

Figure 2-3: Comparison between neutral concentration profiles for steady uniform sediment laden flows in an open wide channel with parabolic neutral eddy viscosity (Equation (2.72)) and with linear-constant neutral eddy viscosity (Equations (2.79), (2.80) and (2.81)). $\alpha = 1$, $\kappa = 0.4$, $g = 9.8\ m^2/s$, $s = 2.65$, $h = 16\ cm$, $u_* = 5\ cm/s$, $z_o = 0.01\ mm$, $w_s = 2\ cm/s$, $C_r = 0.01\ cm^3/cm^3$, $z_r = 2\ mm$. Dashed line: linear-constant neutral eddy viscosity ; Plain line: parabolic neutral eddy viscosity

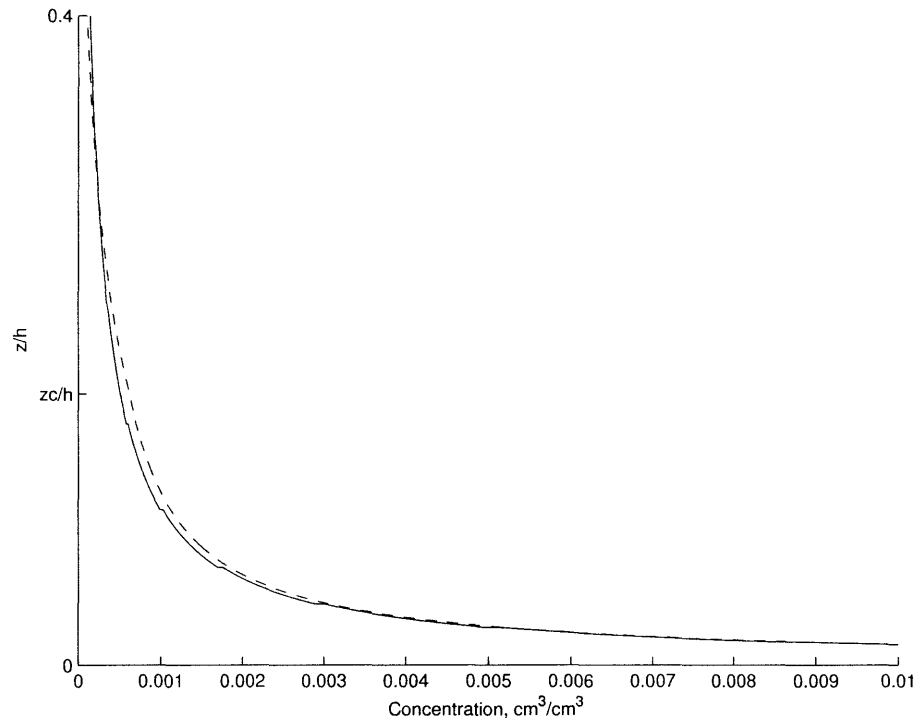

Figure 2-4: Comparison between stratified concentration profiles for steady uniform sediment laden flows in an open wide channel with parabolic neutral eddy viscosity (Equation (2.74)) and with linear-constant neutral eddy viscosity (Equations (2.85), (2.86), (2.87), (2.88) and (2.89)). $\alpha = 1$, $\kappa = 0.4$, $g = 9.8\ m^2/s$, $s = 2.65$, $h = 16\ cm$, $u_* = 5\ cm/s$, $z_o = 0.01\ mm$, $w_s = 2\ cm/s$, $C_r = 0.01\ cm^3/cm^3$, $z_r = 2\ mm$. Dashed line: linear-constant neutral eddy viscosity ; Plain line: parabolic neutral eddy viscosity

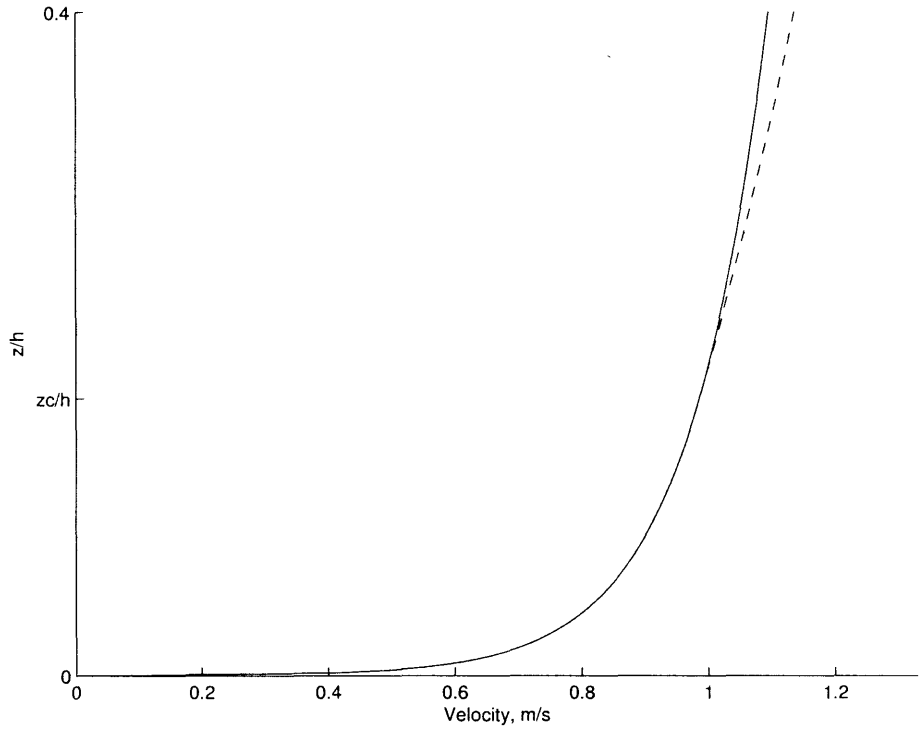

Figure 2-5: Comparison between neutral velocity profiles for steady uniform sediment laden flows in an open wide channel with parabolic neutral eddy viscosity (Equation (2.73)) and with linear-constant neutral eddy viscosity (Equations (2.82), (2.83) and (2.84)). $\alpha = 1$, $\kappa = 0.4$, $g = 9.8\ m^2/s$, $s = 2.65$, $h = 16\ cm$, $u_* = 5\ cm/s$, $z_o = 0.01\ mm$, $w_s = 2\ cm/s$, $C_r = 0.01\ cm^3/cm^3$, $z_r = 2\ mm$. Dashed line: linear-constant neutral eddy viscosity ; Plain line: parabolic neutral eddy viscosity

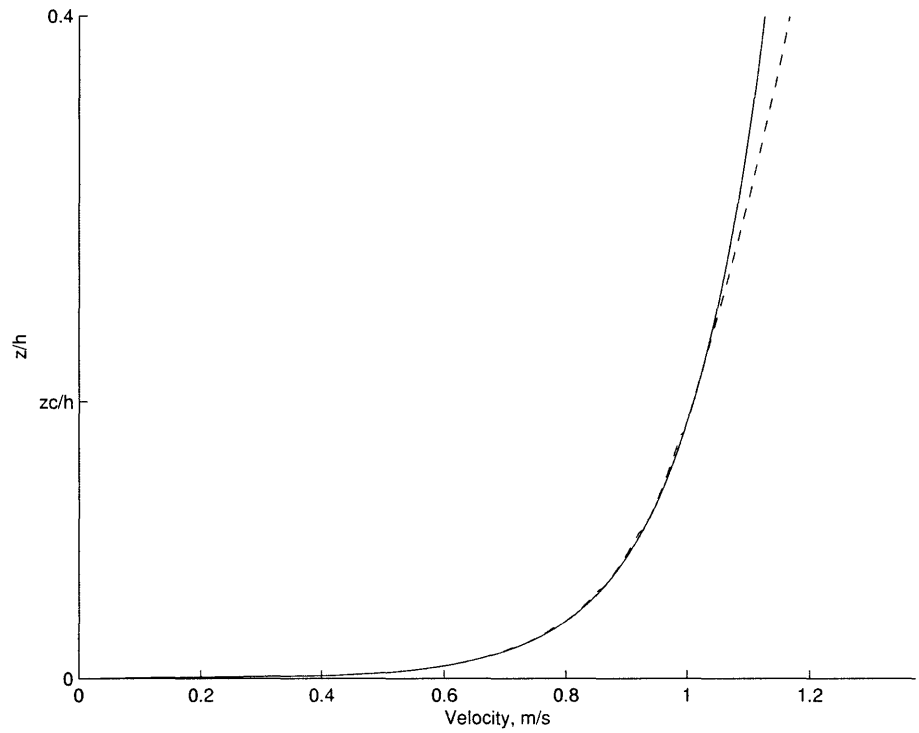

Figure 2-6: Comparison between stratified velocity profiles for steady uniform sediment laden flows in an open wide channel with parabolic neutral eddy viscosity (Equations (2.75) and (2.76)) and with linear-constant neutral eddy viscosity (Equations (2.90), (2.91), (2.92), (2.93), (2.94) and (2.95)). $\alpha = 1$, $\kappa = 0.4$, $g = 9.8\ m^2/s$, $s = 2.65$, $h = 16\ cm$, $u_* = 5\ cm/s$, $z_o = 0.01\ mm$, $w_s = 2\ cm/s$, $C_r = 0.01\ cm^3/cm^3$, $z_r = 2\ mm$. Dashed line: linear-constant neutral eddy viscosity ; Plain line: parabolic neutral eddy viscosity

Chapter 3

Determination of the Stratification Parameters

In Chapter 2, we introduced the effect of stratification on a turbulent flow of water loaded with sediment in a rectangular channel with constant bottom slope, and expressed this effect in terms of two constants α and β. α is the ratio of the eddy viscosity ν_T to the eddy diffusivity ν_S (Equation (1.41)), and β accounts for stratification in the expression of the eddy viscosity and eddy diffusivity (Equations (1.39) and (1.40)): $\nu_T = \nu_{TN}(1 - \beta_u R_f)$ and $\nu_S = \nu_{SN}(1 - \beta_c R_f)$. In this section, we present an analysis of experimental data, based on our theory, to obtain best choice values for these parameters.

3.1 Description of experimental data sets

To calibrate of our model, we use experimental data sets reported by Vanoni (1946) Vanoni and Nomicos (1956) [21], Einstein and Chien (1955) [7], Lyn (1986) [16], Barton and Lin (1955) [2], Brooks (1954) [3], and Coleman (1981) and (1986) [4],[5]. In those experiments, velocity and concentration profiles were measured in laboratory channels over plane beds. These measurements were reported, as well as the water depth h, the settling velocity w_s, the shear velocity u_*, the grain diameter d, in data sets which were generously provided by John Trowbridge (of Villaret & Trowbdridge

(1991) [30]). Only the experiments in which the bed remains flat are considered. There are two types of experiments: "starved-bed" experiments and "equilibrium-bed" experiments. In "starved-bed" experiments, no sand-bed is present, the water flows either over a smooth bottom or over a bottom to which sand particles have been previously glued. In starved-bed experiments, the experimenter introduces sediments in the flow and stops the experiments as soon as sand-bed formation is observed. In "equilibrium-bed" experiments, sediments are provided by the sand-bed, the experimenter begins to take measurements once the equilibrium between the flow and the sand-bed has been established. All investigators use quartz sediment in water, so $s = \frac{\rho_s}{\rho} = 2.65$

3.1.1 Measurements of concentration and velocity

All the investigators used Pitot tubes to measure ensemble averaged velocity U at different elevations z, with the exception of Lyn, who used a two-axis laser-Doppler velocimeter (LDV). In all experiments, ensemble averaged concentration C was measured by means of suction, i.e. suspended sediment samples were taken at different elevations z, dried and weighed in order to determine concentration. The shear velocity u_* was measured from measurements of the depth h and the bottom slope S by using the cross-sectionally integrated momentum balance (1.6): $\tau_o = \rho g R S$ where ρg is the specific weight of the fluid, R is the hydraulic radius equal to the water depth h for a wide rectangular channel and S is the channel slope), with appropriate correction for sidewall friction. Lyn (1986) [16] also conducted LDV measurements of the Reynolds shear stress at the centerline of his channel.

3.1.2 Settling velocity w_s

To measure or compute the sediment settling velocity, w_s, the experimenters used different methods: some of them used experimental methods (e.g. Einstein and Chien), whereas others used graphs or formulae (Lyn). To be scientifically consistent, we need to use a settling velocity obtained by the same method for every experiment.

Table 3.1: Kinematic viscosity for different temperatures

temperature ($°C$)	15	20	25
kinematic viscosity (m^2/s)	$1.14 \cdot 10^{-6}$	$1.0 \cdot 10^{-6}$	$8.96 \cdot 10^{-7}$

Therefore, we use the recent formula for natural sands by Jiménez and Madsen (2003) [14]

$$w_s = W_* \sqrt{(s-1)gd} \tag{3.1}$$

where W_* is the dimensionless settling velocity. Jiménez and Madsen express the dimensionless settling velocity as

$$\frac{1}{W_*} = A + \frac{B}{S_*} \tag{3.2}$$

where S_* is the fluid-sediment parameter introduced by Madsen and Grant (1976), given by:

$$S_* = \frac{d}{4\nu} \sqrt{(s-1)gd} \tag{3.3}$$

with ν being the kinematic viscosity of the fluid and d_n being the nominal sand grain diameter, $d = d_n = d_{sieve}/0.9$. A and B are two coefficient which depend on shape, size and roundness of the sediment grain. For natural quartz sediments, and $S_* \in [0.5, 30]$, typical values for A and B are $A = 0.954$ and $B = 5.121$.

The water's kinematic viscosity depends on the temperature. When the temperature is known, we extrapolate linearly ν from values at $15°C$, $20°C$ and $25°C$ (see Table 3.1). When the temperature of the water was not specified, we assumed it to be approximately equal to $20°C$ and therefore took $\nu = 1.0 \cdot 10^{-6} m^2/s$.

Using equations (3.1), (3.2) and (3.3), we obtain settling velocities similar to those provided by the experimenters: $w_s = (0.92 \pm 0.10) w_{s,s}$ where $w_{s,s}$ is the settling velocity specified by the investigator. The flow and sediment parameters for each experiment are presented in Table B.1 (see Appendix B). In the following analysis, we also use: $\kappa = 0.4$, $g = 9.8 m/s^2$ and $s = 2.65$ (all sediments are quartz and the fluid is water).

3.2 Analysis

The data listed in Table B.1 are first used to determine α and β. The most convenient and consistent choice of reference elevation z_r for the reference concentration C_r would be one that separates the water column into two regions so that sediment transport may be regarded as bed load below z_r and as suspended load above z_r. This suggests z_r to be related to the thickness of the bed load layer, which may be approximated as a multiple of the grain diameter (Madsen (1991) [17]). For this reason, the reference elevation $z_r = 7d = 7d_n$ is adopted here.

It has been observed in Section 2.6 that the effects of stratification seem to occur mainly in the lower layer between the bottom and $z = 0.4h$. Moreover, we expect the data in the upper layer to be influenced by wake and sidewalls effects. We therefore consider only data obtained in the lower layer corresponding to $z \leq 0.4h$.

For a given choice of α and β, the reference concentration C_r remains the only unknown in equations (2.79), (2.80) and(2.81) or (2.85), (2.86), (2.87), (2.88) and(2.89). In order to determine it, we vary C_r in order to minimize the variance

$$\epsilon_c(\alpha, \beta) = \frac{1}{N} \sum_{1}^{N} \left(\frac{C_{predicted} - C_{measured}}{C_{predicted}} \right)^2 \tag{3.4}$$

where $C_{measured}$ is the measured concentration reported in the data set, $C_{predicted}$ corresponds to the concentration predicted by our model at every measurement point and N is the number of considered data points. $\epsilon_c(\alpha, \beta)$ is computed for a wide range of C_r, and we obtain a first $C_{r,min,1}$. The computation is repeated for a finer range of C_r around $C_{r,min,1}$. We then obtain a second $C_{r,min,2}$. This process is repeated five times, and we finally obtain a $C_{r,min}$ with a sufficient precision (with at least four significant digits).

For our given choice of α and β, once C_r has been determined, the concentration can be calculated over the entire depth using equations (2.79), (2.80) and(2.81) or equations (2.85), (2.86), (2.87), (2.88) and(2.89). With the best value of C_r, the stratified concentration can also be integrated numerically, in order to compute the velocity. In the velocity equations (2.82), (2.83), (2.84), or(2.91), (2.92), (2.93), (2.94)

and (2.95), z_o is still unknown. Keeping the same α and β, we use the same method as previously outlined for C_r and obtain the best z_o by minimizing the variance

$$\epsilon_u(\alpha,\beta) = \frac{1}{N}\sum_{1}^{N}\left(\frac{U_{predicted} - U_{measured}}{U_{predicted}}\right)^2 \tag{3.5}$$

We finally obtain a $z_{o,min}$ with a sufficient precision (with at least three significant digits). Introducing this value of z_o in equations (2.82), (2.83), (2.84), or (2.91), (2.92), (2.93), (2.94) and (2.95), we are then able to compute the velocity over the entire depth.

We define relative errors for a given experiment, where the neutral case $\alpha = 1$ and $\beta = 0$ is used as the reference: for each data set, the relative error for the concentration is defined by

$$\epsilon_{c,rel}(\alpha,\beta) = \frac{\epsilon_c(\alpha,\beta)}{\epsilon_c(1,0)} \tag{3.6}$$

Similarly, the relative error for the velocity is defined by

$$\epsilon_{u,rel}(\alpha,\beta) = \frac{\epsilon_u(\alpha,\beta)}{\epsilon_u(1,0)} \tag{3.7}$$

For each couple $[\alpha,\beta]$, we define the absolute average error for the concentration

$$\overline{\epsilon_{c,abs}}(\alpha,\beta) = \sqrt[N_e]{\prod_{N_e}\epsilon_c(\alpha,\beta)} \tag{3.8}$$

and for the velocity

$$\overline{\epsilon_{u,abs}}(\alpha,\beta) = \sqrt[N_e]{\prod_{N_e}\epsilon_u(\alpha,\beta)} \tag{3.9}$$

where N_e is the number of experiments that are considered in our analysis. We also define an average relative error for the concentration

$$\overline{\epsilon_{c,rel}}(\alpha,\beta) = \sqrt[N_e]{\prod_{N_e}\epsilon_{c,rel}(\alpha,\beta)} \tag{3.10}$$

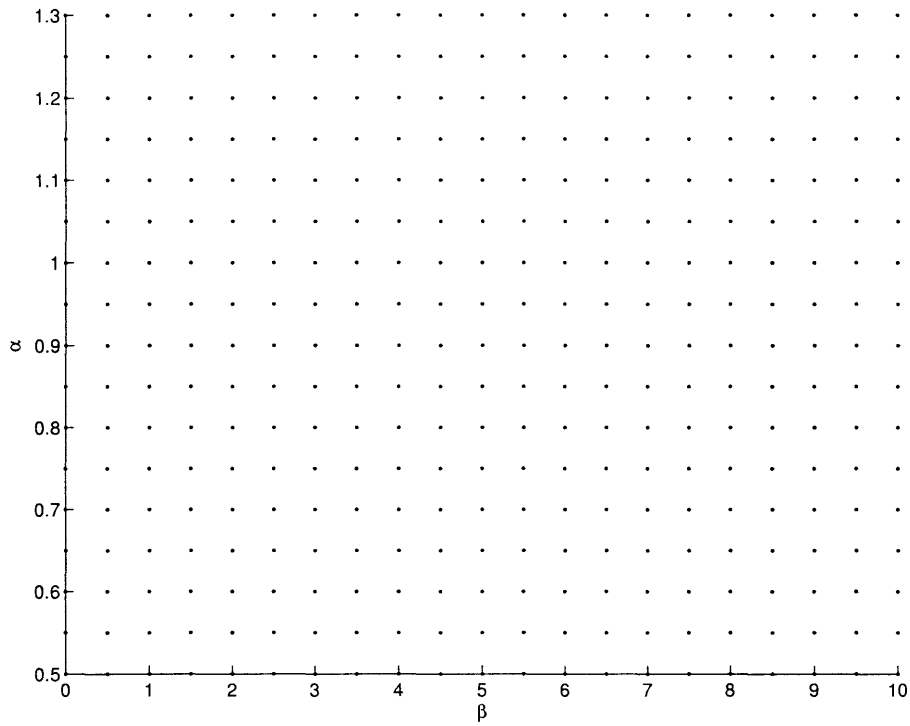

Figure 3-1: Computational $[\alpha, \beta]$ grid-space for absolute and relative errors

and for the velocity

$$\overline{\epsilon_{u,rel}}(\alpha, \beta) = \sqrt[N_e]{\prod_{N_e} \epsilon_{u,rel}(\alpha, \beta)} \tag{3.11}$$

Finally, we also define a "combined" average relative error

$$\overline{\epsilon_{rel}}(\alpha, \beta) = \sqrt[N_e]{\prod_{N_e} \sqrt{\epsilon_{u,rel}(\alpha, \beta)\epsilon_{c,rel}(\alpha, \beta)}} \tag{3.12}$$

Optimal values of the fitting parameters C_r and z_o are computed for every couple of $[\alpha, \beta]$ for $0.5 \leq \alpha \leq 1.3$ with 0.05 intervals and $0 \leq \beta \leq 10$ with 0.5 intervals for stratified cases and $\beta = 0$ for neutral cases. From these computations, we first obtain for each experiment a best couple $[\alpha_c, \beta_c]$ which minimizes the error ϵ_c as defined by (3.4), a best couple $[\alpha_u, \beta_u]$ which minimizes the error ϵ_u as defined by (3.5), and a best couple $[\alpha, \beta]$ which minimizes the product of errors $\epsilon_u \epsilon_c$ (see Table C.1 in Appendix C).

The reference case is defined as the results obtained for the neutral case $[\alpha, \beta]$=[1,0].

All the cases where values of C_r obtained for the neutral reference case are not physically consistent are eliminated from our study. Our consistency criteria is $C_r < C_{r,cr} = 0.1$. The eliminated experiments are: all Coleman (1981) [4] coarse sand experiments and runs 05, 12, 13, 14, 15, 16 by Einstein and Chien (1955) [7] (see Table B.1 in Appendix B).

From these computations, we have the values of the absolute errors $\overline{\epsilon_{c,abs}}(\alpha, \beta)$ as defined by Equation (3.8) and $\overline{\epsilon_{u,abs}}(\alpha, \beta)$ as defined by Equation (3.9) for the points in the $[\alpha, \beta]$ grid-space shown in Figure 3-1. These absolute errors are actually variances, and their square root is the standard deviation. To have an idea about the magnitude of the error, we first plot the contours (using Matlab) for $\overline{\epsilon_{c,abs}}(\alpha, \beta)$ and $\overline{\epsilon_{u,abs}}(\alpha, \beta)$. This is done in Figures 3-2 and 3-3. The absolute error for the concentration is minimum and approximately 13% for $[\alpha, \beta] = [0.8, 4]$. This means that the average difference between the predicted concentration and the observed concentration is roughly $\sqrt{0.13} = 36\%$ of the predicted value. For the velocity, the minimum error being approximately 2.6% for $\beta = 4$, the difference between the predicted velocity and the observed velocity is $\sqrt{0.026} = 16\%$ of the predicted value. Once again, we observe that the value of α does not have a strong influence on the velocity prediction.The model seems to predict more accurately the velocity than the concentration. For the neutral case, which correponds to $\beta = 0$ in Figure 3-2, the minimum for the absolute concentration error occurs at $\alpha = 1$, with an absolute average concentration error of approximately 15%. This means that the difference between the predicted concentration and the observed concentration is $\sqrt{0.15} = 39\%$ of the predicted value. The velocity does not depend on α, as can be seen in equations (2.82), (2.83)and (2.84). The absolute average error for the velocity in the neutral case is approximately 4.2%, roughly a relative error of $\sqrt{0.042} = 20\%$. From these computations, we also have the values of $\overline{\epsilon_{c,rel}}(\alpha, \beta)$, $\overline{\epsilon_{u,rel}}(\alpha, \beta)$, and $\overline{\epsilon_{rel}}(\alpha, \beta)$, as defined by Equation (3.10), (3.11) and (3.12), for the points in the $[\alpha, \beta]$ grid-space shown in Figure 3-1. Using Matlab, we can compute and plot the contours of these functions. We observe a minimum for the average relative error $\overline{\epsilon_{rel}}(\alpha, \beta)$ for $[\alpha, \beta] \approx [0.8, 4]$. We can then plot a precise contour of the average error $\overline{\epsilon_{rel}}(\alpha, \beta)$, the average concentration error

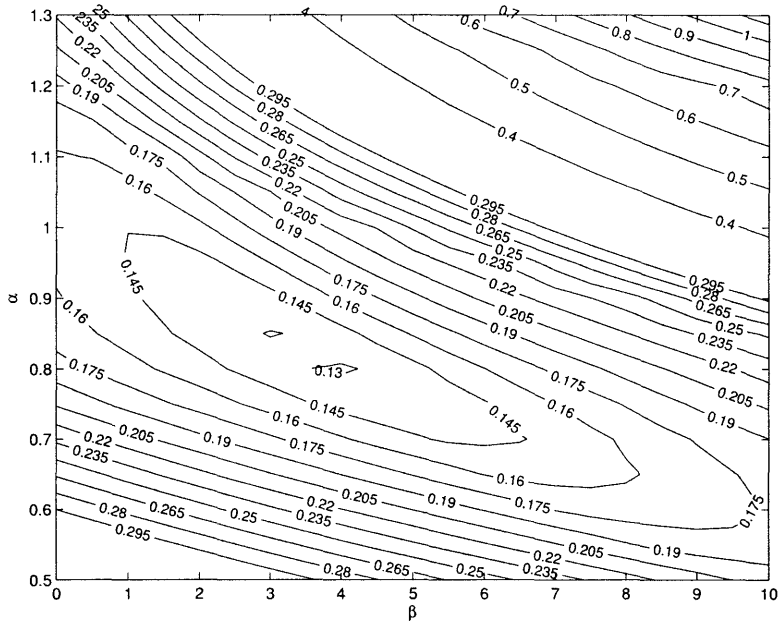

Figure 3-2: Contours of the absolute error (or variance) for the concentration $\overline{\epsilon_{c,abs}}(\alpha, \beta)$ as defined by Equation (3.8)

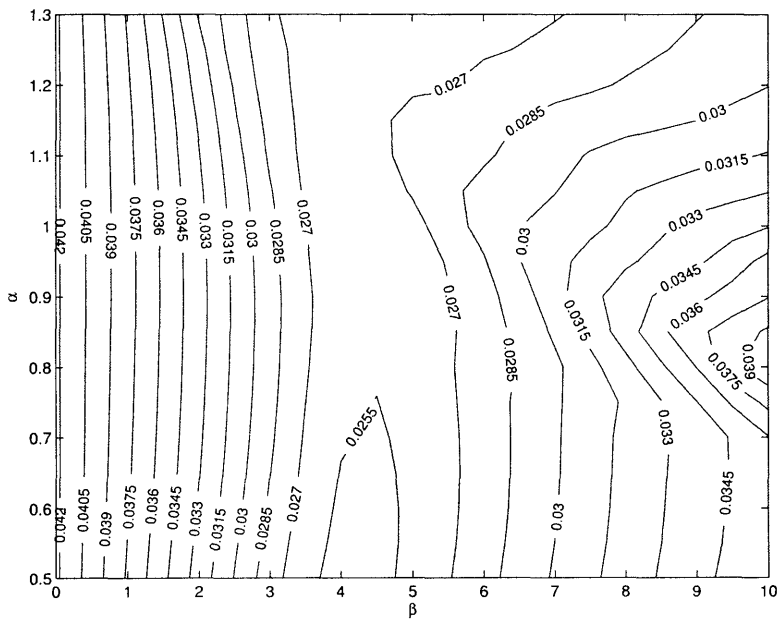

Figure 3-3: Contours of the absolute error (or variance) for the velocity $\overline{\epsilon_{u,abs}}(\alpha, \beta)$ as defined by Equation (3.9)

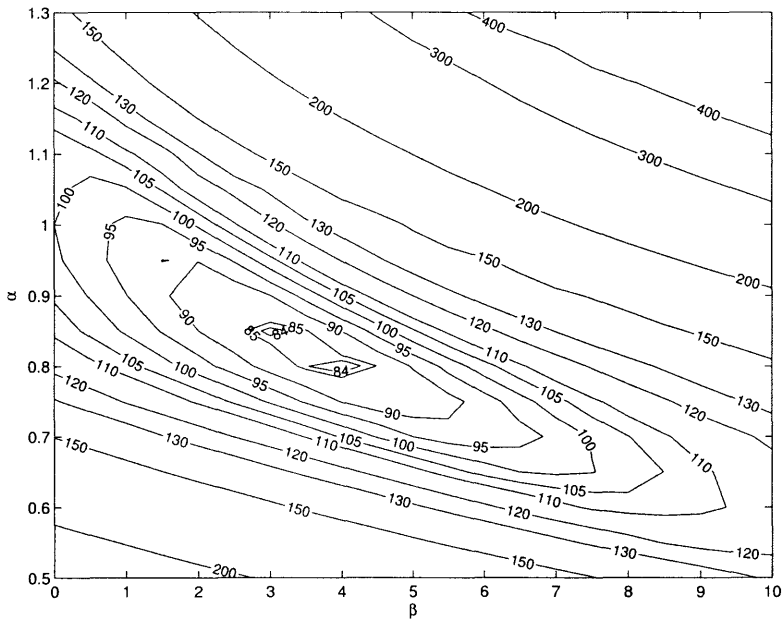

Figure 3-4: Contours of the relative error for the concentration $\overline{\epsilon_{c,rel}}(\alpha, \beta)$ (in percent) as defined by Equation (3.10)

$\overline{\epsilon_{c,rel}}(\alpha, \beta)$ and the average velocity error $\overline{\epsilon_{u,rel}}(\alpha, \beta)$. This is done in Figures 3-4, 3-5 and 3-6. The relative concentration error $\overline{\epsilon_{c,rel}}(\alpha, \beta)$ (which is a ratio of variances) is also mimimum, and equal to 84% for $[\alpha, \beta]$=[0.8,4] as seen from Figure 3-4. For the velocity, we observe in Figure 3-5 a miminum valley of $\overline{\epsilon_{u,rel}}(\alpha, \beta)$ for $\beta = 4$, and the error decreases very slowly as α decreases: the influence of β on the velocity seems to be much more important than the influence of α. This relative error corresponds to a 9% improvement of the concentration prediction compared to the neutral case. The relative error for the velocity is approximately 60%, and corresponds to a 22% improvement of the velocity prediction compared to the neutral case. Villaret and Trowbridge (1991) [30] only examined velocity profiles in order to determine the values of α and β. Since the velocity prediction accuracy does not seem to depend a lot on α, this partially explains why they were not able to obtain definitive results regarding α.

The minimum of the relative average error $\overline{\epsilon_{rel}}(\alpha, \beta)$ is obtained for $[\alpha, \beta]$=[0.8,4], as

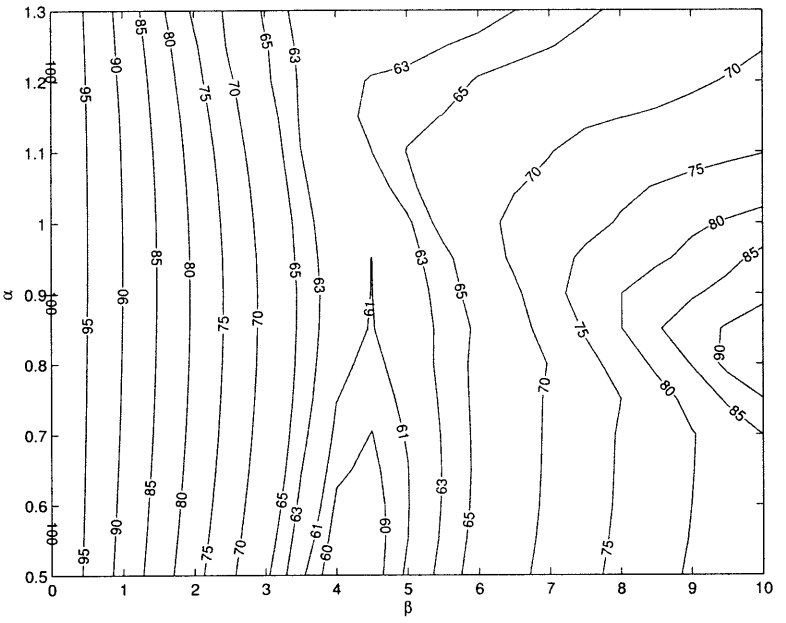

Figure 3-5: Contours of the relative error for the velocity $\overline{\epsilon_{u,rel}}(\alpha, \beta)$ (in percent) as defined by Equation (3.11)

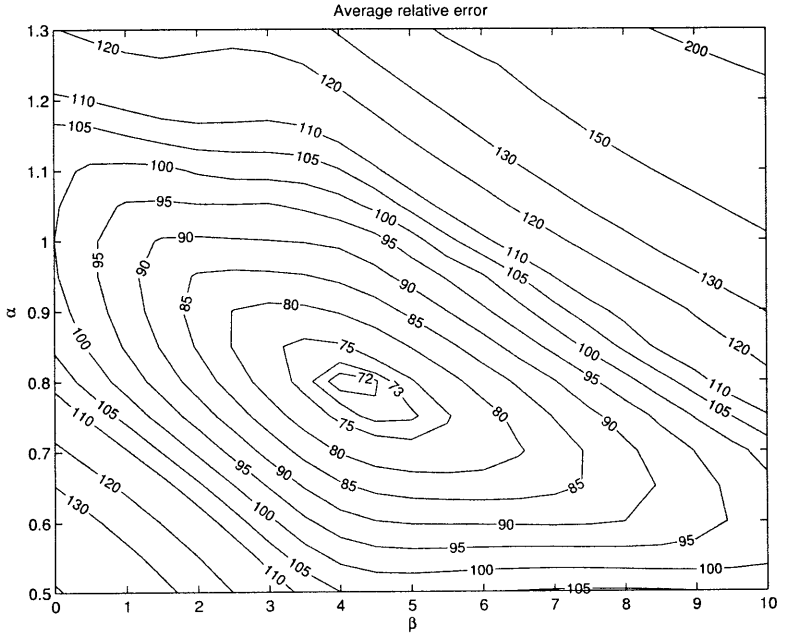

Figure 3-6: Contours of the relative average error $\overline{\epsilon_{rel}}(\alpha, \beta)$ (in percent) as defined by Equation (3.12)

seen from Figure 3-6, and corresponds to an average error of approximately 70%, i.e. an improvement of roughly 16% of the overal prediction capability of the stratification model with $[\alpha, \beta]$=[0.8,4] compared to the neutral case.

3.3 The starved-bed experiment bottom roughness variability

Coleman ran 20 fine sand experiments, keeping the shear stress constant and increasing the sediment load between each run (Coleman, 1981 [4] and Table B.1). Coleman's experiments are all starved bed experiments, with sediment laden water flowing over a plexiglas bottom. For both stratified and neutral cases, it can be observed that the roughness z_o increases with the reference concentration C_r (see Figures 3-7 and 3-8). This can be physically interpreted: the larger C_r is, the more the flow is loaded with sediments, and the larger the near-bottom concentration is. Near the bottom, each sand particle that hits the plexiglas bottom does not bounce elastically, but drags along the bottom a little while before returning to the flow. If the bottom concentration is larger, the number of particles that hit the bottom is also larger, and the particle-induced drag is therefore more important. In practice, this results in a larger bottom roughness, i.e. an increase of z_o. The velocity profile will therefore be influenced by this phenomenon: for a given sediment grain size, we expect the bottom roughness z_o to vary when the sediment load varies. Villaret and Trowbridge (1991) [30] attributed the shift between the neutral velocity profile and the stratified velocity profile solely to the stratification effect, and the bottom roughness for a given sediment size was considered constant in their analysis. Actually, there are two effects: the stratification effect and the bed roughness effect as explained above. Run 20 is the run with the largest amount of sediment in suspension, and consequently with the highest C_r. In Figure 3-9, we show clear water run and run 20 velocity data from Coleman (1981) [4]. We first fit the clear water velocity data between the bed and

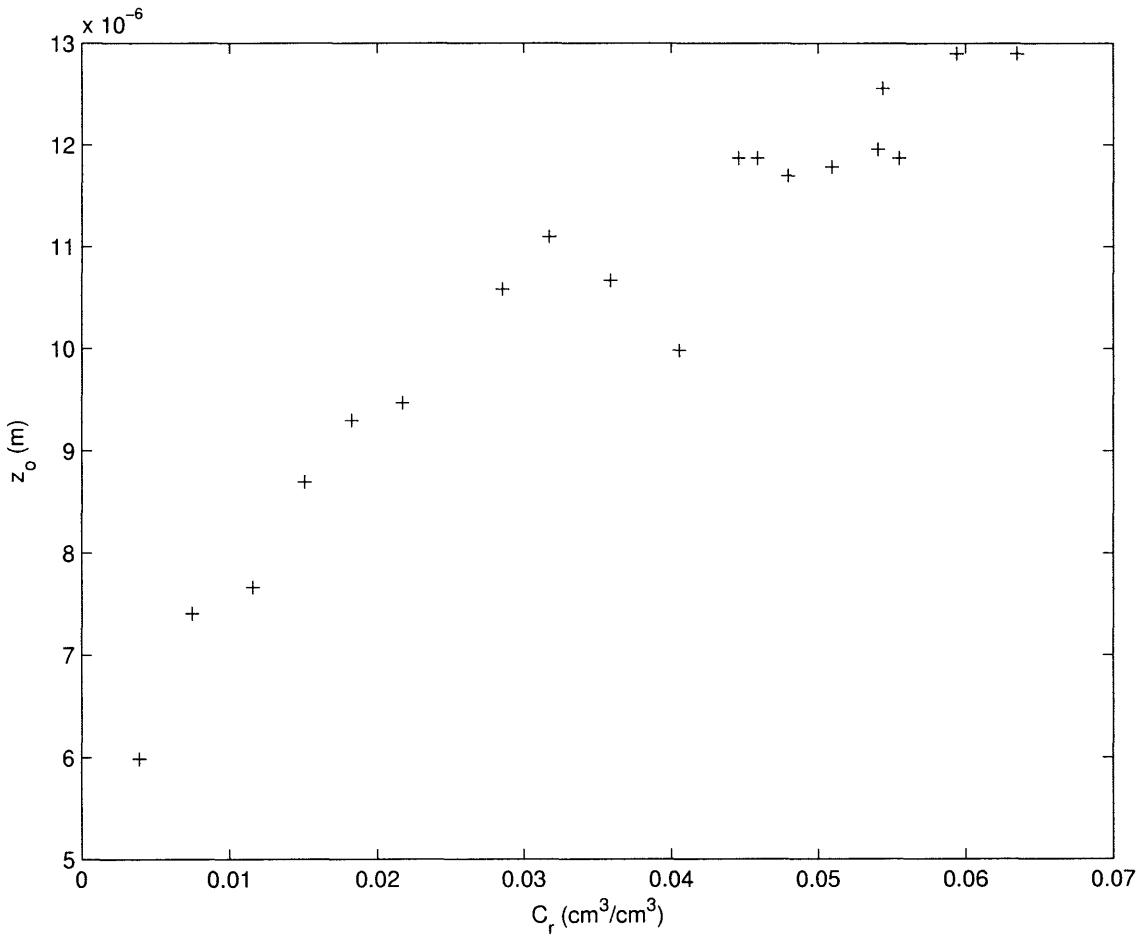

Figure 3-7: $z_o(m)$ versus $C_r(cm^3/cm^3)$ for Coleman fine sand starved-bed experiments, $d = 0.11mm$, neutral case: $\alpha = 1$, $\beta = 0$

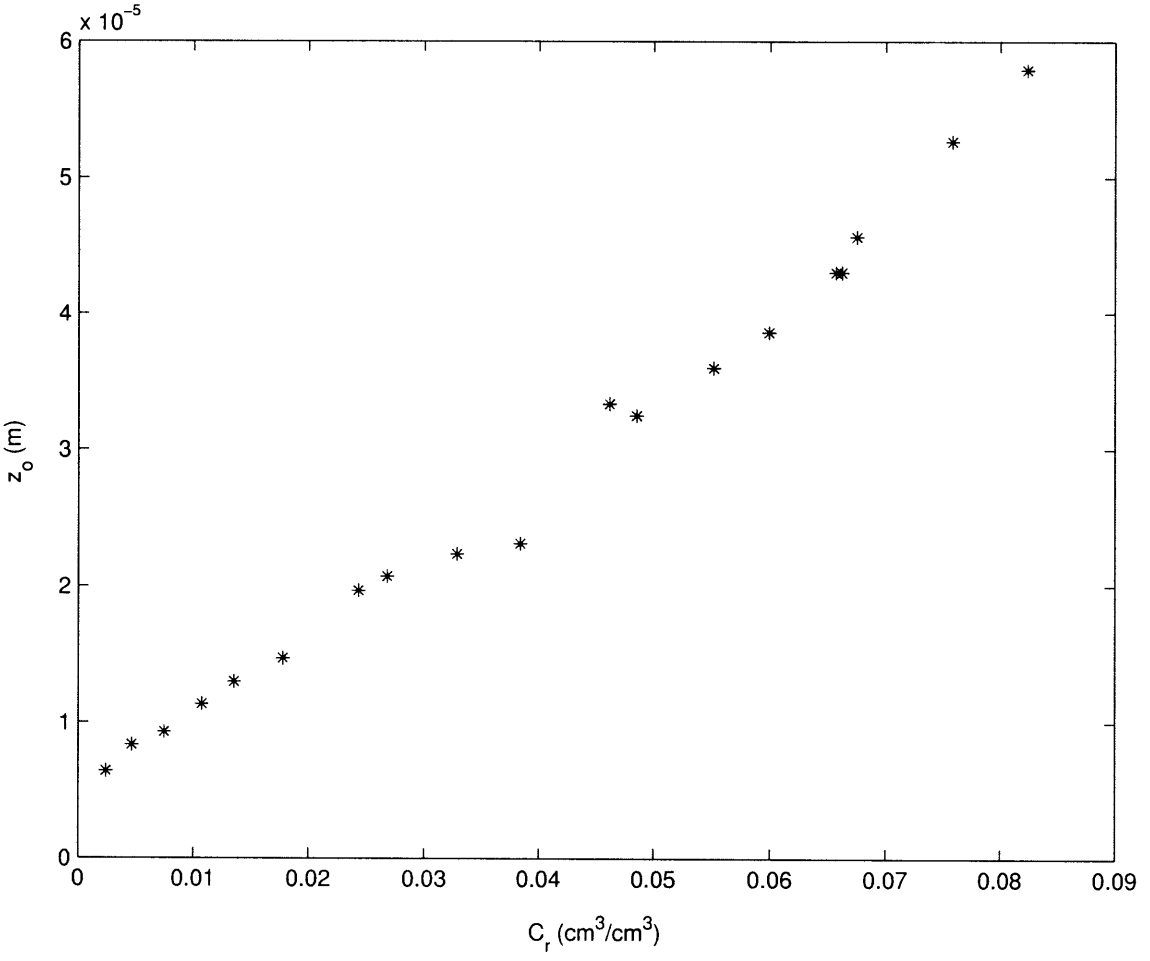

Figure 3-8: $z_o(m)$ versus $C_r(cm^3/cm^3)$ for Coleman fine sand starved-bed experiments, $d = 0.11mm$, stratified case: $\alpha = 0.8$, $\beta = 4$

$0.4h$ indicated by $+$ in Figure 3-9 using the neutral model. We obtain a reasonably good fit (see dotted-dashed line in Figure 3-9) with $z_{o,clearwater} = 5.7 \cdot 10^{-6} m$. When the concentration increases, we would expect the velocity to increase, since the eddy viscosity decreases. However, we can observe in Figure 3-9, where Run 20 is indicated by $*$, that this is not the case. On the contrary, the velocity decreases. If we fit run 20 data using the neutral model, we obtain $z_{o,neutral} = 1.3 \cdot 10^{-5} m$ and the curve shifts to the left (see dashed line in Figure 3-9). As explained above, increasing the sediment concentration increases the bottom roughness by a lot. This can result in a decrease of the velocity. Moreover, the curve obtained with the neutral model fits very poorly the run 20 data. Using the stratified model, we obtain $z_{o,stratified} = 5.2 \cdot 10^{-5} m$, and a curve which fits run 20 data a lot better than the curve obtained when using the neutral model (see full line in Figure 3-9). Using this $z_{o,stratified}$ with the neutral model, we obtain a curve completely shifted to the left (see dotted line in Figure 3-9). This comes from the fact that the neutral model only accounts for bed roughness effects in the velocity profile, whereas the stratified model accounts for both bed roughness effects and stratification effects. Indeed, the velocity profile for the stratified case is given by Equations (2.75) and (2.76)

$$U(z) = \frac{u_*}{\kappa} ln\left(\frac{z}{z_o}\right) = U_N(z), z_o < z \leq z_r$$

$$U(z) = \frac{u_*}{\kappa} ln\left(\frac{z}{z_o}\right) + \frac{u_* \beta a}{\kappa} \int_{z_r}^{z} \frac{C(z')}{1 - \frac{z'}{h}} dz' = U_N(z) + \frac{u_* \beta a}{\kappa} \int_{z_r}^{z} \frac{C(z')}{1 - \frac{z'}{h}} dz', z_r < z \leq h \tag{3.13}$$

where $U_N(z)$ is the neutral velocity profile (corresponding to $\beta = 0$) given by (2.73) and $C(z)$ is given by (2.74). The neutral velocity does not depend on α. From these equations, for a given z_o, we have $U(z) > U_N(z)$ when there is sediment in suspension. Therefore, when we search the best z_o to fit the data, $z_{o,neutral} < z_{o,stratified}$. The dotted line represents the contribution of the bed roughness effects to sediment velocity profile through the term $\frac{u_*}{\kappa} ln\left(\frac{z}{z_o}\right)$, and the difference between the dotted line and the full line represents the contribution of stratification effects through the term $\frac{u_* \beta a}{\kappa} \int_{z_r}^{z} \frac{C(z')}{1 - \frac{z'}{h}} dz'$ in Equation (3.13). For this particular experiment, the stratified

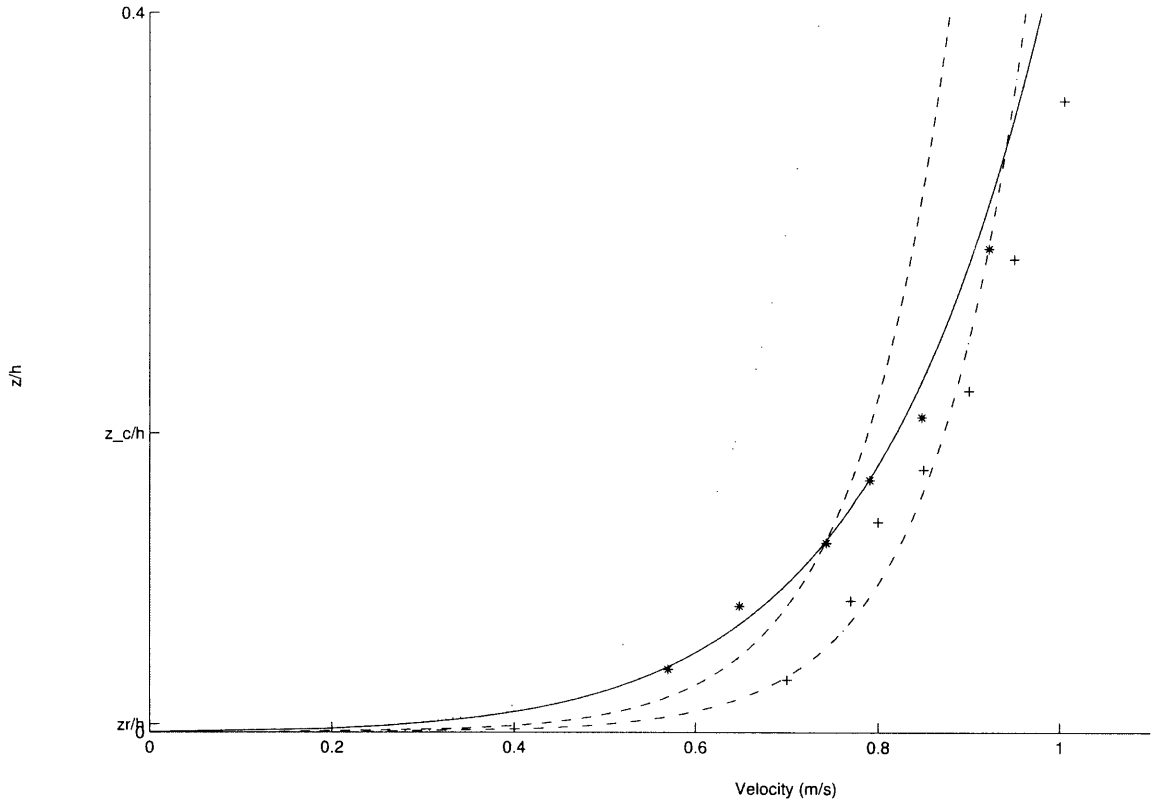

Figure 3-9: Coleman run 20 velocity profile. Full line : best-fit for experiment 20 by Coleman using the stratified model ($z_{o,stratified} = 5.2 \cdot 10^{-5}m$) with $[\alpha, \beta] = [0.8, 4]$. Dashed line : best-fit for experiment 20 by Coleman using the neutral model ($z_{o,neutral} = 1.3 \cdot 10^{-5}m$). Dashed-dotted line: best-fit for clear water by Coleman using the neutral model ($z_{o,clearwater} = 5.7 \cdot 10^{-6}m$). Dotted line : curve obtained with neutral model when taking $z_o = z_{o,stratified} = 5.2 \cdot 10^{-5}m$. $+$: clear water velocity data. $*$: experiment 20 by Coleman velocity data

model seems to fit data much better than the neutral model. This is also the case for the concentration (see Figure 3-10).

For this particular experiment, we examine the results obtained for the velocity profile when assuming that one can use the stratified model until $z_{junction} = 0.4h$ and then the neutral model (Equation (2.73)). This would be in agreement with the assumption that we made previously, stating that stratification seems to occur only below $0.4h$. The velocity has to be continuous at $z_{junction} = 0.4h$, therefore above $0.4h$, $U(z) = \frac{u_*}{\kappa} ln\left(\frac{z}{z_{junction}}\right) + U_{junction}$, where $U_{junction}$ is the value of the velocity obtained when using the stratified model at $z = z_{junction}$. In Figure 3-11, the curve

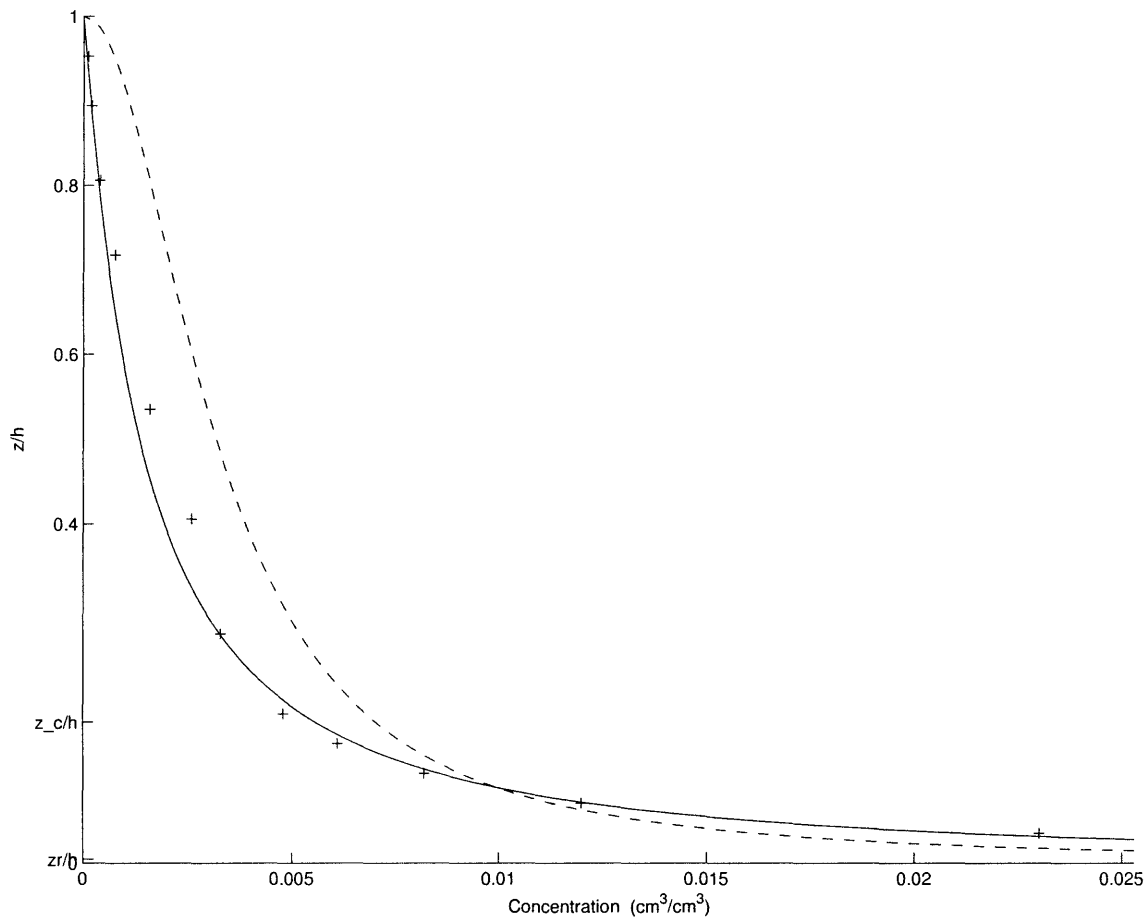

Figure 3-10: Coleman run 20 concentration profile. Full line: best-fit for experiment 20 by Coleman using the stratified model ($C_{r,stratified} = 0.0855cm^3/m^3$). Dashed line: best-fit using the neutral model ($C_{r,neutral} = 0.0448cm^3/m^3$). $*$: experiment 20 by Coleman concentration data

obtained (thick dashed line) seems as acceptable as the curve obtained when accounting for stratification until the surface (thick full line). The linear simplified model was initially limited to $z < z_c = h/6$, we now extend it all the way to $0.4h$. If we used the linear simplified model, using Equations (2.90), (2.91), and (2.92) until $0.4h$, and then (2.73) until the surface, the curve obtained (thick dashed-dotted line) is extremely close to the one obtained by using the parabolic model until $0.4h$. Since Equations (2.90), (2.91), and (2.92) are not computer-time-consuming whereas Equations (2.76) contains integrals that require a lot of time to be numerically evaluated, using Equations (2.90), (2.91), and (2.92) until $0.4h$, and then (2.73) until the surface can have a time advantage while predicting correctly the velocity. We then examine what we obtain by extending the simple linear stratified model all the way to the surface (thin line in Figure 3-11). This curve seems to fit the data as correctly as the curve obtained with the parabolic stratified model. However, the curve obtained when using the neutral model from $0.4h$ to the surface seems to be the best fit for this particular experiment. Doing exactly the same thing, but only until $z_{junction} = z_c = h/6$ does not seem to predict correctly the velocity profile (see dashed and dashed-dotted lines in Figure 3-11).

We show the corresponding neutral and stratified eddy viscosity profiles in Figure 3-12. Between z_o and z_r, the neutral and stratified eddy viscosity are assumed to be equal. Between z_r and h, we multiply the neutral eddy viscosity by the correction term $(1-\beta R_f)$ to obtain the stratified eddy viscosity. Since this correction term is not equal to 1 at $z = z_r$ (see Figure 3-14)), the stratified eddy viscosity is discontinuous at $z = z_r$ (see Figure 3-12(b)). In both cases, the stratified eddy viscosity is smaller than the neutral eddy viscosity. Stratification decreases eddy viscosity as explained in Section 1.2. The difference between linear and parabolic eddy viscosity increases a lot with the elevation z. However, since we assumed the shear stress τ to be linearly varying for the parabolic eddy viscosity (Equation 1.34) and to be constant for the linear eddy viscosity ($z << h$), the governing equation (1.38) for the velocity becomes in both cases

$$\frac{dU}{dz} = \frac{u_*}{\kappa z(1 - \beta R_f)}$$

where the Flux Richardson Number R_f is shown in Figure 3-13. In both cases (linear and parabolic), the Flux Richardson Number is almost constant over the entire depth, and therefore so too is the correction term $(1-\beta R_f)$ (see Figures 3-13 and 3-14). This behavior of the Flux Richardson Number seems to be typical. Indeed, we compute the Flux Richardson Number for all the available experiments (see Table D.1 in Appendix D). In all cases, R_f is almost constant. When we account for stratification through the correction term $(1-\beta R_f)$, we nearly multiply the neutral eddy viscosity by a constant. The effect is therefore nearly the same as multiplying the von Karman's constant κ by a constant smaller than 1, i.e. varying κ, which was the method used by Vanoni (1975) [1] to account for stratification.

Contrary to the governing equation for the velocity, the governing equation for the concentration (1.43)

$$C + \frac{\nu_T}{\alpha w_s}\frac{dC}{dz} = 0$$

is not the same in both cases since ν_T is different. Indeed, in Figure 3-15, we observe that using the linear model until the surface results in a concentration distribution which is quite different from the one obtained when using the parabolic model. The distribution obtained when using the linear model does not fit the concentration data as well as the one obtained when using the parabolic model. Therefore, the linear model provides a good estimate of the velocity profile since the governing equation for the velocity is the same as the governing equation for the parabolic model, but does not provide a good estimate of the concentration distribution, since the governing equation for the concentration is model-dependent. However, since the concentration distribution for parabolic eddy diffusivity does not rely on any numerical integration, this adoption of the parabolic eddy viscosity solution for concentration is not associated with any great increase in computational effort.

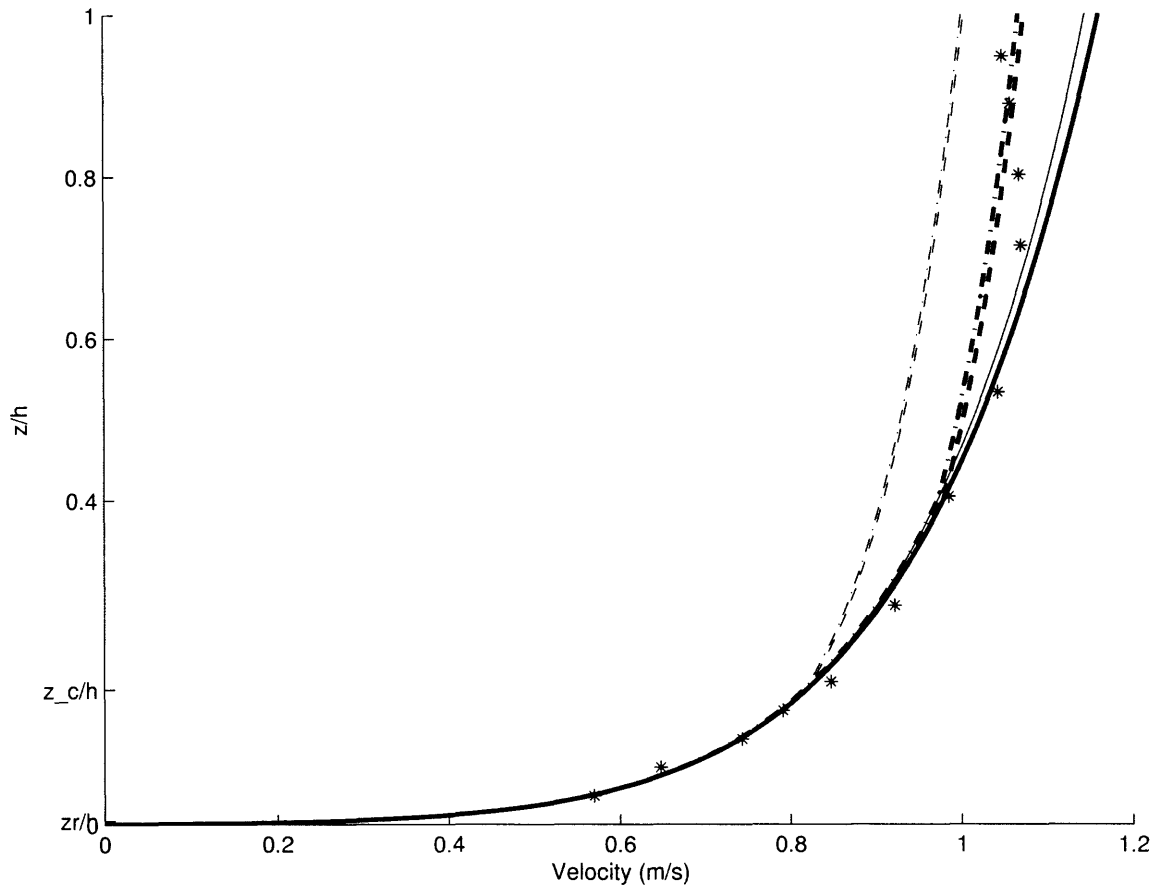

Figure 3-11: Coleman run 20 velocity profile. Thick full line: best-fit for experiment 20 by Coleman with the parabolic stratified model ($z_{o,stratified} = 5.2 \cdot 10^{-5} m$). Thick dashed line: Velocity prediction with the parabolic stratified model until $0.4h$ then the neutral model. Thick dashed-dotted line: Velocity prediction with the simplified "linear" stratified model until $0.4h$ then the neutral model. Dashed line: Velocity prediction with the parabolic stratified model until $z_c = h/6$ then the neutral model. Dashed-dotted line: Velocity prediction with the simplified "linear" stratified model until $z_c = h/6$ then the neutral model. Full line : Velocity prediction with the simplified "linear" stratified model until $z = h$. $*$: experiment 20 by Coleman velocity data

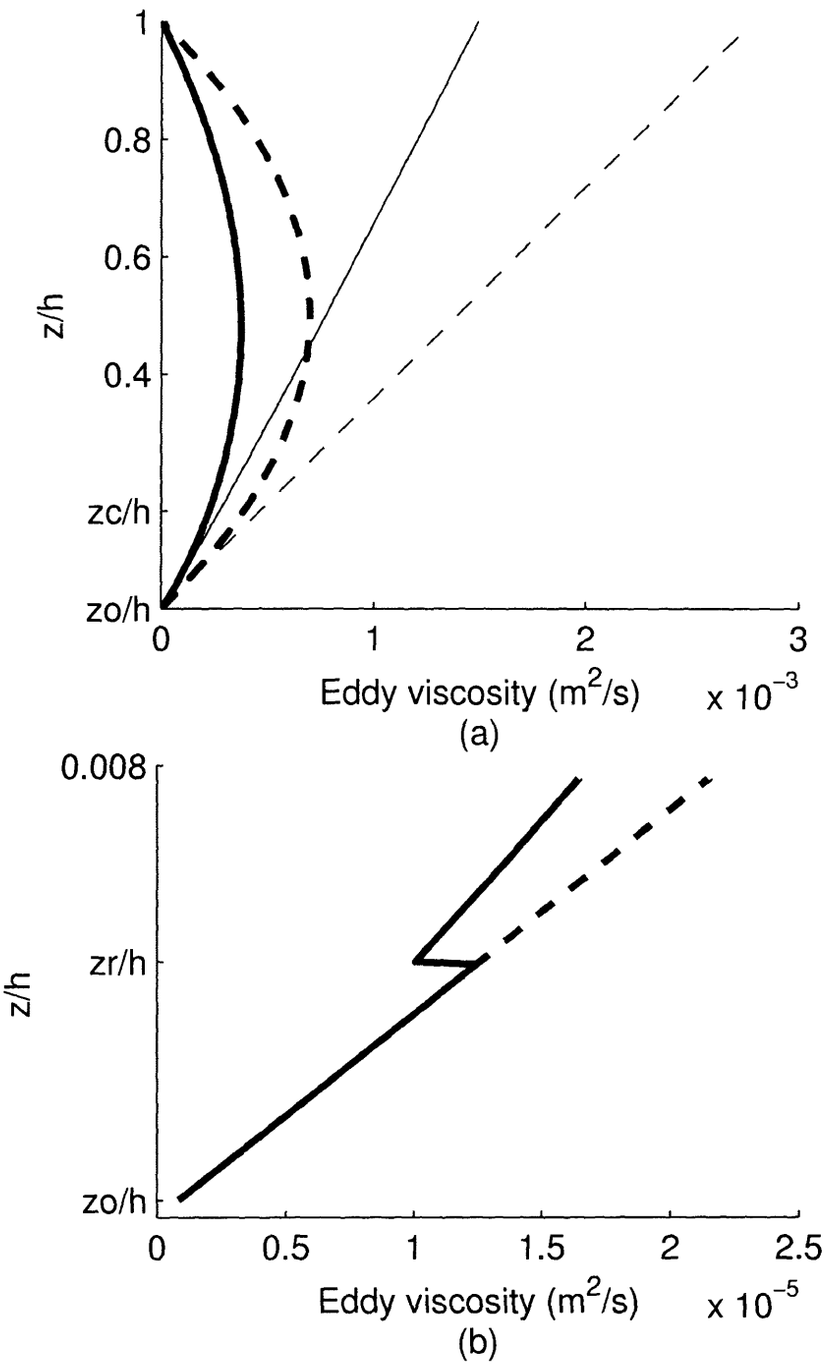

Figure 3-12: Coleman run 20 eddy viscosity. Thick dashed line: parabolic neutral eddy viscosity $\nu_{TN} = \kappa u_* z \left(1 - \frac{z}{h}\right)$. Thick line: parabolic stratified eddy viscosity $\nu_T = \nu_{TN}(1 - \beta R_f)$ with R_f given by (2.14). Dashed line: linear neutral eddy viscosity $\nu_{TN} = \kappa u_* z$. Full line : linear stratified eddy viscosity $\nu_T = \nu_{TN}(1 - \beta R_f)$ with R_f given by (2.39). (a): eddy viscosity profile between z_o and h. (b): eddy viscosity profile discountinuity at $z = z_r$.

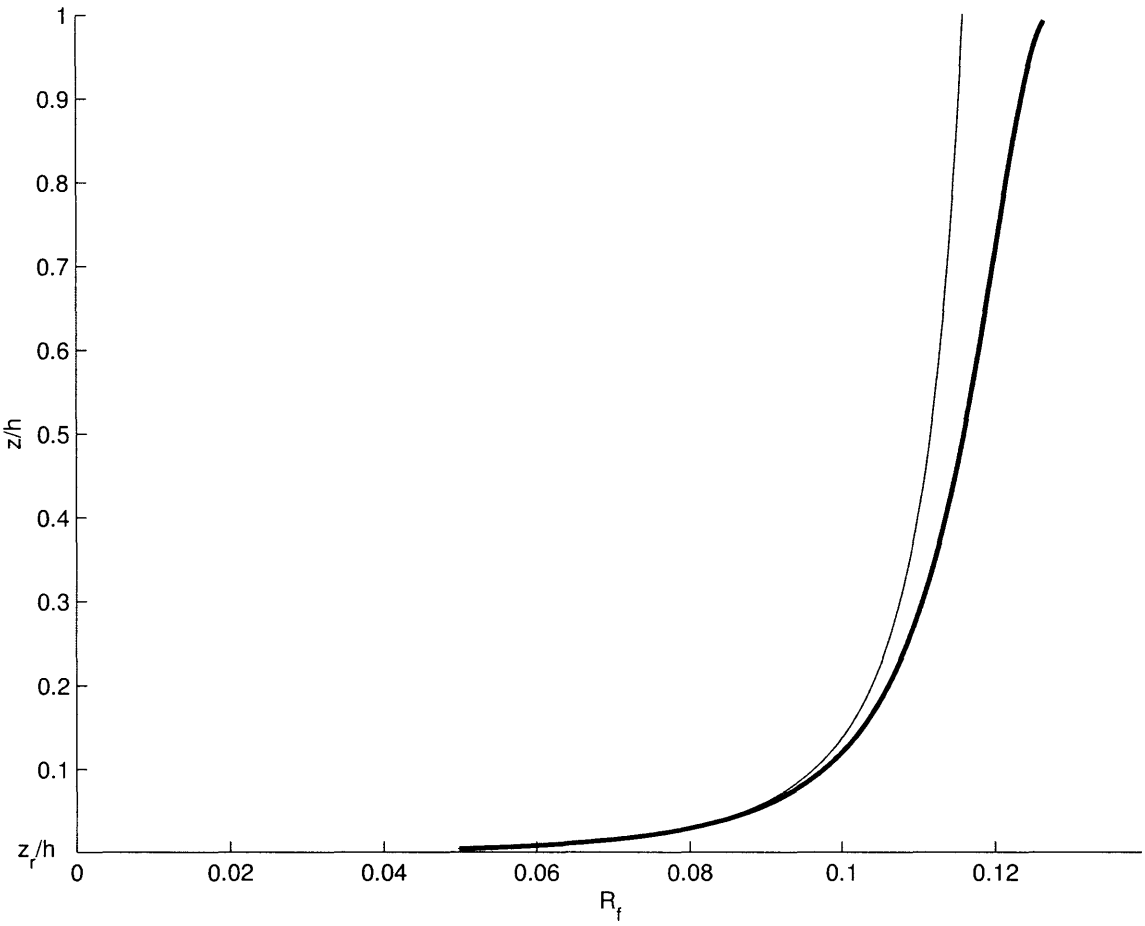

Figure 3-13: Coleman run 20 Flux Richardson Number between z_r and h. Thick full line: R_f with parabolic stratified eddy viscosity given by (2.14). Full line : R_f with linear stratified eddy viscosity given by (2.39)

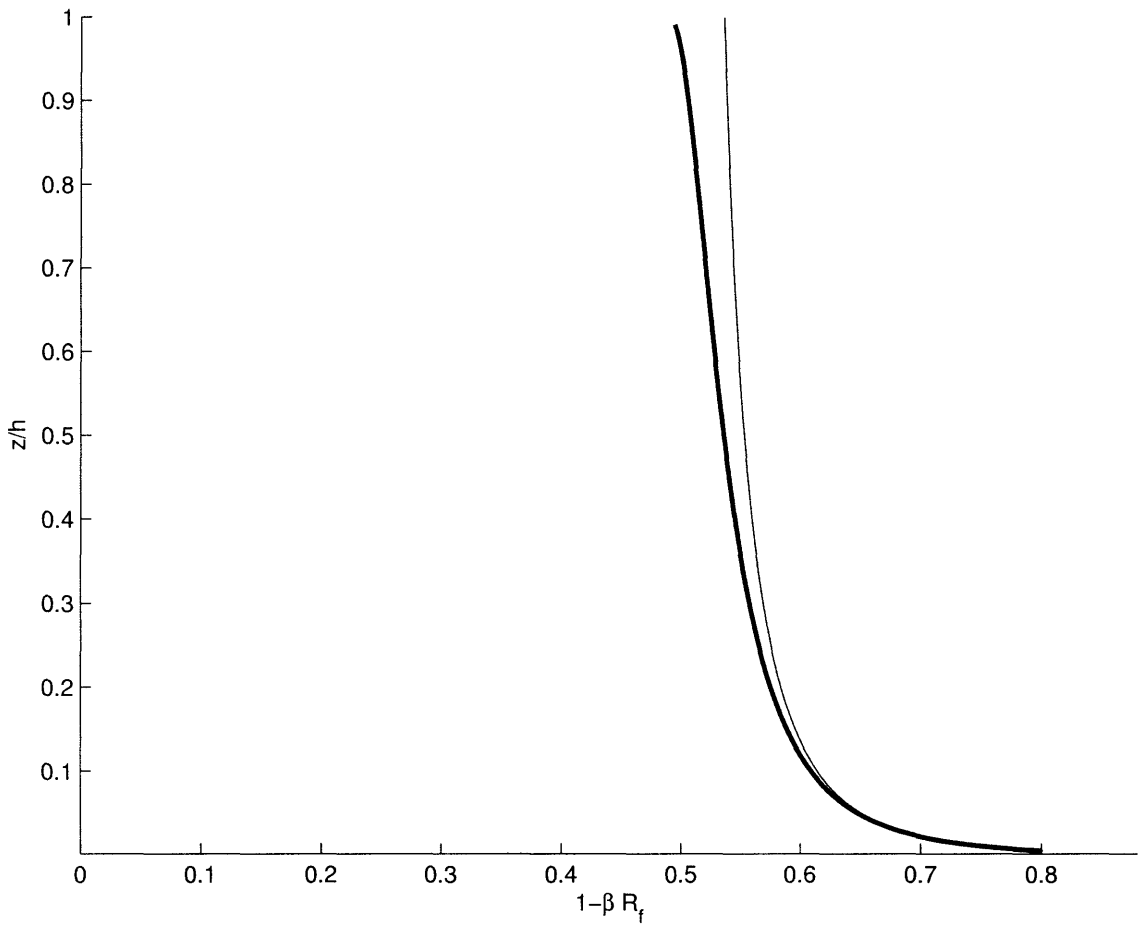

Figure 3-14: Coleman run 20. Correction term $(1 - \beta R_f)$ between z_r and h. Thick full line: $(1 - \beta R_f)$ with parabolic stratified eddy viscosity and R_f given by (2.14). Full line : $(1 - \beta R_f)$ with linear stratified eddy viscosity and R_f given by (2.39)

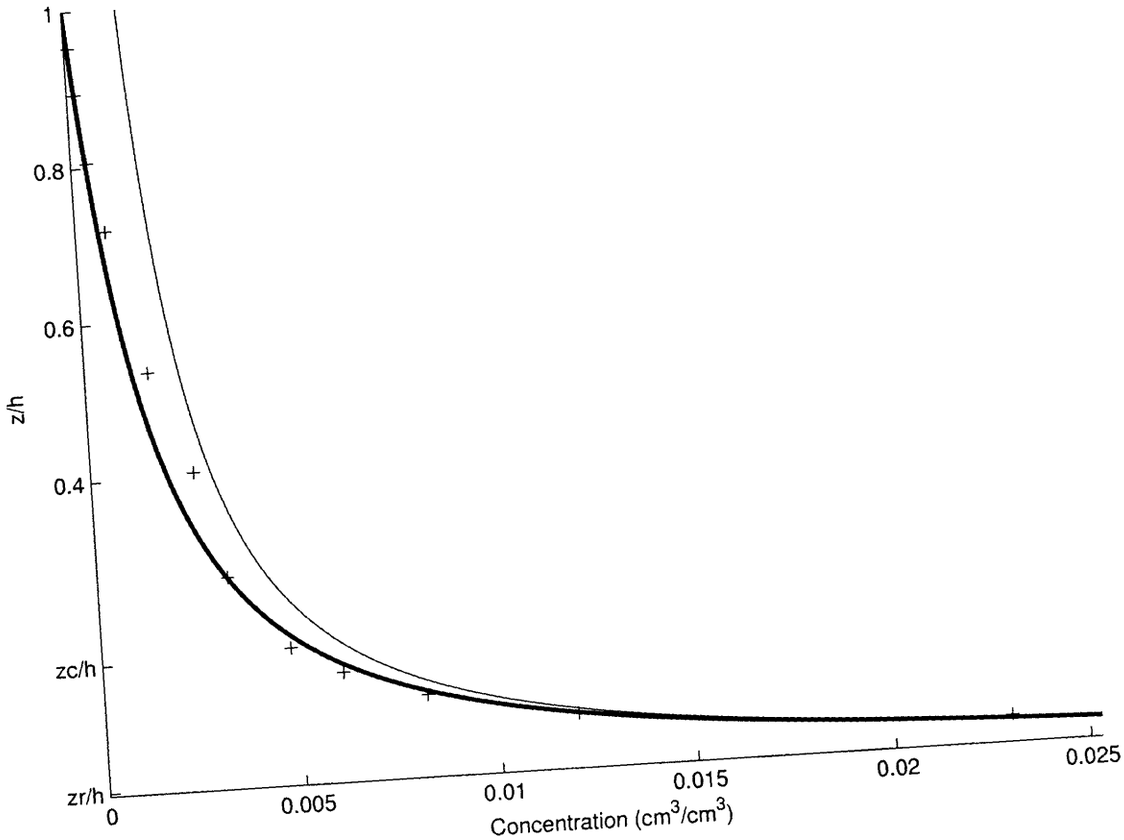

Figure 3-15: Coleman run 20 concentration distribution. Thick full line: best-fit for experiment 20 by Coleman with the parabolic stratified model ($C_{r,stratified} = 0.0855 cm^3/cm^3$). Full line : Concentration prediction with the simplified "linear" stratified model until $z = h$. $*$: experiment 20 by Coleman velocity data

Chapter 4

Determination of movable bed roughness z_O and reference concentration C_r

In Chapter 3, α and β have been determined by applying an optimization method to available experimental data: for each couple $[\alpha, \beta]$, we determined an optimal z_o and an optimal C_r in order to minimize the absolute error for the concentration $\epsilon_c(\alpha, \beta)$, and for the velocity $\epsilon_u(\alpha, \beta)$ for each experiment. The average relative error for the ensemble of the experiments $\overline{\epsilon_{rel}}(\alpha, \beta)$ was then computed for each couple $[\alpha, \beta]$. This average relative error $\overline{\epsilon_{rel}}(\alpha, \beta)$ is minimized for the optimal couple $[\alpha, \beta] = [0.8, 4]$. If we fix $\beta = 0$, which corresponds to neutral conditions, the optimal value of α was found to be 1. The parameters $[\alpha, \beta]$ are now fixed equal to $[\alpha, \beta] = [0.8, 4]$ when stratification is considered and $[\alpha, \beta] = [1, 0]$ when it is not. Using the same optimization method we obtain the optimal values of the bed roughness z_o and the reference concentration C_r that minimize the absolute errors for the concentration $\epsilon_c(\alpha = 0.8, \beta = 4)$ and the velocity $\epsilon_u(\alpha = 0.8, \beta = 4)$ for each experiment. We can also compute the maximum Flux Richardson Number R_f using (2.14) and (2.59). The results are presented in Appendix D (see Table D.1).

It is then possible to determine correlations between z_o and C_r and the parameters of the flow. From a practical point of view, we want to be able to predict velocity profiles

and sediment concentration distributions in natural rivers knowing the parameters of the flow and the sediment. Natural river beds are made of sediment and there is an equilibrium between the sand-bed and the flow, thus natural river beds correspond to "equilibrium bed" experiments. Therefore, we will only use the "equilibrium bed " experiments in our analysis, i.e. all Barton and Lin (1955) [2] runs, all Brooks (1954) [3] runs and Lyn (1986) [16] runs 5, 6, 7, 8. Note that the experiments which were physically "absurd" (i.e. $C_r \geq 0.1$) are not considered here. In all the experiments, the bed remained flat. The available data for this analysis are listed in Table 4.1.

Table 4.1: Fluid-sediment parameter S_*, nominal grain diameter d_n, mm, shear velocity u_*, cm/s, critical Shields Parameter Ψ_{cr}, kinematic viscosity ν, mm^2/s, neutral roughness $z_{o,n}$, mm, neutral reference concentration $C_{r,n}$, cm^3/cm^3, Neutral Reynolds number $Re_{*n} = \frac{30 z_{o,n} u_*}{\nu}$, stratified roughness $z_{o,s}$, mm, stratified reference concentration $C_{r,s}$, cm^3/cm^3, stratified Reynolds number $Re_{*s} = \frac{30 z_{o,s} u_*}{\nu}$

Run	S_*	d_n	u_*	Ψ	Ψ_{cr}	ν	$z_{o,n}$	$C_{r,n} \cdot 10^2$	Re_{*n}	$z_{o,s}$	$C_{r,s} \cdot 10^2$	Re_{*s}
Barton and Lin (1955) [2]												
26 *	2.8	0.20	4.9	0.74	0.053	1.01	0.161	3.92	234	0.319	4.01	464
29 *	2.8	0.20	4.6	0.65	0.053	1.01	0.190	2.69	259	0.305	2.03	416
31	2.8	0.20	3.8	0.45	0.053	1.01	0.019	3.72	22	0.041	3.46	47
35	2.8	0.20	4.9	0.74	0.053	1.01	0.024	3.43	35	0.035	2.39	52
36	2.8	0.20	5.5	0.94	0.053	1.01	0.031	3.63	51	0.050	2.95	82
Brooks (1954) [3]												
2	2.1	0.17	3.6	0.48	0.062	1.01	0.013	2.17	13	0.019	2.07	20
3	2.1	0.17	4.1	0.62	0.062	1.01	0.047	1.03	57	0.054	0.86	66
4	2.1	0.17	4.0	0.59	0.062	1.01	0.029	1.92	34	0.035	1.68	42
6	2.1	0.17	3.8	0.54	0.062	1.01	0.018	1.52	20	0.023	1.34	26
7	2.1	0.17	3.8	0.54	0.062	1.01	0.022	1.72	24	0.029	1.57	32
Lyn (1986) [16]												
5	3.1	0.21	3.9	0.45	0.051	0.99	0.024	0.77	28	0.027	0.53	32
6	4.5	0.27	4.2	0.41	0.043	0.98	0.023	0.87	29	0.027	0.75	34
7	2.2	0.17	3.6	0.48	0.061	0.99	0.022	1.22	23	0.027	0.92	29
8	3.1	0.21	3.7	0.40	0.051	0.98	0.022	1.22	24	0.026	0.81	29

* The values of z_o/d_n for Runs 26 and 29 by Barton and Lin (1955) [2] are one order of magnitude larger than the values obtained for the other experiments for both neutral and stratified conditions. Therefore these runs and are not taken into account in the movable bed roughness and reference concentration analysis

4.1 Movable bed roughness z_o

The Shields Parameter (Shields, 1936) is the ratio of mobilizing (drag) and stabilizing (submerged weight) forces

$$\Psi = \frac{\tau_o}{(\rho_s - \rho)gd} = \frac{u_*^2}{(s-1)gd} \tag{4.1}$$

The critical Shields Parameter Ψ_{cr} expresses the conditions of neutral stability of a sediment grain on the fluid-sediment interface, and is the effective Shields Parameter at which sediment motion starts, i.e. for values $\Psi > \Psi_{cr}$ mobilizing forces exceed stabilizing forces and sediment motion occurs. The critical Shields Parameter Ψ_{cr} is a function of the fluid-sediment parameter S_* introduced by Madsen and Grant (1976) [11]

$$S_* = \frac{d\sqrt{(s-1)gd}}{4\nu} \tag{4.2}$$

where ν is the kinematic viscosity of the fluid and d is the sediment size. In our analysis, we consider the nominal diameter $d_n = d_{sieved}/0.9$ when computing the value of S_* and Ψ. A formula for Ψ_{cr} was given by Soulsby (1997) [26]

$$\Psi_{cr} = 0.095 S_*^{-2/3} + 0.056 \left(1 - exp\left(\frac{-S_*^{3/4}}{20}\right)\right) \tag{4.3}$$

An approximate value of Ψ_{cr} for sand in water is often taken as 0.05 (Nielsen, 1992 [20]), which is consistent with the values of Ψ_{cr} that we have here(see Table 4.1). The effective shear stress τ_{cr} which corresponds to Ψ_{cr} is called the critical shear stress

$$\tau_{cr} = \Psi_{cr}(\rho_s - \rho)gd \tag{4.4}$$

If there is no motion of the sediment, i.e. $\Psi < \Psi_{cr}$, and the flow corresponds to

$$Re_* = \frac{30 z_o u_*}{\nu} > 3.3 \tag{4.5}$$

the flow is considered rough turbulent. This is the case here for all experiments (see Table 4.1). From the extensive experiments by Nikuradse (1933), summarized in most standard fluid mechanics texts, e.g. Schlichting (1968) [23], the value of z_o is then $k_N/30 = d/30$, in which k_N is the equivalent Nikuradse sand grain roughness defined as $k_N = 30z_o$. When the sediment is moving, the equivalent Nikuradse sand grain roughness is $k_N \geq d$. This suggests that a movable bed roughness could be of the type $z_o/d = 1/30 + Constant \cdot (\Psi - \Psi_{cr})$ when $\Psi > \Psi_{cr}$. Similarly, Smith and McLean (1977) [24] suggested that a general expression for z_o could be of the form

$$z_o = \alpha_o \frac{\tau_b - \tau_{cr}}{(\rho_s - \rho)g} + z_n = \alpha_o d(\Psi - \Psi_{cr}) + z_n$$

where z_n is the z_o given by Nikuradse's work (1933) and α_o is a constant. Values of α_o vary among the different studies that have been published. Owen's work (1964) [22] yields $\alpha_o = 22.8$ and Smith and McLean (1977) [24] gives $\alpha_o = 26.3$. Wilson (1987) [31] also suggested that when sediment motion occurs k_N should be of the form $k_N = 5\Psi d$ for steady sheet-flow in closed conduits. Wilson did not suggest $k_N = 5(\Psi - \Psi_{cr})d$, however, in his analysis (and in the present study, see Table 4.1), $\Psi >> \Psi_{cr}$ and $5(\Psi - \Psi_{cr})d \approx 5\Psi d$.

For stratified conditions ($[\alpha, \beta] = [0.8, 4]$), we plot $y = ln\left(\frac{z_o}{d_n}\right)$ versus $x = ln(\Psi)$, $x = ln\,(\Psi - .05)$, $x = ln\,(\Psi - \Psi_{cr})$ and $x = ln\left(\frac{\Psi}{\Psi_{cr}} - 1\right)$ and perform a linear regression analysis in the form of $y = ax + b$. We also plot $y = \left(\frac{z_o}{d_n}\right)$ versus $x = (\Psi)$, $x = (\Psi - .05)$, $x = (\Psi - \Psi_{cr})$ and $x = \left(\frac{\Psi}{\Psi_{cr}} - 1\right)$ and perform a linear regression analysis in the form of $y = bx + a$. The same analysis is performed for neutral conditions ($[\alpha, \beta] = [1, 0]$). We also perform this analysis for $y = ln\left(\frac{z_o}{d_n} - \frac{1}{15}\right)$ and $y = ln\left(\frac{z_o}{d_n} - \frac{1}{30}\right)$. The values of z_o/d_n for Runs 26 and 29 by Barton and Lin (1955) [2] are one order of magnitude larger than the values obtained for the other experiments for both neutral and stratified conditions (see Table 4.1). Therefore these values are not taken into account when we perform our best-fit analysis. In order to be consistent, these two experiments are not taken into account when performing the best-fit analysis for the reference concentration C_r in Section 4.2, even if they are

within the same range as the other values.

For each analysis, a measure of the error is given by

$$\overline{x_{z_o}} = average\left(x_{z_o}\right) \tag{4.6}$$

where x_{z_o} is the ratio of the best z_o valued obtained from the measured velocity and the value predicted by the regression formula obtained here, i.e.

$$x_{z_o} = \frac{\left(\frac{z_o}{d_n}\right)_{observed}}{\left(\frac{z_o}{d_n}\right)_{predicted}} \tag{4.7}$$

We also compute the standard deviation

$$\sigma_{z_o} = \sqrt{\frac{\sum\left(x_{z_o} - \overline{x_{z_o}}\right)^2}{N-1}} \tag{4.8}$$

where N is the number of experiments considered.

The results are shown in Tables 4.2 and 4.3 and in Figures 4-1 through 4-5. The linear fit analysis of the logarithm of the terms considered here is performed in order to check to extent to which the linear assumption is correct, i.e. if we assume $y = \frac{z_o}{d_n}$ to be related to $x = (\Psi - \Psi_{cr})$ by a function of the form $y = ax^b$, and take the logarithm of these terms, a linear regression analysis provides a value of b, respectively 0.717 and 0.843 for the neutral and the stratified case (see Table 4.3 and Figure 4-3). These values are reasonably close to 1, and therefore justify the assumption of a linear relationship between $\frac{z_o}{d_n}$ and $\Psi - \Psi_{cr}$. This is further brought out by the errors, σ_{z_o}, being identical for the logarithmic and linear fits (Tables 4.2 and 4.3). From our analysis, the formula for the bottom roughness as function of the Shields Parameter that is the most accurate (see Table 4.2 and Figure 4-1) is:

$$\left\{\frac{z_o}{d_n}\right\}_{neutral} = \left\{0.151\left(\Psi - \Psi_{cr}\right) + 0.0558\right\}\left(1 \pm 0.36\right) \tag{4.9}$$

Table 4.2: A linear best-fit analysis is performed between the parameters x and y. a and b are the zero and first-order coefficients in the equation $y = bx+a$. The subscript $_n$ denotes the neutral coefficients and the subscript $_s$ denotes the stratified coefficient. The error $\overline{x_{z_o}}$ as defined by (4.7) and the standard deviation σ_{z_o} as defined by (4.8) are also presented. Experiments bar_{26} and bar_{29} are not considered

$y = z_o/d_n$vs.	b_n	a_n	$\overline{x_{z_o}}$	σ_{z_o}	b_s	a_s	$\overline{x_{z_o}}$	σ_{z_o}
$x = \Psi - \Psi_{cr}$	1.51E-1	5.58E-2	1.00	0.36	2.48E-1	5.23E-2	1.00	0.29
$x = \Psi/\Psi_{cr} - 1$	4.99E-3	8.65E-2	1.00	0.41	9.93E-3	8.74E-2	1.00	0.33
$x = \Psi - .05$	1.55E-1	5.28E-2	1.00	0.36	2.52E-1	4.90E-2	1.00	0.29
$x = \Psi$	1.55E-1	4.50E-2	1.00	0.36	2.52E-1	3.64E-2	1.00	0.29

Table 4.3: A power best-fit analysis is performed between the parameters x and y. a and b are the coefficients in the equation $y = ax^b$. The subscript $_n$ denotes the neutral coefficients and the subscript $_s$ denotes the stratified coefficient. The error $\overline{x_{z_o}}$ as defined by (4.7) and the standard deviation σ_{z_o} as defined by (4.8) are also presented. Experiments bar_{26} and bar_{29} are not considered

$y = z_o/d_n$vs.	b_n	a_n	$\overline{x_{z_o}}$	σ_{z_o}	b_s	a_s	$\overline{x_{z_o}}$	σ_{z_o}
$x = \Psi - \Psi_{cr}$	7.17E-1	2.08E-1	1.05	0.36	8.43E-1	3.09E-1	1.03	0.29
$x = \Psi/\Psi_{cr} - 1$	4.93E-1	4.26E-2	1.06	0.42	6.17E-1	4.41E-2	1.04	0.34
$x = \Psi - .05$	7.26E-1	2.08E-1	1.04	0.36	8.51E-1	3.08E-1	1.03	0.29
$x = \Psi$	7.89E-1	2.01E-1	1.04	0.36	9.27E-1	2.96E-1	1.03	0.29
$y = z_o/d_n - 1/15$ vs.								
$x = \Psi - \Psi_{cr}$	1.7	0.167	1.10	0.40	1.46	0.272	1.06	0.31
$x = \Psi/\Psi_{cr} - 1$	1.27	0.00314	1.12	0.46	1.02	0.0103	1.08	0.36
$x = \Psi - .05$	1.71	0.164	1.10	0.39	1.48	0.272	1.06	0.31
$x = \Psi$	1.86	0.152	1.10	0.40	1.61	0.254	1.06	0.31
$y = z_o/d_n - 1/30$ vs.								
$x = \Psi - \Psi_{cr}$	0.985	0.18	1.06	0.37	1.06	0.285	1.04	0.30
$x = \Psi/\Psi_{cr} - 1$	0.688	0.0199	1.08	0.43	0.767	0.0252	1.06	0.35
$x = \Psi - .05$	0.996	0.179	1.06	0.37	1.07	0.283	1.04	0.30
$x = \Psi$	1.08	0.171	1.06	0.37	1.17	0.27	1.04	0.30

which is equivalent to

$$\{k_N\}_{neutral} = \{4.53\,(\Psi - \Psi_{cr}) + 1.67\}\,d_n\,(1 \pm 0.36) \tag{4.10}$$

for the neutral case and

$$\left\{\frac{z_o}{d_n}\right\}_{stratified} = \{0.248\,(\Psi - \Psi_{cr}) + 0.0523\}\,(1 \pm 0.29) \tag{4.11}$$

which is equivalent to

$$\{k_N\}_{stratified} = \{7.44\,(\Psi - \Psi_{cr}) + 1.57\}\,d_n\,(1 \pm 0.29) \tag{4.12}$$

for the stratified case, where $k_N = z_o/30$ is the Nikuradse roughness.

As reported by Nielsen (1992) [20], several authors (e.g. Engelund and Hansen (1972)[8], Nielsen (1976)[20]) have suggested that since it is not physically possible to obtain a monolayer bed, the roughness height k_N should be more than d even if there is no sediment motion. Engelund and Hansen suggested $2d_{65}$ whereas Nielsen suggested the value $2.5d_{50}$ for the grain roughness of a flat bed of sand with median size d_{50}. It can therefore be expected that with sediment motion, k_N should be of the form $const(\Psi - \Psi_{cr}) + Constant \cdot d$. If we force the additive constant in (4.10) and (4.12) to be equal to 2, performing a linear-fit analysis (see Figure 4-6), we obtain

$$\{k_N\}_{neutral} = \{3.93\,(\Psi - \Psi_{cr}) + 2\}\,d_n\,\{0.99 \pm 0.37\} \tag{4.13}$$

$$\{k_N\}_{stratified} = \{6.66\,(\Psi - \Psi_{cr}) + 2\}\,d_n\,\{0.99 \pm 0.29\} \tag{4.14}$$

The standard deviations are almost the same than in (4.12) and (4.10). This suggest that the roughness height k_N is equal to $2d_n$ when there is no sediment motion.

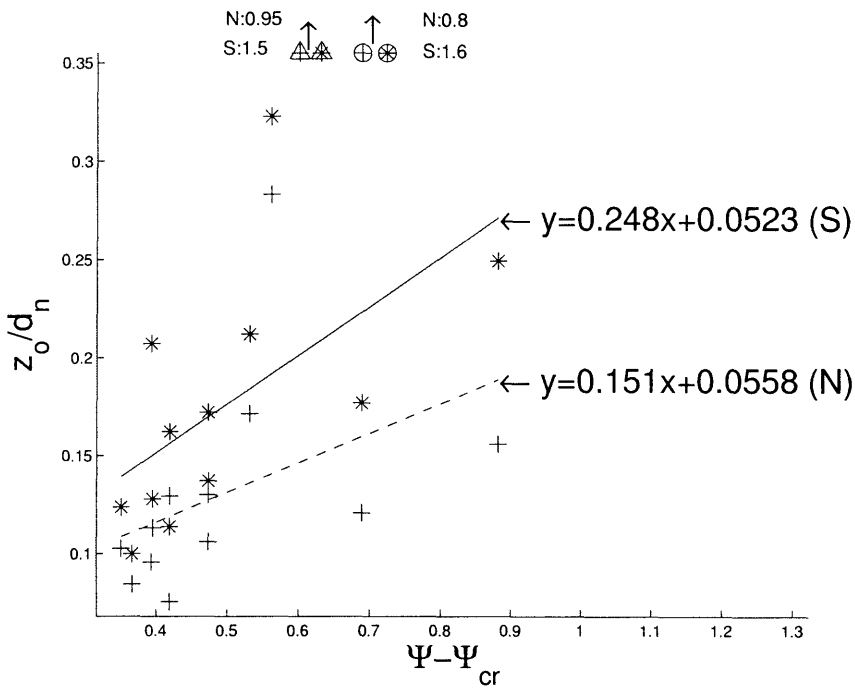

Figure 4-1: z_o/d_n vs. $\Psi - \Psi_{cr}$. Linear fit analysis. Dashed line and + : neutral. Plain line and * : stratified. △ : Barton 29 ◯ : Barton 26, S: stratified, N: neutral

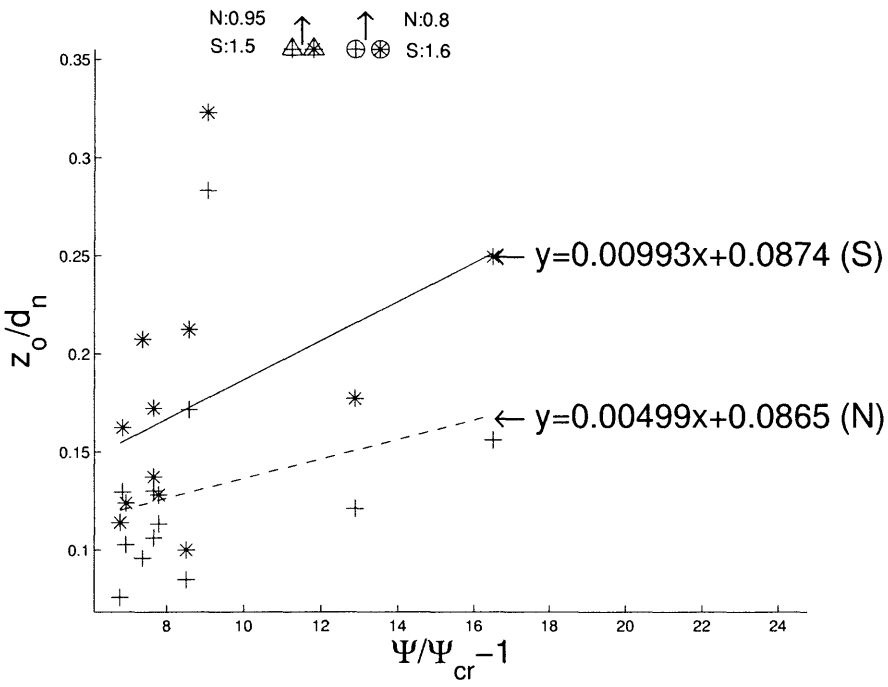

Figure 4-2: z_o/d_n vs. $\frac{\Psi}{\Psi_{cr}} - 1$. Linear fit analysis. Dashed line and + : neutral. Plain line and * : stratified. △ : Barton 29 ◯ : Barton 26, S: stratified, N: neutral

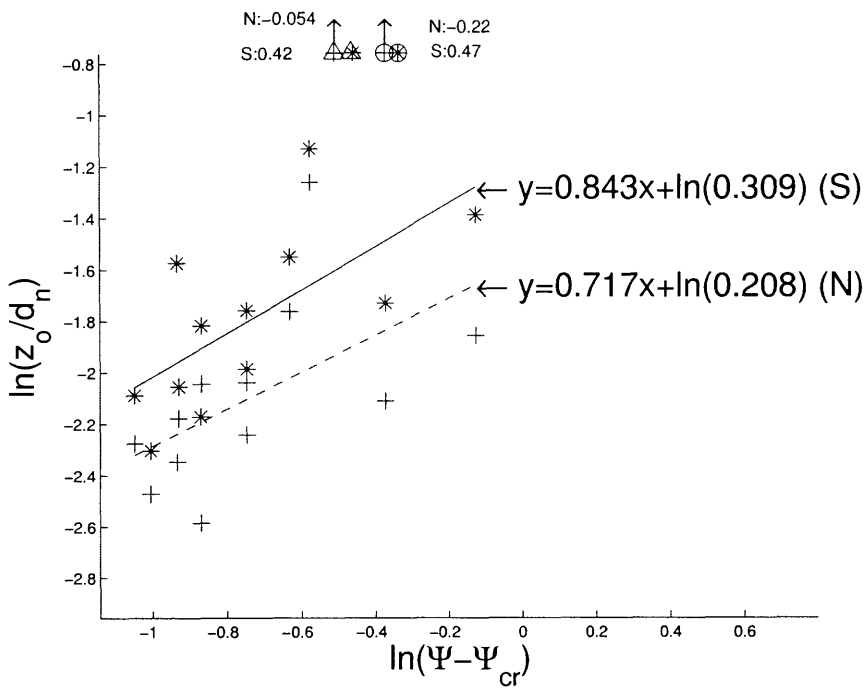

Figure 4-3: z_o/d_n vs. $\Psi - \Psi_{cr}$. Power fit analysis. Dashed line and + : neutral. Plain line and * : stratified. $\triangle$: Barton 29 $\bigcirc$: Barton 26, S: stratified, N: neutral

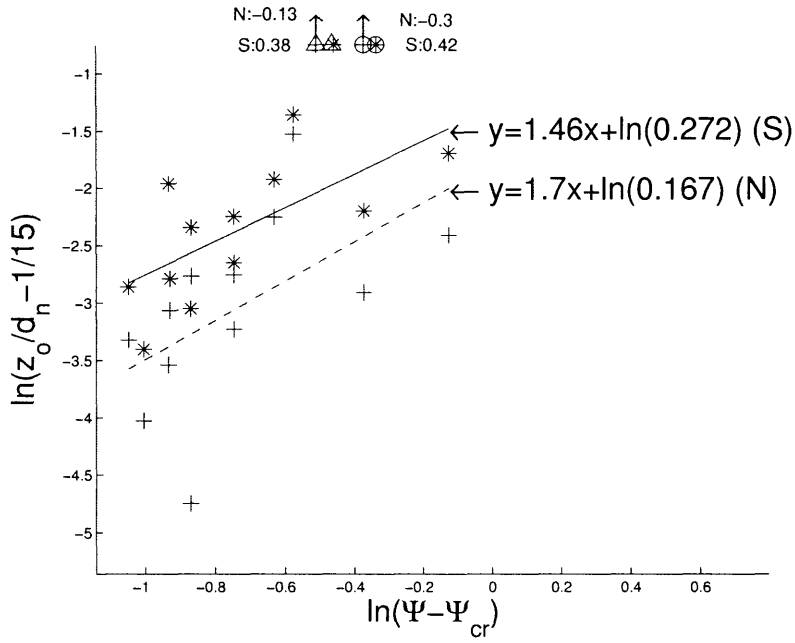

Figure 4-4: $z_o/d_n - 1/15$ vs. $\Psi - \Psi_{cr}$. Power fit analysis. Dashed line and + : neutral. Plain line and * : stratified. $\triangle$: Barton 29 $\bigcirc$: Barton 26, S: stratified, N: neutral

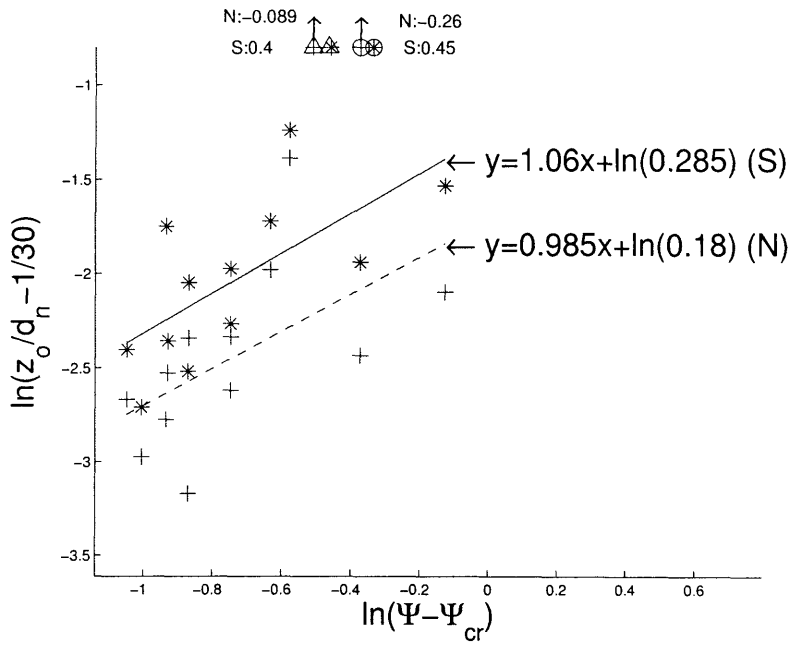

Figure 4-5: $z_o/d_n - 1/30$ vs. $\Psi - \Psi_{cr}$. Power fit analysis. Dashed line and + : neutral. Plain line and * : stratified. $\triangle$: Barton 29 $\bigcirc$: Barton 26, S: stratified, N: neutral

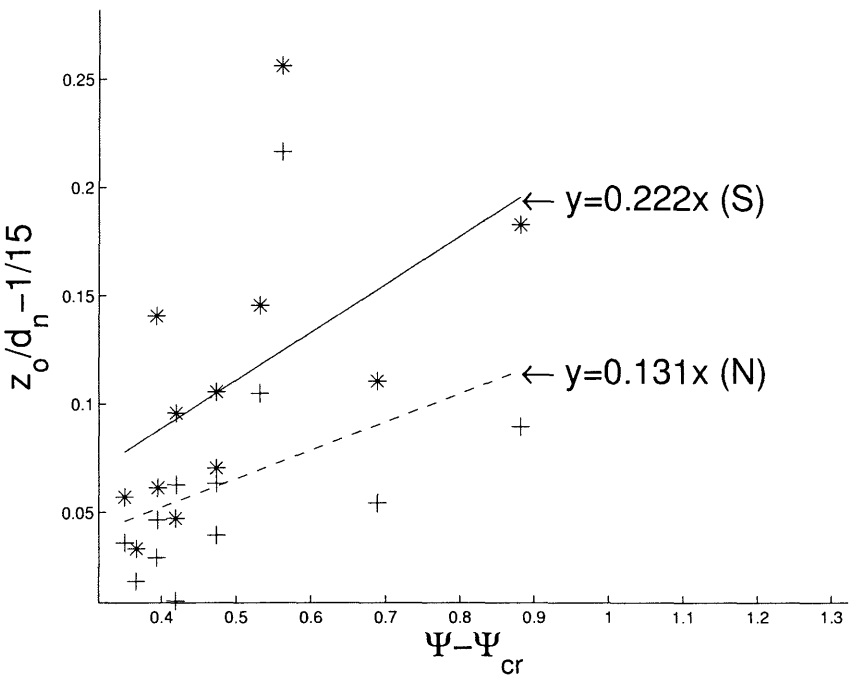

Figure 4-6: $z_o/d_n - 1/15$ vs. $\frac{\Psi}{\Psi_{cr}} - 1$. Linear fit analysis. Dashed line and + : neutral. Plain line and * : stratified. $\triangle$: Barton 29 $\bigcirc$: Barton 26, S: stratified, N: neutral

4.2 Reference concentration C_r

When there is no sediment motion, i.e. $\Psi < \Psi_{cr}$, there is no suspended sediment and the reference concentration C_r at $z_r = 7d_n$ is equal to 0. Performing a Taylor expansion, we therefore have

$$C_r(\Psi - \Psi_{cr}) = C_r(\Psi_{cr}) + \alpha\,(\Psi - \Psi_{cr}) + H.O.T = \alpha\,(\Psi - \Psi_{cr}) + H.O.T$$

where $\alpha = \frac{\partial C_r}{\partial \Psi}|_{\Psi=\Psi_{cr}}$. This suggests that the reference concentration C_r could be proportional to the difference $\Psi - \Psi_{cr}$ and therefore to the excess shear stress $\tau_b - \tau_{cr}$. Smith (1977) [25] and Smith and McLean (1977) [24] suggested that the near-bottom reference concentration C_r at their reference elevation z_r (that they did not take equal to $7d_n$ but approximately equal to z_o) should be proportional to the excess shear stress $\tau_b - \tau_{cr}$ normalized by the critical shear stress τ_{cr}. Thus, the relationship that is suggested in the literature by Smith and McLean is $C_r = \gamma_o C_o \left(\frac{\tau_b - \tau_{cr}}{\tau_{cr}}\right) = \gamma_1 \left(\frac{\tau_b}{\tau_{cr}} - 1\right)$ where γ_o is an empirical constant of the order of 10^{-3}, C_o is a maximum permissible concentration and $\gamma_1 = \gamma_o C_o$. Smith and McLean's work yields $\gamma_1 = 2.4 \cdot 10^{-3}$. The ratio of the bottom shear stress τ_b to the critical shear stress τ_{cr} is proportional to the ratio of the Shields Parameter Ψ to the critical Shields Parameter Ψ_{cr}. Following Smith and McLean, we may therefore expect the reference concentration C_r to be a function of this ratio $\frac{\Psi}{\Psi_{cr}} - 1$.

We plot $y = C_r$ versus $x = \left(\frac{\Psi}{\Psi_{cr}} - 1\right)$, $x = (\Psi - \Psi_{cr})$ and $x = (\Psi - .05)$ and perform a linear regression analysis of the form $y = ax$. In order to check the consistency of the assumption of a linear relationship between these parameters, we also plot $y = ln(C_r)$ versus $x = ln\left(\frac{\Psi}{\Psi_{cr}} - 1\right)$, $x = ln\,(\Psi - \Psi_{cr})$ and $x = ln\,(\Psi - .05)$, and perform a linear regression analysis of the form $y = bx + ln(a)$.

For each analysis, a measure of the average error is given by

$$\overline{x_{C_r}} = average\,(x_{C_r}) \tag{4.15}$$

where x_{C_r} is the ratio of the best C_r value obtained from the measured concentration and the value predicted by the regression formula presented here, i.e.

$$x_{C_r} = \frac{C_{r,measured}}{C_{r,predicted}} \tag{4.16}$$

We also compute the standard deviation

$$\sigma_{C_r} = \sqrt{\frac{\sum \left(x_{C_r} - \overline{x_{C_r}}\right)^2}{N-1}} \tag{4.17}$$

where N is the number of experiments considered.

This analysis is performed for neutral ($[\alpha, \beta] = [1, 0]$) and stratified ($[\alpha, \beta] = [0.8, 4]$) conditions. The results are shown in Tables 4.4 and 4.5 and in Figures 4-7 and 4-8.

When we perform a power-fit analysis of the form $y = ax^b$ with $x = \frac{\Psi}{\Psi_{cr}} - 1$ and

Table 4.4: A linear best-fit analysis is performed between the parameters x and y. a is the first-order coefficient in the equation $y = ax$. The subscript $_n$ denotes the neutral coefficients and the subscript $_s$ denotes the stratified coefficient. The error $\overline{x_{C_r}}$ as defined by (4.16) and the standard deviation σ_{z_o} as defined by (4.17) are also presented. Experiments bar_{26} and bar_{29} are not considered

$y = C_r$vs.	a_n	$\overline{x_{C_r}}$	σ_{C_r}	a_s	$\overline{x_{C_r}}$	σ_{C_r}
$x = \Psi - \Psi_{cr}$	0.0393	0.992	0.521	0.0322	1.01	0.619
$x = \Psi/\Psi_{cr} - 1$	0.00218	1	0.513	0.00179	1.03	0.619
$x = \Psi - .05$	0.0388	0.992	0.522	0.0319	1.01	0.619

Table 4.5: A power best-fit analysis is performed between the parameters x and y. a and b are coefficients in the equation $y = ax^b$. The subscript $_n$ denotes the neutral coefficients and the subscript $_s$ denotes the stratified coefficient. The error $\overline{x_{C_r}}$ as defined by (4.16) and the standard deviation σ_{z_o} as defined by (4.17) are also presented. Experiments bar_{26} and bar_{29} are not considered

$y = C_r$vs.	b_n	a_n	$\overline{x_{C_r}}$	σ_{C_r}	b_s	a_s	$\overline{x_{C_r}}$	σ_{C_r}
$x = \Psi - \Psi_{cr}$	1.15	0.0393	1.11	0.596	1.14	0.0319	1.14	0.715
$x = \Psi/\Psi_{cr} - 1$	1.01	0.00195	1.11	0.569	0.926	0.00189	1.15	0.678
$x = \Psi - .05$	1.15	0.0387	1.11	0.597	1.15	0.0316	1.14	0.716

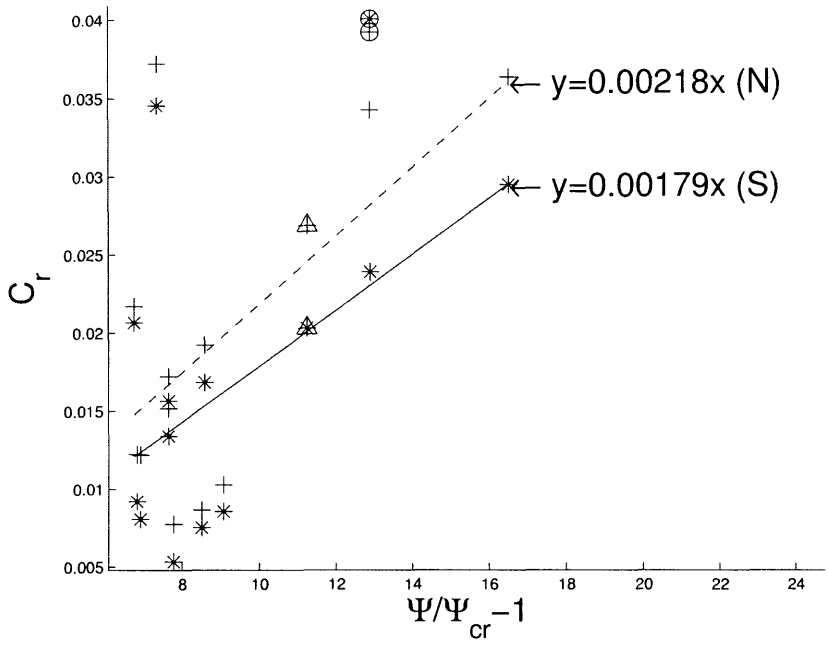

Figure 4-7: C_r vs. $\Psi - \Psi_{cr}$. Linear fit analysis. Dashed line and + : neutral. Plain line and * : stratified. △ : Barton 29 ◯ : Barton 26

$y = C_r$, we obtain for b 1.01 and 0.926 for the neutral and stratified cases, respectively, (Figure 4-8 and Table 4.5). These values are very close to one and therefore suggest a linear relationship between C_r and $\frac{\Psi}{\Psi_{cr}} - 1$. This is further brought out by the error σ_{C_r}, being minimum for the linear and power fit analysis between C_r and $\left(\frac{\Psi}{\Psi_{cr}} - 1\right)$ (Tables 4.4 and 4.5).

We obtain the following predictive formulae

$$\{C_r\}_{neutral} = \left\{0.00218\left(\frac{\Psi}{\Psi_{cr}} - 1\right)\right\}(1 \pm 0.51) \tag{4.18}$$

for the neutral case, and

$$\{C_r\}_{stratified} = \left\{0.00179\left(\frac{\Psi}{\Psi_{cr}} - 1\right)\right\}(1 \pm 0.62) \tag{4.19}$$

for the stratified case (see Figure 4-7 and Table 4.4). The values of the coefficient are very close to the $2.4 \cdot 10^{-3}$ proposed by Smith and McLean (1977) [24]. This

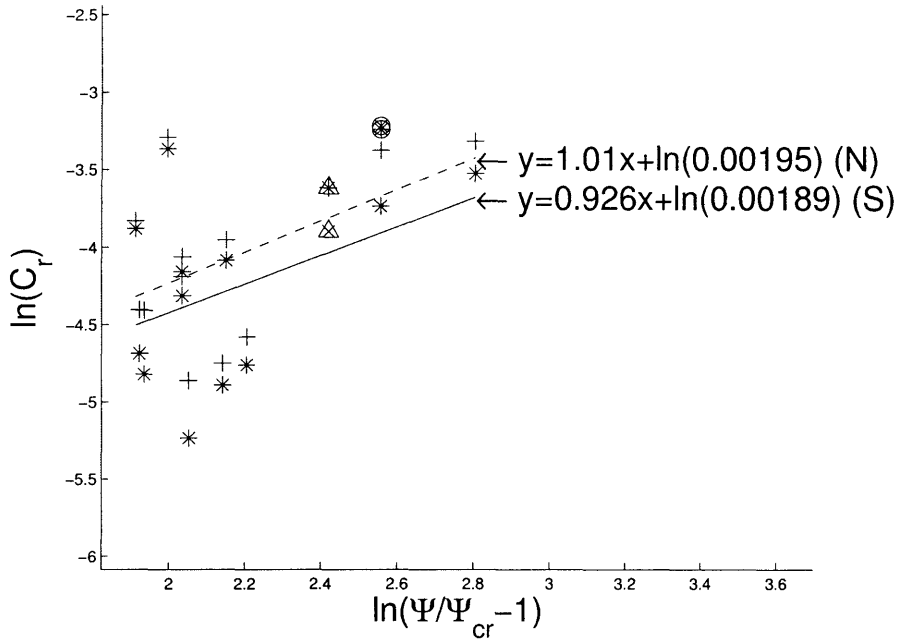

Figure 4-8: C_r vs. $\Psi - \Psi_{cr}$. Power fit analysis. Dashed line and + : neutral. Plain line and * : stratified. $\triangle$: Barton 29 $\bigcirc$: Barton 26

agreement is, however, purely coincidental since Smith and McLean did not use the same definition of z_r as the one used here, $z_r = 7d_n$, but used $z_r = z_o$.

For given Ψ and Ψ_{cr}, the neutral reference concentration is larger than the stratified reference concentration (Equations (4.18) and (4.19)). In Chapter 2, Equation (2.28) relates the stratified and neutral concentration

$$C(z) = C_N(z)\frac{1}{1 + \frac{h^2 q\beta a z_r^q C_r Z_r(z)}{(h-z_r)^q}}, z_r < z < h$$

with $Z_r(z) > 0$ given by Equations (2.24) and (2.25). From this equation, for given q and C_r, $C(z) < C_N(z)$. To fit a same data set, we would therefore expect that $C_{r,neutral} < C_{r,stratified}$. This is not the case in Equations (4.18) and (4.19), due to the fact that $\alpha = 1$ for the neutral case and $\alpha = 0.8$ for the stratified case, thus $q = \frac{w_s \alpha}{\kappa u_*}$ is not the same for the neutral case and the stratified case. We observed in Figure 2-1 that if α is different for the neutral case and the stratified case, for example $\alpha = 0.8$ for the stratified case and $\alpha = 1$ for the neutral case, the concentration can

be larger for the stratified case than for the neutral case. To fit a same data set, the stratified reference concentration should then be smaller than the neutral reference concentration. This is consistent with the formulae (4.18) and (4.19) that we obtained for the reference concentration.

Chapter 5

Implication of results

5.1 Summary of Model for the prediction of suspended sediment concentration distribution and velocity profiles

In the previous chapters, we have taken into account the effects of self-induced sediment stratification in the equations governing a two-dimensional flow of water loaded with sediment through the parameters α (the ratio of eddy viscosity to eddy diffusivity) and β (the parameter that accounts for stratification by scaling the Flux Richardson Number in the eddy viscosity and diffusivity expressions (1.39) and (1.40)). We then solved those equations and obtained explicit mathematical formulae for the ensemble averaged velocity and concentration fields of sediment in a stratified environment. Comparing our model with available data has allowed us to determine the value of α and β. We also used those data to determine explicit formulae for the movable bed roughness z_o and C_r and reference concentration for both neutral and stratified case.

Therefore, to compute the velocity profile and concentration profiles and the transport rate in a channel, we need to know : the depth h, the sediment size d_{sieve}, the slope of the channel S, the sediment density ρ_s, the temperature T. Moreover, we use $g = 9.8m/s^2$, $\kappa = 0.4$, $[\alpha, \beta] = [1, 0]$ for the neutral cases and $[\alpha, \beta] = [0.8, 4]$ for

the stratified cases. From these parameters, we can compute:

- the kinematic viscosity ν by extrapolating linearly from values at $15°C$, $20°C$ and $25°C$ (see Table 3.1)
- the nominal diameter $d_n = d_{sieved}/0.9$
- the relative density of sediment $s = \rho_s/\rho_{water}$. $s = 2.65$ is generally used for quartz sand
- the fluid sediment parameter $S_* = \frac{d_n}{4\nu}\sqrt{(s-1)gd_n}$
- the shear velocity $u_* = \sqrt{ghS}$
- the settling velocity, using the Madsen and Jimenez (2003) (Equation 3.1): $w_{s,J\&M} = W_*\sqrt{(s-1)gd_n}$ with $W_* = \left(A + \frac{B}{S_*}\right)^{-1}$. For natural quartz sediments, and $S_* \in [0.5, 30]$, the values for A and B are 0.954 and 5.121, respectively.
- the Shield parameter $\Psi = \frac{\tau_o}{(\rho_s-\rho)gd_n} = \frac{u_*^2}{(s-1)gd_n}$
- the critical Shield parameter $\Psi_{cr} = 0.095S_*^{-2/3} + 0.056\left(1 - exp\left(\frac{-S_*^{3/4}}{20}\right)\right)$
- the reference concentration C_r: for neutral cases, $C_{r,neutral} = 0.00218\left(\frac{\Psi}{\Psi_{cr}} - 1\right)$, and for stratified cases, $C_{r,stratified} = 0.00179\left(\frac{\Psi}{\Psi_{cr}} - 1\right)$
- the roughness z_o: for neutral cases $z_{o,neutral} = d_n(0.151\left(\Psi - \Psi_{cr}\right) + 0.0558)$ and for stratified cases, $z_{o,stratified} = d_n\left(0.248\left(\Psi - \Psi_{cr}\right) + 0.0523\right)$
- the parabolic neutral eddy viscosity $\nu_T(z) = \kappa u_* z\left(1 - \frac{z}{h}\right)$ for $z_o \leq z \leq h$
- the simplified linear-constant neutral eddy viscosity $\nu_T(z) = \kappa u_* z$ for $z_o < z < z_c$ and $\nu_T(z) = \nu_o = \kappa u_* z_c$ for $z_c \leq z \leq h$ where $z_c = h/6$
- the extremely simplified linear neutral eddy viscosity $\nu_T(z) = \kappa u_* z$ for $z_o < z < h$
- the parameters $a = \frac{g(s-1)w_s\kappa}{u_*^3}$, $b = \frac{g(s-1)w_s\nu_o}{u_*^4}$, $p = \frac{w_s\alpha}{nu_o}$ and $q = \frac{w_s\alpha}{\kappa u_*}$

- For the parabolic model, the neutral concentration distribution over the entire water colum is given by

  $C_N(z) = C_r\left(\frac{(h-z)z_r}{(h-z_r)z}\right)^q, z_r < z \leq h$

  and the neutral velocity is given by

  $U_N(z) = \frac{u_*}{\kappa} ln\left(\frac{z}{z_o}\right), z_o < z \leq h$

- $Z_r(z)$ is defined by

  $Z_r(z) = \frac{1}{h(q-1)}\left[\left(\frac{h}{z_r}-1\right)^{q-1} - \left(\frac{h}{z}-1\right)^{q-1}\right], q \neq 1$

  $Z_r(z) = \frac{1}{h} ln\left|\frac{h/z_r-1}{h/z-1}\right| = \frac{1}{h} ln\frac{z(h-z_r)}{z_r(h-z)}, q = 1$

- For the parabolic model, the stratified concentration distribution is given by

  $C(z_r) = C_r$

  $C(z) = \frac{(h-z)^q}{h^2 q\beta a z^q\left(Z_r(z)+\frac{(h-z_r)^q}{h^2 q\beta a C_r z_r^q}\right)}, z_r \leq z \leq h$

  the stratified velocity is given by

  $U(z) = \frac{u_*}{\kappa} ln\left(\frac{z}{z_o}\right), z_o < z \leq z_r$

  $U(z_r) = \frac{u_*}{\kappa} ln\left(\frac{z_r}{z_o}\right)$

  $U(z) = \frac{u_*}{\kappa} ln\left(\frac{z}{z_o}\right) + \frac{u_*\beta a}{\kappa}\int_{z_r}^{z} \frac{C(z')}{1-\frac{z'}{h}} dz', z_r < z \leq h$

  and the Flux Richardson Number is given by

  $R_f(z) = \frac{azC}{1-\frac{z}{h}+\beta azC}$

- For the simplified linear-constant model, the neutral concentration distribution over the entire water colum is given by

  $C_N(z) = C_r\left(\frac{z_r}{z}\right)^q, z_r < z \leq z_c$

  $C_{Nc} = C_N(z_c) = C_r\left(\frac{z_r}{z_c}\right)^q$

  $C_N(z) = C_{Nc} e^{-p(z-z_c)}, z_c \leq z \leq h$

  and the neutral velocity profile is given by

  $U_N(z) = \frac{u_*}{\kappa} ln\left(\frac{z}{z_o}\right), z_o < z \leq z_c$

  $U_{Nc} = U_N(z_c) = \frac{u_*}{\kappa} ln\left(\frac{z_c}{z_o}\right)$

  $U_N(z) = \frac{u_*^2}{\nu_o}\left(z - z_c + \frac{z_c^2-z^2}{2h}\right) + U_{Nc}, z_c \leq z \leq h$

- $W_c(z) = h^2 p e^{-ph}\left[\frac{e^{-p(z_c-h)}}{p(z_c-h)} - \frac{-e^{p(z-h)}}{p(z-h)} - E_i(p(z_c-h)) + E_i(p(z-h))\right]$, where $E_i(z) = \int_z^\infty \frac{e^{-x}}{x} dx$

- For the simplified linear-constant model, the stratified concentration distribution is given by totally closed analytical formulae

  $C(z_r) = C_r$

  $C(z) = \frac{1}{\beta a z\left(ln\left(\frac{z}{z_r}\right)+\frac{1}{C_r\beta a z_r}\right)}, z_r \leq z \leq z_c, q = 1$

  $C(z) = \frac{1-q}{q\beta a\left(z+z_r^{-q}\left(\frac{1-q}{C_r q\beta a}-z_r\right)z^q\right)}, z_r \leq z \leq z_c, q \neq 1$

  $C(z_c) = \frac{1}{\beta a z_c\left(ln\left(\frac{z_c}{z_r}\right)+\frac{1}{C_r\beta a z_r}\right)} = C_c, q = 1$

  $C(z_c) = \frac{1-q}{q\beta a\left(z_c+z_r^{-q}\left(\frac{1-q}{C_r q\beta a}-z_r\right)z_c^q\right)} = C_c, q \neq 1$

  $C(z) = \frac{C_c exp(-pz)}{exp(-pz_c)+C_c\beta bpW_c(z)}, z_c \leq z \leq h$

  the stratified velocity profile is given by

  $U(z) = \frac{u_*}{\kappa} ln\left(\frac{z}{z_o}\right), z_o < z \leq z_r$

  $U(z_r) = \frac{u_*}{\kappa} ln\left(\frac{z_r}{z_o}\right)$

  $U(z) = \frac{u_*}{\kappa}\left(ln\left(\frac{z}{z_o}\right) + ln\left|C_r\beta a z_r ln\left(\frac{z}{z_r}\right)+1\right|\right), z_r < z \leq z_c, q = 1$

  $U(z) = \frac{u_*}{\kappa} ln\left(\frac{z}{z_o}\right) + \frac{u_*}{\kappa q} ln\left|1+\frac{C_r q\beta a z_r^q}{1-q}(z^{1-q}-z_r^{1-q})\right|, z_r < z \leq z_c, q \neq 1$

  $U(z_c) = \frac{u_*}{\kappa}\left(ln\left(\frac{z_c}{z_o}\right) + ln\left|C_r\beta a z_r ln\left(\frac{z_c}{z_r}\right)+1\right|\right), q = 1$

  $U(z_c) = \frac{u_*}{\kappa} ln\left(\frac{z_c}{z_o}\right) + \frac{u_*}{\kappa q} ln\left|1+\frac{C_r q\beta a z_r^q}{1-q}(z_c^{1-q}-z_r^{1-q})\right| = U_c = U_{Nc}+U_{Sc}, q \neq 1$

  $U(z) = \frac{u_*^2}{\nu_o}\left(z - z_c + \frac{z_c^2-z^2}{2h} + \int_{z_c}^{z}\frac{\beta bC(z')}{1-\frac{z'}{h}}dz'\right) + U_c, z_c \leq z \leq h$

  and the Flux Richardson Number is given by

  $R_f(z) = \frac{azC}{1+\beta azC}, z_r \leq z \leq z_c$

  $R_f(z) = \frac{bC}{\left(1-\frac{z}{h}\right)^2+\beta bC}, z_c \leq z \leq h$

- For the extremely simplified linear model, the neutral concentration distribution over the entire water colum is given by

  $C_N(z) = C_r\left(\frac{z_r}{z}\right)^q, z_r < z \leq h$

  and the neutral velocity profile is given by

  $U_N(z) = \frac{u_*}{\kappa} ln\left(\frac{z}{z_o}\right), z_o < z \leq h$

- For the extremely simplified linear model, the stratified concentration distribution is given by totally closed analytical formulae

  $C(z_r) = C_r$

  $C(z) = \frac{1}{\beta a z\left(ln\left(\frac{z}{z_r}\right)+\frac{1}{C_r\beta a z_r}\right)}, z_r \leq z \leq h, q = 1$

  $C(z) = \frac{1-q}{q\beta a\left(z+z_r^{-q}\left(\frac{1-q}{C_r q\beta a}-z_r\right)z^q\right)}, z_r \leq z \leq h, q \neq 1$

the stratified velocity profile is given by

$U(z) = \frac{u_*}{\kappa} ln\left(\frac{z}{z_o}\right), z_o < z \leq z_r$

$U(z_r) = \frac{u_*}{\kappa} ln\left(\frac{z_r}{z_o}\right)$

$U(z) = \frac{u_*}{\kappa}\left(ln\left(\frac{z}{z_o}\right) + ln\left|C_r \beta a z_r ln\left(\frac{z}{z_r}\right) + 1\right|\right), z_r < z \leq h, q = 1$

$U(z) = \frac{u_*}{\kappa} ln\left(\frac{z}{z_o}\right) + \frac{u_*}{\kappa q} ln\left|1 + \frac{C_r q \beta a z_r^q}{1-q}(z^{1-q} - z_r^{1-q})\right|, z_r < z \leq h, q \neq 1$

and the Flux Richardson Number is given by

$R_f(z) = \frac{azC}{1+\beta azC}, z_r \leq z \leq h$

- All the integrals in the parabolic velocity formulae and the simplified linear-constant velocity formulae for the Outer Layer Region can be computed numerically. However, the extremely simplified linear model initially assumed to be valid between z_o and z_c provides a very good estimate of the parabolic stratified velocity profile when we extend it until the surface.

We can then compute numerically the average velocity

$$\overline{U} = \frac{1}{h}\int_{z_o}^{h} U(z)dz \tag{5.1}$$

the average concentration

$$\overline{C} = \frac{1}{h}\int_{z_r}^{h} C(z)dz \tag{5.2}$$

and the transport rate

$$q_s = \int_{z_r}^{h} C(z)U(z)dz \tag{5.3}$$

Finally, for each experimental run, we compute the concentration error (as defined by (3.5))

$$\epsilon_c = \frac{1}{N_c}\sum_{N_c}\left(\frac{c_{predicted} - c_{measured}}{c_{predicted}}\right)^2$$

where N_c is the number of concentration data points for the experiment, and the velocity error (as defined by (3.5))

$$\epsilon_u = \frac{1}{N_u}\sum_{N_u}\left(\frac{u_{predicted} - u_{measured}}{u_{predicted}}\right)^2$$

where N_u is the number of velocity data points for the experiment. Note that these errors are actually variances, i.e. their square root are the standard deviations.

5.2 Example for a specific case

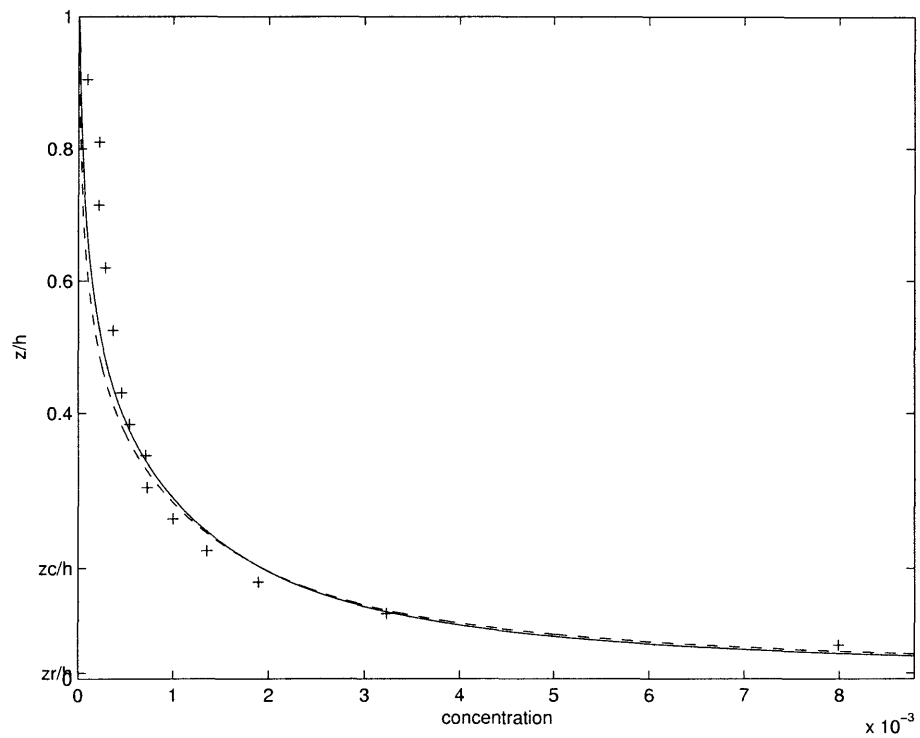

Figure 5-1: Concentration prediction for Barton and Lin, run 36. $h = 16.2cm$, $d_s = 0.18mm$, $u_* = 5.5cm/s$, $w_s = 2.05cm/s$. Dashed line: neutral. Full line: stratified. +:data

The equilibrium-bed experiment for which we obtained the highest reference concentration is run 36 by Barton and Lin (1955) ([2]) (see Table D.1 in Appendix D). We therefore expect to observe the largest stratification effects and run our model for this experiment. The values of h, u_*, d and w_s are presented in Table D.1 (Appendix D). Using the formulae presented in Section 5.1, we compute C_r, z_o, $U(z)$, $C(z)$, $\overline{U}$, $\overline{C}$, q_s, ϵ_c (as defined by (3.4)) and ϵ_u (as defined by (3.5)) with the neutral model ($\alpha = 1$, $\beta = 0$) and the stratified model ($\alpha = 0.8$, $\beta = 4$). The results are presented in Table 5.1 and Figures 5-1 and 5-2. We can evaluate the ratios of

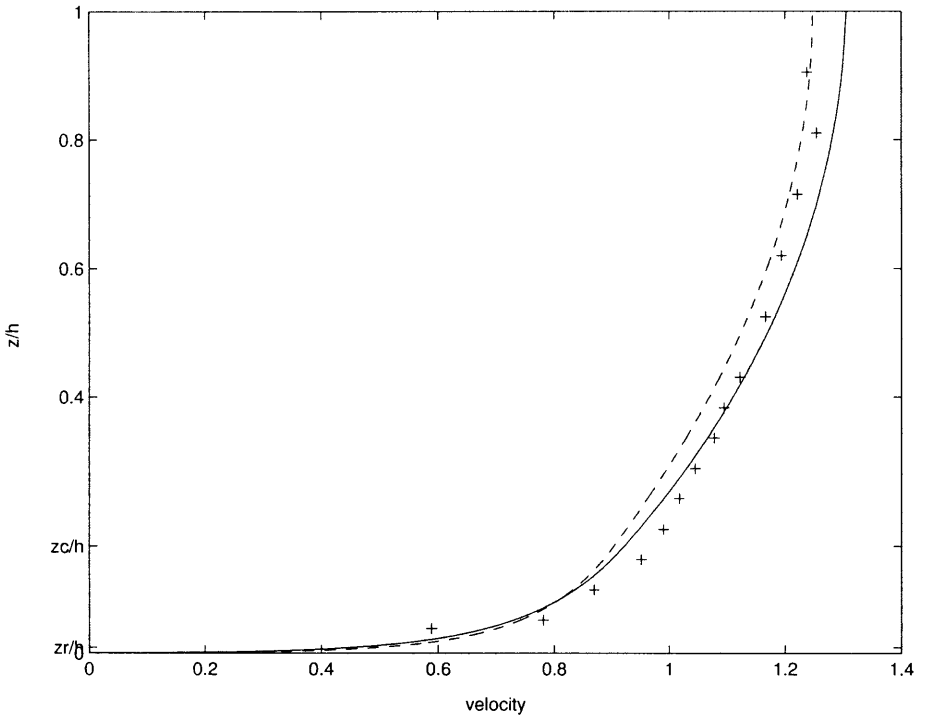

Figure 5-2: Velocity prediction for Barton and Lin, run 36. $h = 16.2cm$, $d_s = 0.18mm$, $u_* = 5.5cm/s$, $w_s = 2.05cm/s$. Dashed line: neutral. Full line: stratified. +:data

the stratified error (or variance) to the neutral error (variance) for the concentration and velocity predictions for this particular experiment: $\frac{\epsilon_{c,S}}{\epsilon_{c,N}} = 0.74$ and $\frac{\epsilon_{u,S}}{\epsilon_{u,N}} = 0.69$, where the subscripts $_N$ and $_S$ refer to the neutral and stratified cases, respectively. For this particular experiment, taking the stratification effects into account in our model therefore improves slightly the concentration and velocity prediction accuracy by roughly 15%.

The ratio between the stratified mean concentration $\overline{C}_s$ and the neutral mean concen-

Table 5.1: Run 36 by Barton and Lin (1954) [2]. Movable bed roughness z_o, reference concentration C_r, average concentration , average velocity , transport rate , concentration error and velocity error (as defined by (3.4) obtained by using our model for the neutral (N) and stratified (S) cases

N	z_o	C_r	$\overline{C}$	$\overline{U}(m/s)$	$q_s(m^2/s)$	ϵ_c	ϵ_u
	3.78e-005	0.036	0.0013	1.07	1.58e-4	0.225	0.00402
S	z_o	C_r	$\overline{C}$	$\overline{U}(m/s)$	$q_s(m^2/s)$	ϵ_c	ϵ_u
	5.42e-005	0.0296	0.0012	1.11	1.54e-4	0.167	0.00276

tration $\overline{C}_n$ is 0.96, the ratio between the stratified mean velocity $\overline{U}_s$ and the neutral mean velocity $\overline{U}_n$ is 1.03 and the ratio between the stratified sediment transport rate $q_{s,S}$ and the neutral sediment transport rate $q_{s,N}$ is 0.97.

In Tables 5.2 and 5.3, we present the results obtained for all equilibrium-bed experiments, i.e. all runs by Barton and Lin (1954) [2], all runs by Brooks (1955) [3], and runs 5, 6, 7, 8 by Lyn (1986) [16]. Using the stratified model improved the velocity prediction by more than 10% for 2 of the 14 equilibrium-bed experiments and lowered it by more than 10% for 2 of the 14 equilibrium-bed experiments in comparison with the neutral model results (see Table 5.3). Using the stratified model improved the velocity prediction by more than 5% for 7 of the 14 equilibrium-bed experiments and lowered it by more than 5% for 3 of the 14 equilibrium-bed experiments in comparison with the neutral model results. Using the stratified model improved the concentration prediction by more than 10% for 4 of the 14 equilibrium-bed experiments and lowered by more than 10% for 6 of the 14 equilibrium-bed experiments in comparison with the neutral model results. Using the stratified model improved the concentration prediction by more than 5% for 6 of the 14 equilibrium-bed experiments and lowered it by more than 5% for 6 of the 14 equilibrium-bed experiments in comparison with the neutral model results.

We consider $x_c = ln\sqrt{\frac{\epsilon_{c,S}}{\epsilon_{c,N}}}$ and $x_u = ln\sqrt{\frac{\epsilon_{u,S}}{\epsilon_{u,N}}}$. $e^{\overline{x}}$, where the overbar represents the mean, is the relative bias between stratified and neutral predictive capability. We obtain $e^{\overline{x_c}} = 1.12$ for the concentration and $e^{\overline{x_u}} = 0.98$ for the velocity. The neutral concentration predictive capability is 12% more accurate than the stratified concentration predictive capability and the stratified velocity predictive capability is 2% more accurate than the neutral velocity predictive capability. e^{σ_x}-1, where σ_x is the variance of x, is approximately the coefficient of variation between neutral and stratified errors. We obtain $e^{\sigma_{x,c}} - 1 = 0.39$ for the concentration and $e^{\sigma_{x,u}} - 1 = 0.18$ for the velocity.

Table 5.2: Neutral model: movable bed roughness $z_{o,N}$, reference concentration $C_{r,N}$, average concentration $\overline{C_N}$, average velocity $\overline{U_N}(m/s)$, transport rate $q_{s,N}(m^2/s)$, concentration error $\epsilon_{c,N}$ (as defined by (3.5) and velocity error $\epsilon_{u,N}$ (as defined by (3.4))

run	$z_{o,N}$	$C_{r,N}$	$\overline{C_N}$	$\overline{U_N}$	$q_{s,N}$	$\epsilon_{c,N}$	$\epsilon_{u,N}$
Barton and Lin (1955) [2]							
26	3.20e-5	0.0281	6.43e-4	1.01	9.43e-5	0.392	0.108
29	2.93e-5	0.0245	5.46e-4	0.94	6.46e-5	0.384	0.273
31	2.30e-5	0.016	3.26e-4	0.765	2.16e-5	0.618	0.003
35	3.20e-5	0.0281	7.51e-4	0.982	8.82e-5	0.354	0.002
36	3.78e-5	0.036	1.26e-3	1.07	1.58e-4	0.225	0.004
Brooks (1954)[3]							
2	1.98e-5	0.0148	5.37e-4	0.703	2.36e-5	0.105	0.004
3	2.34e-5	0.0198	1.01e-3	0.768	4.28e-5	1.901	0.021
4	2.27e-5	0.0187	9.34e-4	0.749	3.75e-5	0.069	0.002
6	2.12e-5	0.0167	7.47e-4	0.721	2.93e-5	0.461	0.002
7	2.12e-5	0.0167	7.46e-4	0.721	2.93e-5	1.733	0.002
Lyn (1986) [16]							
5	2.44e-5	0.017	6.14e-4	0.701	1.74e-5	1.459	0.002
6	2.96e-5	0.0186	4.91e-4	0.748	1.64e-5	2.843	0.003
7	1.99e-5	0.0149	6.55e-4	0.677	2.10e-5	0.178	0.001
8	2.30e-5	0.0151	4.51e-4	0.683	1.40e-5	0.366	0.001

Table 5.3: Stratified model: movable bed roughness $z_{o,S}$, reference concentration $C_{r,S}$, average concentration $\overline{C_S}$, average velocity $\overline{U_S}(m/s)$, transport rate $q_{s,S}(m^2/s)$, ratio of stratified transport rate to neutral transport rate $q_{s,S}/q_{s,N}$, concentration error $\epsilon_{c,S}$ (as defined by (3.5)) and velocity error $\epsilon_{u,S}$ (as defined by (3.4)), square root of the ratio of the stratified concentration error to the neutral concentration error $\sqrt{\frac{\epsilon_{c,S}}{\epsilon_{c,N}}}$, square root of the ratio of the stratified velocity error to the neutral velocity error $\sqrt{\frac{\epsilon_{u,S}}{\epsilon_{u,N}}}$.

run	$z_{o,S}$	$C_{r,S}$	$\overline{C_S}$	$\overline{U_S}$	$q_{s,S}$	$q_{s,S}/q_{s,N}$	$\epsilon_{c,S}$	$\epsilon_{u,S}$	$\sqrt{\frac{\epsilon_{c,S}}{\epsilon_{c,N}}}$	$\sqrt{\frac{\epsilon_{u,S}}{\epsilon_{u,N}}}$
Barton and Lin (1955) [2]										
26	4.46e-5	0.0231	6.29e-4	1.04	9.47e-5	1.005	0.329	0.122	0.92	1.06
29	4.03e-5	0.0201	5.36e-4	0.965	6.50e-5	1.007	0.314	0.270	0.90	0.99
31	3.00e-5	0.0132	3.21e-4	0.778	2.17e-5	1.004	0.464	0.001	0.87	0.72
35	4.46e-5	0.0231	7.30e-4	1.01	8.77e-5	0.995	0.291	0.003	0.91	1.47
36	5.42e-5	0.0296	1.21e-3	1.11	1.54e-4	0.974	0.167	0.003	0.86	0.83
Brooks (1954)[3]										
2	2.60e-5	0.0121	5.36e-4	0.715	2.40e-5	1.018	0.211	0.004	1.42	1.00
3	3.19e-5	0.0162	9.92e-4	0.78	4.25e-5	0.992	4.72	0.022	1.58	1.00
4	3.07e-5	0.0154	9.17e-4	0.761	3.72e-5	0.993	0.025	0.002	0.60	0.91
6	2.83e-5	0.0137	7.38e-4	0.732	2.94e-5	1.001	1.43	0.001	1.76	0.92
7	2.83e-5	0.0137	7.37e-4	0.732	2.94e-5	1.002	5.92	0.002	1.85	0.92
Lyn (1986) [16]										
5	3.17e-5	0.0139	5.73e-4	0.707	1.64e-5	0.939	2.67	0.002	1.35	1.03
6	3.82e-5	0.0152	4.33e-4	0.754	1.45e-5	0.881	6.23	0.002	1.48	0.93
7	2.61e-5	0.0122	6.46e-4	0.685	2.09e-5	0.999	0.166	0.002	0.96	1.23
8	2.94e-5	0.0124	4.23e-4	0.689	1.32e-5	0.947	0.386	0.001	1.03	0.95

5.3 Effects of reference concentration and movable bed roughness uncertainty on predictions

In Section 5.2, we observed for a specific example that taking the stratification effects into account can improve the concentration and velocity prediction accuracy by roughly 15%. However, the formulae that we established in Chapter 4 predict the bed roughness z_o and the reference concentration C_r with a relative accuracy. For stratified conditions, we can indeed predict z_o with a 29% accuracy and C_r with a 60% accuracy (see Tables 4.2 and 4.4). We therefore investigate the effects of this uncertainty on the predictive capability of our model.

For the experiment 36 by Barton and Lin analysed in Section 5.2, we vary the reference concentration and the bed roughness in order to investigate the effect of their variability on the mean concentration, mean velocity and sediment transport rate prediction. We compute $\overline{C}$, $\overline{U}$, q_S for $z_o \in [0.6z_{o,predicted}, 1.4z_{o,predicted}]$ and $C_r \in [0.4C_{r,predicted}, 1.6C_{r,predicted}]$ for neutral and stratified cases, where the subscript $_{predicted}$ indicates that we consider the value of the parameter obtained by using one of our formulae (4.9), (4.11), (4.18) or (4.19). Using Matlab, we can then plot the contours of $\frac{\overline{C}}{\overline{C}_{predicted}}$, $\frac{\overline{U}}{\overline{U}_{predicted}}$, $\frac{q_s}{q_{s,predicted}}$. The results are presented in Figures 5-3, 5-4 and 5-5 for neutral case, and in Figures 5-6, 5-7 and 5-8 for stratified case.

We can first observe in Figures 5-3 and 5-6 that the movable bed roughness does not affect the neutral and stratified average concentration predictions. Indeed the movable bed roughness does not appear in the neutral and stratified concentration formulae (2.72) and (2.74), neither in the average concentration formulae (5.2), since z_r is the lower bound of the integration we perform to calculate the average concentration trough the water column. Similarly we can observe in Figure 5-4 that the reference concentration does not affect the average neutral velocity prediction significantly. This is in agreement with Equation (2.73), indeed the reference concentration does not appear in the neutral velocity formula. However, the reference concentration does affect the average neutral velocity prediction (see Figure 5-7), since it appears indirectly in Equation (2.76) through the concentration in the integral term.

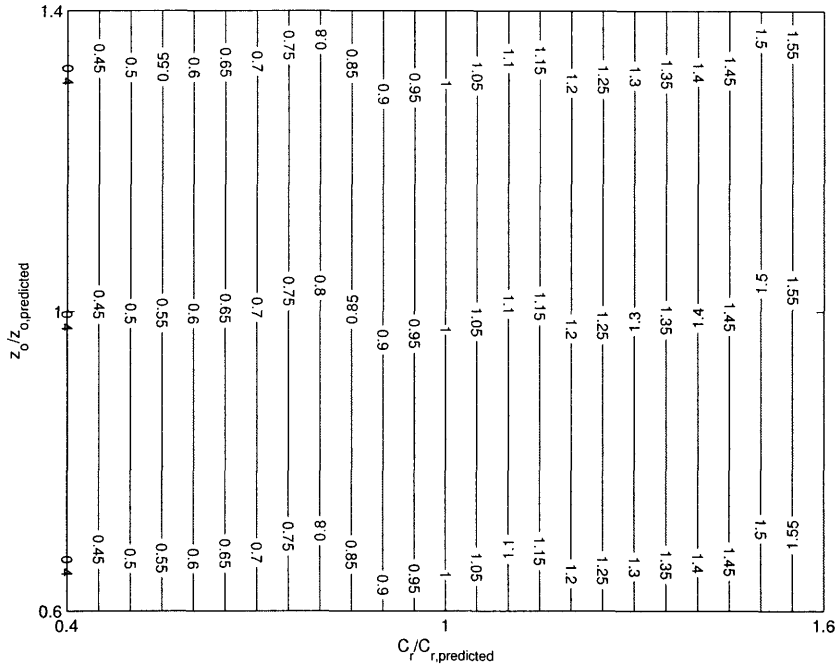

Figure 5-3: Mean neutral concentration variability

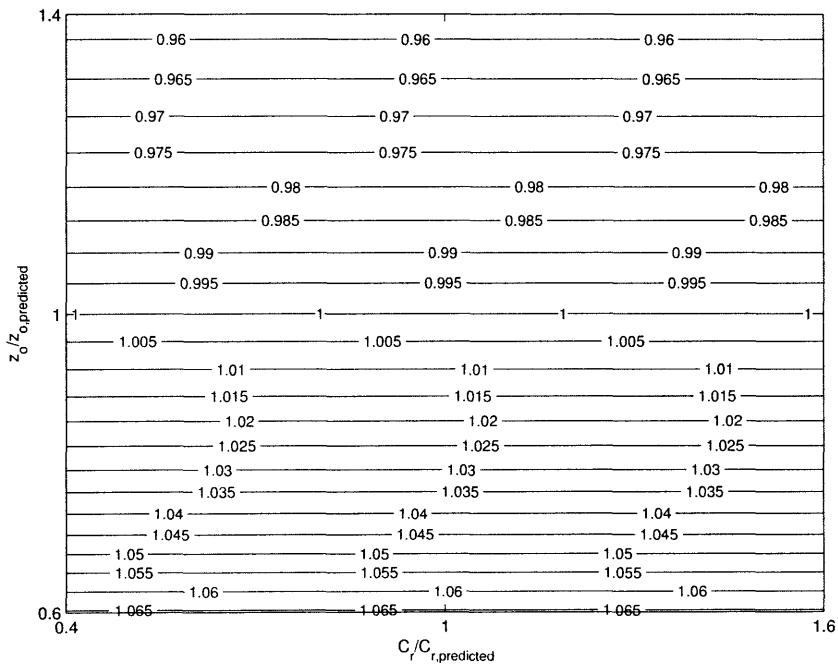

Figure 5-4: Mean neutral velocity variability

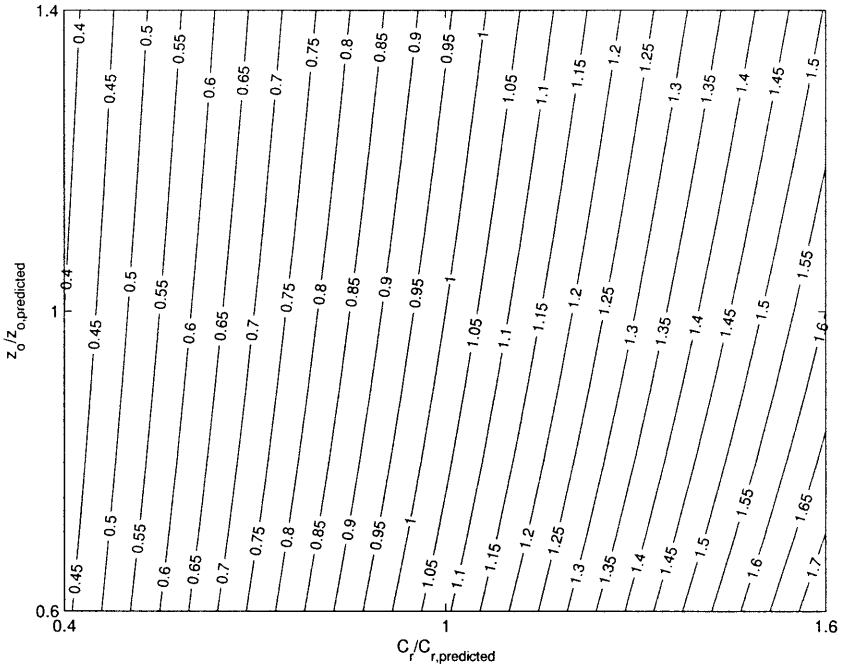

Figure 5-5: Neutral transport rate variability

From Section 5.2, when using values of z_o and C_r predicted by Equations (4.9), (4.11), (4.18) and (4.19), the ratio $\frac{\overline{C}_S}{\overline{C}_N}$ is 0.96 (this corresponds to a 4% difference), the ratio $\frac{\overline{U}_S}{\overline{U}_N}$ is 1.03 (this corresponds to a 3% difference), and the ratio $\frac{\overline{q}_{s,S}}{\overline{q}_{s,N}}$ is 0.97 (this corresponds to a 3% difference).

If z_o is kept constant and equal to $z_{o,predicted}$, a 60% difference between C_r and $C_{r,predicted}$ induces approximately a 55% difference between $\overline{C}_S$ and $\overline{C}_{S,predicted}$ (see Figure 5-6), a 4% difference between $\overline{U}_S$ and $\overline{U}_{S,predicted}$ (see Figure 5-7) and a 50% difference between $\overline{q}_{s,S}$ and $\overline{q}_{s,S,predicted}$ (see Figure 5-8).

If C_r is kept constant and equal to $C_{r,predicted}$, a 40% difference between z_o and $z_{o,predicted}$ induces approximately a 6% difference between $\overline{U}_S$ and $\overline{U}_{S,predicted}$ (see Figure 5-7) and a 10% difference between $\overline{q}_{s,S}$ and $\overline{q}_{s,S,predicted}$ (see Figure 5-8).

From these figures, we can also observe the effects of combined prediction errors on z_o and C_r, which can result in even larger differences. In all the cases, it is clearly seen from Figures 5-6, 5-7 and 5-8 that the error associated with uncertainty in C_r and z_o

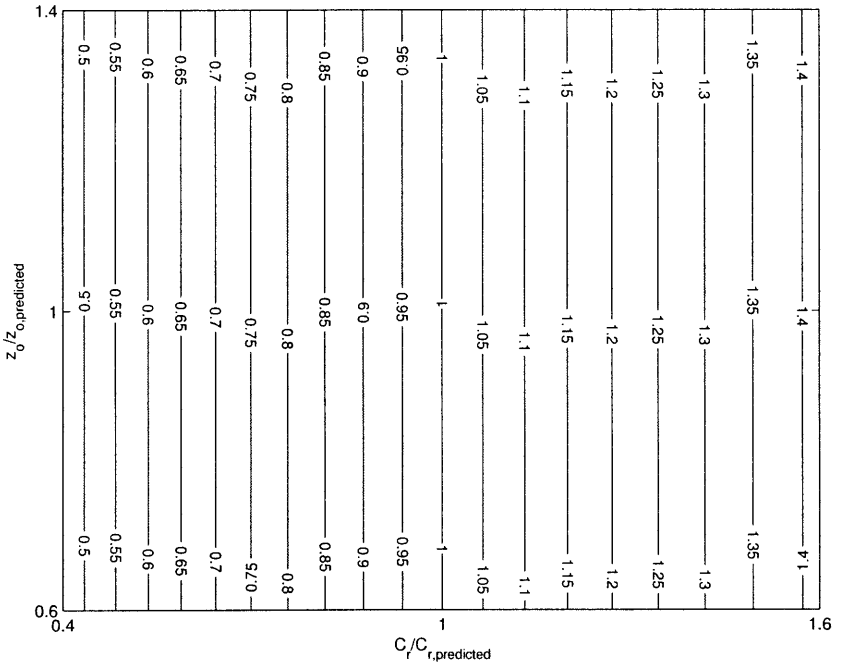

Figure 5-6: Mean stratified concentration variability

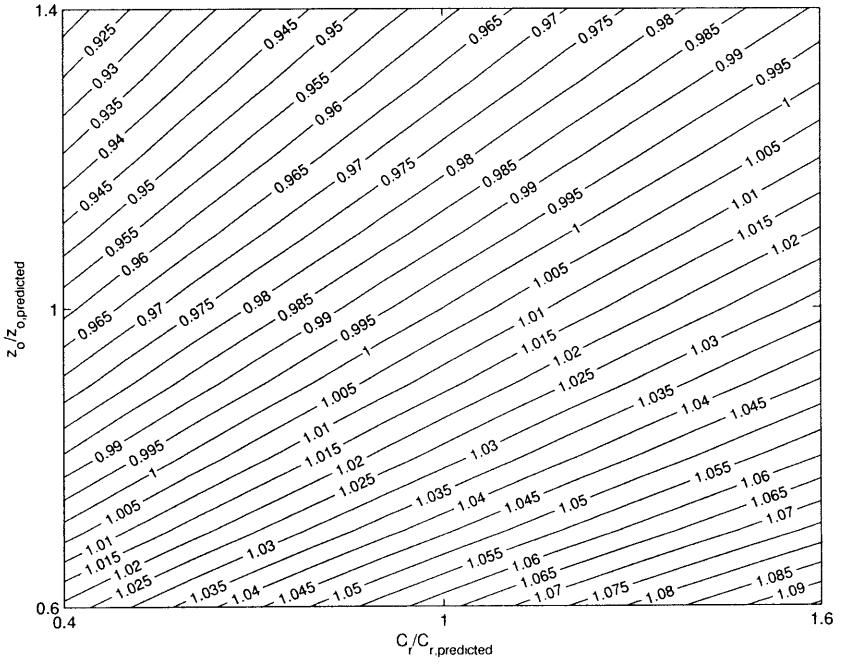

Figure 5-7: Mean stratified velocity variability

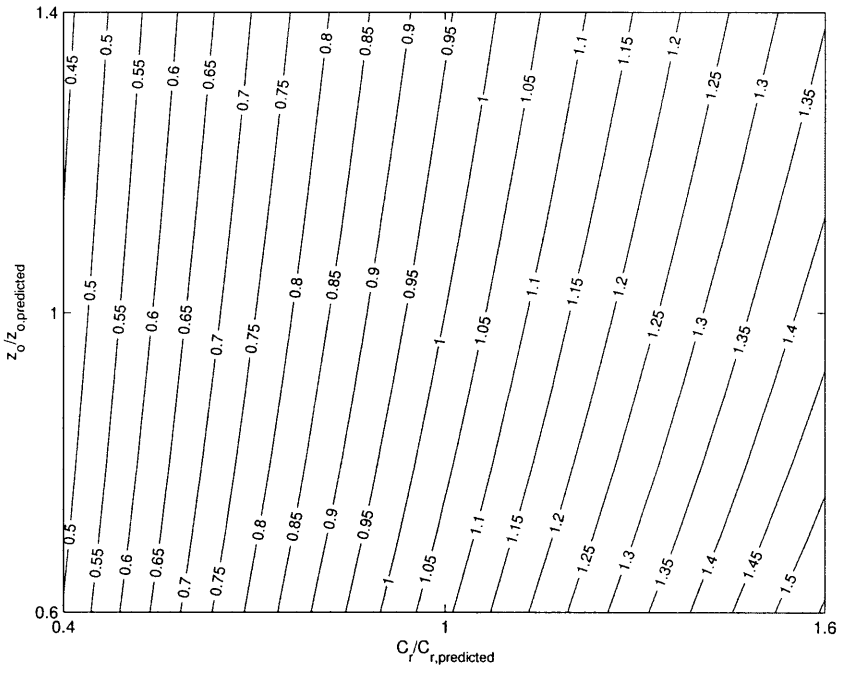

Figure 5-8: Stratified transport rate variability

is as important, if not more important as than, the difference between the stratified and neutral models' predictions for $\overline{C}$, $\overline{U}$ and q_s. Thus, the improvement due to the fact that stratification is taken into account appears to be masked by the variability induced by the uncertainty in our predictions of C_r and z_o.

Chapter 6

Discussion and Conclusions

The effects of sediment-induced stratification on velocity and sediment concentration profiles in a fluid loaded with sediment in suspension and flowing in a rectangular channel with a constant slope have been examined in this work.

The early work concerning sediment stratification relates stratification with von Karman's constant's variability (Vanoni (1975) [1]). Subsequent attempts to account for sediment-induced stratification in turbulent flows were based on the stratified flow analogy (Smith and McLean (1977) [24], Glenn and Grant (1987) [10], Styles and Glenn (2000) [28]). These investigators assumed that, similarly to thermal stratification, sediment stratification can be expressed through a modification to neutral eddy viscosity $\nu_{T,N}$ and eddy diffusivity $\nu_{T,S}$. They introduced the parameters α and β, where α is the ratio between the eddy viscosity ν_T and the eddy diffusivity ν_S and β accounts for stratification by scaling the Flux Richardson Number in the stratified eddy viscosity and diffusivity expressions

$$\nu_T = \nu_{T,N}(1 - \beta R_f)$$

$$\nu_S = \nu_{S,N}(1 - \beta R_f) = \frac{\nu_{T,N}}{\alpha}(1 - \beta R_f)$$

The values of α and β were assumed to be the same as those obtained for thermally stratified atmospheric boundary layers (Businger et al. 1971). However, the correct-

ness of this assumption was not demonstrated.

Villaret and Trowbridge (1991) [30] were the first investigators to attempt to account for stratification effects using suspended sediment data. Following these investigators, we also assume that stratification effects are expressed through the parameters α and β. We solve the governing equations for velocity and sediment concentration for a sediment-induced stratified steady unidirectional flow in an open rectangular channel for three neutral eddy viscosity models: a parabolic neutral eddy viscosity model, a simplified linear-constant neutral eddy viscosity model and an extremely simplified linear neutral eddy viscosity model. Analytically closed form solutions are obtained for both velocity profile and sediment concentration distribution. This is in contrast with other works, e.g. Styles and Glenn (2000) [28], where the two equations are solved iteratively. For the parabolic and linear-constant models, the velocity formulae contain integrals that must be evaluated through time-consuming numerical computation. The concentration formulae and the linear model velocity formulae do not call for numerical integration at all. The average velocity, average concentration and transport rate can finally be estimated through numerical computation.

We use our model with the extensive data set used by Villaret and Trowbridge (1991) [30]. These data were generously provided by Dr. Trowbridge. In contrast to Villaret and Trowbridge, who examined only velocity profiles, we consider both concentration and velocity measurements. Most importantly we vary not only α and β but also the movable bed roughness z_o (which was kept constant by Villaret and Trowbridge) to obtain the optimal set $[\alpha, \beta]$ for the suspended sediment experiments. For neutral conditions, i.e. when stratification effects are not accounted for, $\nu_T = \alpha\nu_S$ and $\beta = 0$ by definition, the optimal value $\alpha = 1$ is obtained. If we want to predict sediment velocity and concentration by accounting for stratification, i.e. $\beta \neq 0$, the optimal values $\alpha = 0.8$ and $\beta = 4.0$ are obtained. For a Flux Richardson Number equal to 0.25 stratification effects would thus completely annihilate turbulent mixing. This result is in agreement with the Miles theorem (1961) [18] which introduces the criti-

cal Flux Richardson Number $R_{f,critical} = 0.25$ above which turbulence production is eliminated. Accounting for stratification slightly improves the prediction of velocity and concentration in comparison with the case where we do not account for stratification. Indeed, when comparing our model to the data set used in its establishment, we observe a 16% improvement of the overal predictive capability of the stratified model compared to the neutral model, a 9% improvement of the concentration prediction, and a 22% improvement of the velocity prediction.

For predictive purposes, we need to know the movable bed roughness z_o and the reference concentration C_r at $z_r = 7d$. We analyse a subset of equilibrium bed experiments, which correspond to natural river conditions, in order to establish a relationship between these parameters and the sediment and flow parameters, namely the density ratio s, the sediment diameter d_n, the shear velocity u_* and the fluid's kinematic viscosity ν and density ρ. From previous studies, we expect a relationship between the ratio of the movable bed roughness z_o to the nominal diameter d_n and the difference between the Shield Parameter Ψ and the critical Shield Parameter Ψ_{cr}. After linear and power series regression analyses, we establish relationships for neutral, $[\alpha, \beta] = [1, 0]$, conditions

$$z_{o,neutral} = d_n(0.151\,(\Psi - \Psi_{cr}) + 0.0558)$$

and for stratified conditions, $[\alpha, \beta] = [0.8, 4]$,

$$z_{o,stratified} = d_n\,(0.248\,(\Psi - \Psi_{cr}) + 0.0523)$$

Knowing the flow and sediment parameters, we are then able to predict the movable bed roughness z_o under neutral conditions with a 36% uncertainty, and with a 29% uncertainty if we account for sediment-induced stratification effects.

Also, from previous works, we expect a linear relationship between the reference concentration C_r and the relative difference between the Shield Parameter Ψ and the critical Shield Parameter Ψ_{cr}. After linear and power series regression analyses, we

establish linear relationships for neutral, $[\alpha, \beta] = [1, 0]$, conditions

$$C_{r,neutral} = 0.00218 \left(\frac{\Psi}{\Psi_{cr}} - 1 \right), z_r = 7d$$

and for stratified conditions, $[\alpha, \beta] = [0.8, 4]$,

$$C_{r,stratified} = 0.00179 \left(\frac{\Psi}{\Psi_{cr}} - 1 \right), z_r = 7d$$

Knowing the flow and sediment parameters, we are then able to predict the reference concentration C_r under neutral conditions with a 51% uncertainty, and with a 62% uncertainty if we account for stratification effects.

The formulae established for the reference concentration and the movable bed roughness only provide estimates of these parameters. A study of the effects of the uncertainty in the values for z_o and C_r on the velocity, concentration and transport rate prediction capability of our model reveals that this uncertainty overshadows the slight improvement resulting from accounting for stratification.

We compare the parabolic, linear-constant and linear neutral eddy viscosity models by example computations. The velocity and concentration formulae that we established are intended to predict velocity and concentration between the bed and $0.4h$, where stratification effects are expected to be most pronounced. Above $0.4h$, other processes affect the flow and stratification is not expected to be significant. With both parabolic and linear-constant models, the concentration is given by totally closed analytical formulae. However, using these models requires time-consuming numerical evaluation of integrals in order to obtain the velocity profiles. Extending the linear model all the way to the surface provides excellent estimates of velocity and concentration profiles and does not require time-consuming numerical computations of integrals.

Finally, by example computations, our model expressing stratification appears to be nearly equivalent to changing von Karman's constant κ by multiplying it by a constant smaller than 1. This is actually equivalent to the "old" method proposed by

Vanoni (1975) [1] but is here derived from fundamentally sound considerations of stratified flow hydrodynamics.

Given the simplicity of our extremely simplified model with a linear eddy viscosity over the entire depth, it is feasible to account for stratification in the governing equations for a two-dimensional steady uniform flow carrying sediment in suspenstion. However, this simple model accounting for stratification awaits better determination of the reference concentration C_r and the movable bed roughness z_o to become of practical importance.

Appendix A

The Ricatti Equation

We consider $y(x)$ which is the solution to the first-order equation

$$\frac{dy}{dx} + P(x)y(x) + Q(x)y^2(x) = R(x) \tag{A.1}$$

where $P(x)$, $Q(x)$ and $R(x)$ are function of x , with $Q(x) \neq 0 \forall x$ and $Q(x)$ a differentiable function of x. We introduce $u(x)$ so that

$$\frac{u'(x)}{u(x)} = y(x)Q(x) \tag{A.2}$$

Then

$$y'(x) = \frac{u''(x)}{Q(x)u(x)} - \frac{u'^2(x)}{Q(x)u^2(x)} - \frac{Q'(x)u'(x)}{Q^2(x)u(x)} \tag{A.3}$$

Introducing

$$y(x) = \frac{u'(x)}{Q(x)u(x)}$$

in equation A.1, we get

$$\frac{u''(x)}{Q(x)u(x)} - P(x)\frac{u'(x)}{Q(x)u(x)} - \frac{Q'(x)u'(x)}{Q^2(x)u(x)} - R(x) = 0 \tag{A.4}$$

Multiplying equation A.4 by $Q(x)u(x)$, we obtain

$$u''(x) + \left(P(x) - \frac{Q'(x)}{Q(x)}\right)u'(x) - R(x)Q(x)u(x) = 0 \tag{A.5}$$

which is an linear second order differential equation.

Appendix B

Parameters for each experiment

Table B.1: Flow and sediment parameters: depth h, shear velocity u_*, sieve grain diameter $d_s = d_{50}$, bottom roughness sediment size d_b ($= d_s$ for equilibrium experiments), kinematic viscosity ν, fluid-sediment parameter S_*, specified settling velocity $w_{s,s}$, Jiménez and Madsen (2003) [14] settling velocity $w_{s,J\&M}$. NS: not specified. ST: starved-bed. EQ: equilibrium-bed. P: no glued sand, plexiglas bed

Run	h, cm	$u_*, cm/s$	d_s, mm	d_b, mm	$T, ^\circ C$	$\nu, mm^2/s$	S_*	$w_{s,s}$	$w_{s,J\&M}$	bed
Barton and Lin (1955) [2]										
26	21.00	4.9	0.18	0.18	NS	1.010	2.82	2.00	2.05	EQ
29	18.30	4.6	0.18	0.18	NS	1.010	2.82	2.00	2.05	EQ
31	12.80	3.8	0.18	0.18	NS	1.010	2.82	2.00	2.05	EQ
35	17.10	4.9	0.18	0.18	NS	1.010	2.82	2.00	2.05	EQ
36	16.20	5.5	0.18	0.18	NS	1.010	2.82	2.00	2.05	EQ
Brooks (1954)[3]										
2	8.65	3.6	0.15	0.15	NS	1.010	2.14	1.70	1.55	EQ
3	7.40	4.1	0.15	0.15	NS	1.010	2.14	1.70	1.55	EQ
4	7.20	4.0	0.15	0.15	NS	1.010	2.14	1.70	1.55	EQ
6	7.40	3.8	0.15	0.15	NS	1.010	2.14	1.70	1.55	EQ
7	7.41	3.8	0.15	0.15	NS	1.010	2.14	1.70	1.55	EQ

Table B.1 (cont.)

Run	h, cm	$u_*, cm/s$	d_s, mm	d_b, mm	$T, ^\circ C$	$\nu, mm^2/s$	S_*	$w_{s,s}$	$w_{s,J\&M}$	bed
Lyn (1986) [16]										
5	5.70	3.9	0.19	0.19	20.9	0.989	3.12	2.50	2.25	EQ
6	6.50	4.2	0.24	0.24	21.3	0.980	4.47	3.30	3.13	EQ
7	6.45	3.6	0.15	0.15	20.7	0.994	2.18	1.80	1.57	EQ
8	6.50	3.7	0.19	0.19	21.1	0.985	3.13	2.50	2.26	EQ
10	5.70	3.7	0.19	0.15	21.1	0.985	3.13	2.50	2.26	ST
11	5.70	3.7	0.19	0.15	21.4	0.978	3.15	2.50	2.27	ST
12	6.60	3.6	0.19	0.15	21.1	0.985	3.13	2.50	2.26	ST
14	5.80	4.2	0.19	0.15	21.1	0.985	3.13	2.50	2.26	ST
15	5.80	4.3	0.19	0.15	21.1	0.985	3.13	2.50	2.26	ST
16	5.80	4.3	0.19	0.15	21.6	0.974	3.17	2.50	2.27	ST
17	5.70	4.3	0.19	0.15	21.3	0.980	3.15	2.50	2.26	ST
Einstein and Chien (1955) [7]										
1	13.80	11.5	1.30	1.30	22.9	0.943	58.50	15.70	14.67	ST
2	12.00	12.8	1.30	1.30	17.2	1.082	50.99	15.70	14.49	ST
3	11.60	13.3	1.30	1.30	18.3	1.053	52.39	15.70	14.53	ST
4	11.50	14.3	1.30	1.30	21.0	0.988	55.87	15.70	14.62	ST
5	11.00	14.5	1.30	1.30	16.9	1.090	50.65	15.70	14.48	ST
6	14.30	11.8	0.90	0.90	25.0	0.896	35.48	12.40	11.58	ST
7	14.20	11.8	0.90	0.90	19.2	1.032	30.82	12.40	11.35	ST
8	13.90	11.5	0.90	0.90	21.8	0.969	32.82	12.40	11.46	ST
9	13.50	11.8	0.90	0.90	22.8	0.947	33.58	12.40	11.49	ST
10	13.00	12.6	0.90	0.90	24.2	0.915	34.75	12.40	11.55	ST
11	13.30	10.6	0.27	0.27	19.9	1.014	5.15	3.90	3.58	ST
12	13.20	10.1	0.27	0.27	21.1	0.985	5.30	3.90	3.63	ST
13	13.40	10.5	0.27	0.27	20.4	1.000	5.22	3.90	3.60	ST
14	12.40	12.1	0.27	0.27	19.4	1.025	5.10	3.90	3.56	ST
15	12.40	11.0	0.27	0.27	18.5	1.050	4.98	3.90	3.51	ST
16	11.90	12.5	0.27	0.27	16.9	1.090	4.79	3.90	3.44	ST
Vanoni And Nomicos (1960) [21]										
7	7.80	4.1	0.16	NS	NS	1.010	2.36	1.90	1.72	ST
Coleman (1981) [4] Coarse Sand										
22	17.00	4.1	0.21	P	23.8	0.923	3.88	3.00	2.70	ST
23	17.00	4.1	0.21	P	23.8	0.923	3.88	3.00	2.70	ST

Table B.1 (cont.)

Run	h, cm	$u_*, cm/s$	d_s, mm	d_b, mm	$T, ^\circ C$	$\nu, mm^2/s$	S_*	$w_{s,s}$	$w_{s,J\&M}$	bed
24	16.90	4.1	0.21	P	23.8	0.923	3.88	3.00	2.70	ST
25	16.70	4.0	0.21	P	23.9	0.921	3.89	3.00	2.71	ST
26	17.10	4.1	0.21	P	19.5	1.023	3.50	3.00	2.54	ST
27	16.80	4.1	0.21	P	23.0	0.942	3.81	3.00	2.67	ST
28	17.00	4.1	0.21	P	22.9	0.944	3.80	3.00	2.67	ST
29	16.80	4.0	0.21	P	23.3	0.935	3.83	3.00	2.68	ST
30	16.80	4.1	0.21	P	23.7	0.926	3.87	3.00	2.70	ST
31	17.20	4.1	0.21	P	23.9	0.921	3.89	3.00	2.71	ST
33	17.40	4.1	0.42	P	22.5	0.953	10.63	6.30	6.05	ST
34	17.20	4.1	0.42	P	23.3	0.935	10.84	6.30	6.09	ST
35	17.20	4.1	0.42	P	23.0	0.942	10.76	6.30	6.08	ST
36	17.10	4.1	0.42	P	23.6	0.928	10.92	6.30	6.11	ST
37	16.70	4.1	0.42	P	21.7	0.971	10.43	6.30	6.01	ST
38	16.70	4.3	0.42	P	22.1	0.962	10.53	6.30	6.03	ST
39	17.10	4.4	0.42	P	22.3	0.958	10.58	6.30	6.04	ST
40	17.10	4.5	0.42	P	22.9	0.944	10.74	6.30	6.07	ST
Coleman (1981) [4] Fine Sand										
2	17.10	4.1	0.11	P	24.6	0.905	1.50	1.10	1.02	ST
3	17.20	4.1	0.11	P	25.0	0.896	1.52	1.10	1.03	ST
4	17.10	4.1	0.11	P	25.3	0.889	1.53	1.10	1.03	ST
5	17.10	4.1	0.11	P	23.9	0.921	1.47	1.10	1.00	ST
6	17.00	4.1	0.11	P	24.0	0.919	1.48	1.10	1.01	ST
7	17.10	4.1	0.11	P	22.7	0.948	1.43	1.10	0.98	ST
8	17.30	4.1	0.11	P	23.3	0.935	1.45	1.10	0.99	ST
9	17.20	4.1	0.11	P	24.4	0.910	1.49	1.10	1.01	ST
10	17.10	4.1	0.11	P	23.9	0.921	1.47	1.10	1.00	ST
11	16.90	4.1	0.11	P	24.2	0.914	1.49	1.10	1.01	ST
12	17.30	4.1	0.11	P	24.7	0.903	1.50	1.10	1.02	ST
13	17.10	4.1	0.11	P	22.7	0.948	1.43	1.10	0.98	ST
14	17.10	4.1	0.11	P	22.7	0.948	1.43	1.10	0.98	ST
15	17.10	4.1	0.11	P	22.9	0.944	1.44	1.10	0.99	ST
16	17.10	4.1	0.11	P	23.0	0.942	1.44	1.10	0.99	ST
17	17.10	4.1	0.11	P	23.8	0.923	1.47	1.10	1.00	ST
18	17.12	4.1	0.11	P	22.8	0.946	1.44	1.10	0.98	ST

Table B.1 (cont.)

Run	h, cm	$u_*, cm/s$	d_s, mm	d_b, mm	$T, ^\circ C$	$\nu, mm^2/s$	S_*	$w_{s,s}$	$w_{s,J\&M}$	bed
19	17.00	4.1	0.11	P	23.4	0.932	1.46	1.10	0.99	ST
20	17.00	4.1	0.11	P	23.9	0.921	1.47	1.10	1.00	ST

Appendix C

Best α and β for each experiment

Table C.1: Best-fit α and β for each experiment: run, minimum error $\sqrt{\epsilon_c}_{min}$ as defined by (3.4), β_c and α_c which minimize $\sqrt{\epsilon_c}$, corresponding $C_{r,c}$ (cm^3/cm^3) and $z_{o,c}$ (m), minimum error $\sqrt{\epsilon_u}_{min}$ as defined by (3.5), β_u and α_u which minimize $\sqrt{\epsilon_u}$, corresponding $C_{r,u}$ (cm^3/cm^3) and $z_{o,u}$ (m), minimum error $\sqrt{\sqrt{\epsilon_u}\sqrt{\epsilon_c}}_{min}$,β and α which minimize $\epsilon = \sqrt{\sqrt{\epsilon_u}\sqrt{\epsilon_c}}$, corresponding C_r (cm^3/cm^3) and z_o (m)

Table C.1

Barton and Lin(1955)[2]															
26	0.55	0.85	8.5	2.01	1.80e-2	0.14	1.05	4.5	1.47	3.11e-3	0.27	1.00	5.0	5.88e-1	1.71e-3
29	0.39	0.75	10.0	4.32e-2	8.13e-4	0.30	0.90	10.0	9.30e-1	9.66e-3	0.36	0.75	10.0	4.32e-2	8.13e-4
31	0.32	0.70	9.0	1.41e-1	2.50e-4	0.10	1.25	9.0	3.12	7.53e-4	0.19	0.70	9.5	4.42e-1	8.53e-4
35	0.44	0.60	10.0	1.66e-2	4.96e-5	0.18	0.70	0.5	1.29e-2	2.50e-5	0.29	0.80	0.5	1.79e-2	2.52e-5
36	0.37	0.75	9.0	5.02e-2	1.09e-4	0.22	1.10	5.5	2.14	9.83e-4	0.29	0.75	9.0	5.02e-2	1.09e-4
Brooks(1954)[3]															
2	0.19	1.20	5.5	4.30e-1	7.90e-5	0.07	1.20	5.5	4.30e-1	7.90e-5	0.12	1.20	5.5	4.30e-1	7.90e-5
3	0.07	1.25	6.5	2.62e-2	6.58e-5	0.13	0.50	10.0	6.59e-3	6.46e-5	0.10	1.20	9.5	2.86e-2	7.78e-5
4	0.07	1.10	1.5	2.95e-2	3.16e-5	0.09	1.25	5.0	8.60e-2	5.14e-5	0.09	1.00	4.5	3.09e-2	3.88e-5
6	0.30	1.15	8.5	6.51e-2	4.57e-5	0.13	1.10	9.5	6.05e-2	4.90e-5	0.20	1.10	10.0	6.77e-2	5.38e-5
7	0.41	1.30	9.5	8.47e-1	2.80e-4	0.16	1.30	10.0	1.27	4.00e-4	0.25	1.30	10.0	1.27	4.00e-4
Lyn(1986)[16]															
5	0.45	1.00	10.0	2.15e-2	4.23e-5	0.19	1.15	10.0	7.00e-1	2.27e-4	0.30	1.00	10.0	2.15e-2	4.23e-5
6	0.42	1.10	10.0	4.28e-1	1.23e-4	0.19	0.50	10.0	6.78e-3	3.56e-5	0.29	1.10	10.0	4.28e-1	1.23e-4
7	0.35	0.90	10.0	2.45e-2	4.90e-5	0.10	1.10	9.5	4.03e-1	2.56e-4	0.18	0.90	10.0	2.45e-2	4.90e-5
8	0.42	0.85	10.0	2.41e-2	4.57e-5	0.13	1.00	10.0	6.42e-1	2.61e-4	0.24	0.85	10.0	2.41e-2	4.57e-5
10	0.37	0.75	10.0	3.49e-3	9.08e-6	0.10	1.30	2.5	8.48e-2	1.15e-5	0.20	0.80	5.0	3.71e-3	8.27e-6
11	0.36	0.70	10.0	1.28e-3	7.90e-6	0.11	1.30	1.5	2.88e-2	8.19e-6	0.20	0.70	4.5	1.21e-3	7.53e-6
12	0.45	0.90	10.0	4.54e-2	3.99e-5	0.13	1.00	10.0	7.09e-1	1.85e-4	0.25	0.90	10.0	4.54e-2	3.99e-5
14	0.29	0.85	10.0	2.19e-2	1.98e-5	0.14	0.50	10.0	5.91e-3	1.55e-5	0.21	0.85	10.0	2.19e-2	1.98e-5
15	0.28	0.80	7.5	4.56e-3	9.45e-6	0.15	1.20	10.0	2.51e-1	3.95e-5	0.21	0.80	10.0	4.89e-3	1.00e-5
16	0.25	0.80	6.5	2.60e-3	8.19e-6	0.12	1.30	10.0	1.56e-1	2.50e-5	0.18	0.80	10.0	2.74e-3	8.56e-6
17	0.22	0.80	10.0	1.85e-3	6.19e-6	0.12	1.30	10.0	2.11e-2	8.34e-6	0.17	0.80	10.0	1.85e-3	6.19e-6

Table C.1 cont.

Run	$\sqrt{\epsilon_c}$	α_c	β_c	$C_{r,c}$	$z_{o,c}$	$\sqrt{\epsilon_u}$	α_u	β_u	$C_{r,u}$	$z_{o,u}$	ϵ	α	β	C_r	z_o
Einstein and Chien(1955)[7]															
1	0.33	0.55	10.0	1.04e-2	1.27e-4	0.14	1.15	10.0	6.45e-2	1.33e-4	0.23	0.55	10.0	1.04e-2	1.27e-4
2	0.41	0.65	2.5	2.95e-2	6.06e-5	0.17	0.80	10.0	2.01e-1	8.95e-5	0.31	0.50	10.0	3.43e-2	7.58e-5
3	0.41	0.60	3.5	3.86e-2	7.89e-5	0.19	0.80	9.5	3.06e-1	1.15e-4	0.32	0.50	8.0	4.24e-2	9.16e-5
4	0.37	0.80	0.5	6.60e-2	1.31e-4	0.17	0.65	10.0	2.13e-1	2.03e-4	0.32	0.50	10.0	9.28e-2	1.92e-4
6	0.37	1.00	0.5	1.14e-2	7.32e-5	0.22	1.30	10.0	4.01e-2	8.38e-5	0.31	0.85	10.0	1.17e-2	7.96e-5
7	0.36	1.00	0.5	2.75e-2	7.53e-5	0.18	1.30	7.5	6.50e-1	1.13e-4	0.32	0.70	10.0	2.87e-2	9.22e-5
8	0.50	0.95	0.5	2.80e-2	8.03e-5	0.21	1.15	10.0	2.91e-1	1.10e-4	0.37	0.60	10.0	2.88e-2	9.78e-5
9	0.42	0.95	0.5	5.07e-2	9.43e-5	0.20	1.00	10.0	5.61e-1	1.54e-4	0.34	0.50	10.0	5.30e-2	1.36e-4
10	0.40	1.00	0.5	8.25e-2	1.27e-4	0.16	0.90	10.0	4.03e-1	1.92e-4	0.29	0.50	10.0	8.86e-2	1.83e-4
11	0.28	0.95	10.0	2.37e-2	4.24e-5	0.12	1.15	0.5	2.73e-2	3.88e-5	0.18	1.05	0.5	2.41e-2	3.88e-5
Vanoni and Nomicos(1960)[21]															
7	0.18	1.20	9.5	3.08e-2	5.22e-5	0.22	1.30	10.0	7.08e-2	6.02e-5	0.22	1.20	10.0	3.29e-2	5.34e-5
Coleman(1981)[4] Fine Sand															
2	0.16	0.70	8.5	2.20e-3	6.80e-6	0.07	0.50	9.5	1.45e-3	6.80e-6	0.11	0.70	8.5	2.20e-3	6.80e-6
3	0.19	0.75	2.5	4.54e-3	7.92e-6	0.10	0.50	8.5	2.85e-3	9.12e-6	0.14	0.70	7.5	4.37e-3	9.12e-6
4	0.17	0.85	1.0	8.61e-3	8.01e-6	0.07	0.95	7.0	1.37e-2	1.15e-5	0.11	0.75	6.5	7.98e-3	1.04e-5
5	0.24	0.85	0.5	1.12e-2	8.95e-6	0.11	0.50	4.5	6.08e-3	1.10e-5	0.16	0.75	4.5	1.04e-2	1.14e-5
6	0.16	0.95	0.5	1.69e-2	9.64e-6	0.09	0.50	3.5	7.55e-3	1.17e-5	0.13	0.85	3.0	1.55e-2	1.18e-5
7	0.16	0.95	0.5	2.04e-2	9.98e-6	0.09	0.50	5.5	9.78e-3	1.50e-5	0.13	0.75	5.5	1.73e-2	1.62e-5
8	0.33	0.80	0.5	1.88e-2	1.13e-5	0.11	0.90	3.0	3.10e-2	1.68e-5	0.19	0.70	3.0	1.76e-2	1.54e-5
9	0.19	0.95	1.5	3.32e-2	1.40e-5	0.12	0.50	4.0	1.43e-2	1.81e-5	0.15	0.80	4.0	2.91e-2	2.01e-5
10	0.12	1.05	0.5	4.23e-2	1.17e-5	0.10	0.50	4.0	1.70e-2	1.88e-5	0.12	0.80	4.5	3.65e-2	2.34e-5
11	0.21	1.05	0.5	4.81e-2	1.11e-5	0.12	0.50	4.0	1.94e-2	1.89e-5	0.16	0.75	4.5	3.77e-2	2.36e-5
12	0.34	0.90	0.5	3.92e-2	1.33e-5	0.13	0.80	3.5	4.75e-2	2.81e-5	0.21	0.70	3.5	3.42e-2	2.55e-5
13	0.20	0.85	3.0	4.77e-2	2.33e-5	0.13	0.50	4.0	2.24e-2	2.44e-5	0.16	0.75	4.5	4.38e-2	3.14e-5
14	0.20	1.00	1.0	5.62e-2	1.51e-5	0.11	0.50	4.0	2.46e-2	2.58e-5	0.16	0.75	4.0	4.62e-2	2.99e-5
15	0.22	1.10	0.5	6.79e-2	1.35e-5	0.10	0.50	4.0	2.68e-2	2.75e-5	0.15	0.75	4.5	5.43e-2	3.77e-5
16	0.22	1.15	0.5	8.09e-2	1.39e-5	0.12	0.55	4.5	3.40e-2	3.42e-5	0.17	0.75	4.5	6.03e-2	4.21e-5
17	0.27	1.15	0.5	8.34e-2	1.39e-5	0.13	0.50	4.5	3.12e-2	3.42e-5	0.20	0.75	4.5	6.29e-2	4.30e-5
18	0.24	1.10	1.0	8.08e-2	1.72e-5	0.10	0.50	3.5	2.89e-2	2.82e-5	0.16	0.80	4.0	6.56e-2	3.95e-5
19	0.23	1.20	0.5	9.89e-2	1.54e-5	0.13	0.55	4.0	3.76e-2	3.68e-5	0.18	0.80	4.0	7.63e-2	4.65e-5
20	0.25	1.15	1.0	1.10e-1	1.90e-5	0.13	0.50	4.0	3.65e-2	3.86e-5	0.19	0.80	4.5	9.65e-2	6.49e-5

Appendix D

Results for each experiment with neutral and stratified model

Table D.1: For each experiment, number of measurements points N_c between the bed and $0.4h$ in the concentration dataset, number of measurements points N_u between the bed and $0.4h$ in the concentration dataset, neutral movable bed roughness $z_{o,n}(m)$, neutral reference concentration $C_{r,n}(cm^3/cm^3)$, neutral concentration error $\sqrt{\epsilon_{c,n}}$ as defined by (3.4), neutral velocity error $\sqrt{\epsilon_{u,n}}$ as defined by (3.5), stratified movable bed roughness $z_{o,s}(m)$, stratified reference concentration $C_{r,s}(cm^3/cm^3)$, stratified concentration error $\sqrt{\epsilon_{c,s}}$ as defined by (3.4), stratified velocity error $\sqrt{\epsilon_{u,s}}$ as defined by (3.5), and $Max_{z_o<z<0.4h}\{R_f(z)\}$ with R_f defined by (2.14) and (2.59)

Run	N_c	N_u	$z_{o,n}$	$C_{r,n}$	$\sqrt{\epsilon_{c,n}}$	$\sqrt{\epsilon_{u,n}}$	$z_{o,s}$	$C_{r,s}$	$\sqrt{\epsilon_{c,s}}$	$\sqrt{\epsilon_{u,s}}$	$R_{f,max}$
Barton and Lin (1955) [2]											
26	8	9	1.61e-4	4.38e-2	0.632	0.270	3.19e-4	4.48e-2	0.644	0.193	0.051
29	7	8	1.90e-4	3.02e-2	0.422	0.426	3.05e-4	2.27e-2	0.434	0.397	0.034
31	5	6	1.91e-5	4.30e-2	0.461	0.234	4.15e-5	4.10e-2	0.352	0.194	0.084
35	9	9	2.42e-5	3.83e-2	0.584	0.173	3.54e-5	2.65e-2	0.507	0.236	0.037
36	8	9	3.12e-5	4.01e-2	0.400	0.261	4.99e-5	3.22e-2	0.404	0.240	0.046
Brooks (1954)[3]											
2	4	7	1.26e-5	2.44e-2	0.509	0.177	1.90e-5	2.31e-2	0.530	0.109	0.044
3	4	5	4.72e-5	1.14e-2	0.510	0.198	5.38e-5	9.33e-3	0.580	0.174	0.026

Table D.1 (cont.)

Run	N_c	N_u	$z_{o,n}$	$C_{r,n}$	$\sqrt{\epsilon_{c,n}}$	$\sqrt{\epsilon_{u,n}}$	$z_{o,s}$	$C_{r,s}$	$\sqrt{\epsilon_{c,s}}$	$\sqrt{\epsilon_{u,s}}$	$R_{f,max}$
4	4	5	2.86e-5	2.13e-2	0.321	0.175	3.54e-5	1.85e-2	0.389	0.119	0.039
6	5	8	1.77e-5	1.69e-2	0.542	0.174	2.29e-5	1.48e-2	0.589	0.146	0.033
7	5	5	2.17e-5	1.92e-2	0.637	0.226	2.87e-5	1.73e-2	0.658	0.198	0.036
Lyn (1986) [16]											
5	12	14	2.39e-5	9.05e-3	0.503	0.214	2.70e-5	6.10e-3	0.621	0.209	0.019
6	17	17	2.25e-5	1.06e-2	0.607	0.217	2.66e-5	9.07e-3	0.730	0.210	0.036
7	10	10	2.16e-5	1.38e-2	0.400	0.156	2.71e-5	1.02e-2	0.479	0.130	0.025
8	12	18	2.17e-5	1.44e-2	0.466	0.180	2.61e-5	9.37e-3	0.510	0.166	0.032
10	12	12	7.45e-6	7.11e-3	0.541	0.105	8.12e-6	3.60e-3	0.376	0.104	0.013
11	12	10	7.23e-6	4.14e-3	0.636	0.106	7.53e-6	1.78e-3	0.434	0.106	0.007
12	13	15	1.38e-5	1.37e-2	0.489	0.167	1.69e-5	8.79e-3	0.551	0.156	0.032
14	10	8	9.75e-6	1.57e-2	0.341	0.170	1.20e-5	1.10e-2	0.429	0.161	0.026
15	11	10	8.19e-6	7.67e-3	0.455	0.175	8.79e-6	4.19e-3	0.285	0.169	0.010
16	11	13	7.53e-6	4.79e-3	0.458	0.139	7.90e-6	2.51e-3	0.253	0.135	0.006
17	10	14	5.70e-6	3.22e-3	0.401	0.131	5.89e-6	1.75e-3	0.234	0.128	0.004
Einstein and Chien (1955) [7]											
1	9	24	1.16e-4	1.18e-2	0.614	0.226	1.20e-4	1.06e-2	0.499	0.203	0.051
2	10	22	5.56e-5	4.18e-2	0.576	0.310	6.47e-5	4.48e-2	0.589	0.270	0.110
3	10	21	6.82e-5	5.12e-2	0.561	0.335	8.14e-5	5.92e-2	0.603	0.291	0.121
4	10	19	1.27e-4	8.26e-2	0.475	0.371	1.61e-4	1.21e-1	0.619	0.296	0.152
6	9	19	7.32e-5	1.12e-2	0.368	0.271	7.60e-5	9.75e-3	0.424	0.258	0.026
7	11	17	7.46e-5	2.67e-2	0.358	0.313	8.17e-5	2.61e-2	0.415	0.286	0.059
8	13	17	7.88e-5	2.88e-2	0.502	0.337	8.66e-5	2.84e-2	0.509	0.307	0.067
9	11	17	9.22e-5	5.09e-2	0.414	0.377	1.09e-4	5.55e-2	0.454	0.331	0.100
10	12	17	1.24e-4	7.79e-2	0.396	0.373	1.50e-4	9.20e-2	0.458	0.303	0.119
11	8	22	3.86e-5	2.25e-2	0.285	0.120	4.01e-5	1.85e-2	0.344	0.139	0.019
Vanoni And Nomicos (1960) [21]											
7	5	19	3.94e-5	8.48e-3	0.478	0.366	4.16e-5	5.98e-3	0.567	0.352	0.016
Coleman (1981) [4] Fine Sand											
2	6	6	5.99e-6	3.94e-3	0.343	0.096	6.37e-6	2.64e-3	0.212	0.084	0.020
3	6	6	7.40e-6	7.48e-3	0.332	0.129	8.35e-6	5.19e-3	0.226	0.111	0.035
4	6	6	7.66e-6	1.16e-2	0.258	0.134	9.29e-6	8.41e-3	0.173	0.096	0.048
5	6	6	8.69e-6	1.51e-2	0.284	0.140	1.12e-5	1.14e-2	0.251	0.109	0.059
6	6	6	9.29e-6	1.83e-2	0.168	0.131	1.27e-5	1.45e-2	0.182	0.090	0.067

Table D.1 (cont.)

Run	N_c	N_u	$z_{o,n}$	$C_{r,n}$	$\sqrt{\epsilon_{c,n}}$	$\sqrt{\epsilon_{u,n}}$	$z_{o,s}$	$C_{r,s}$	$\sqrt{\epsilon_{c,s}}$	$\sqrt{\epsilon_{u,s}}$	$R_{f,max}$
7	6	6	9.47e-6	2.17e-2	0.159	0.173	1.41e-5	1.80e-2	0.163	0.111	0.076
8	7	7	1.06e-5	2.86e-2	0.393	0.164	1.87e-5	2.52e-2	0.417	0.115	0.086
9	6	6	1.11e-5	3.17e-2	0.219	0.186	2.01e-5	2.91e-2	0.191	0.122	0.088
10	6	6	1.07e-5	3.59e-2	0.236	0.193	2.12e-5	3.46e-2	0.153	0.106	0.094
11	6	6	9.98e-6	4.05e-2	0.254	0.207	2.20e-5	4.11e-2	0.213	0.125	0.098
12	7	7	1.19e-5	4.58e-2	0.353	0.218	3.33e-5	5.21e-2	0.446	0.135	0.103
13	6	6	1.19e-5	4.45e-2	0.273	0.224	2.90e-5	4.77e-2	0.205	0.132	0.104
14	6	6	1.17e-5	4.79e-2	0.274	0.226	3.14e-5	5.37e-2	0.218	0.121	0.107
15	6	6	1.18e-5	5.09e-2	0.318	0.233	3.42e-5	5.88e-2	0.226	0.109	0.109
16	6	6	1.20e-5	5.40e-2	0.333	0.248	3.77e-5	6.52e-2	0.225	0.135	0.111
17	6	6	1.19e-5	5.55e-2	0.371	0.252	3.86e-5	6.82e-2	0.280	0.144	0.110
18	6	6	1.26e-5	5.44e-2	0.365	0.227	3.95e-5	6.56e-2	0.242	0.102	0.111
19	6	6	1.29e-5	5.94e-2	0.396	0.249	4.65e-5	7.63e-2	0.241	0.134	0.113
20	6	6	1.29e-5	6.35e-2	0.417	0.259	5.18e-5	8.55e-2	0.256	0.137	0.114

List of Figures

List of Tables

Bibliography

[1] ASCE - Manuals and reports on engineering practice. *Sedimentation Engineering*, 1975.

[2] J. R. Barton and P. N. Lin. A study of the sediment transport in alluvial streams. Technical report, Colorado A&M College, Civil Engineering Department, Fort Collins, CO, USA, 1955.

[3] N. H. Brooks. *Laboratory studies of the mechanics of motion of streams flowing over a movable bed of fine sand.* PhD thesis, California Institute of Technology, 1954.

[4] N. L. Coleman. Velocity profiles with suspended sediment. *Journal of Hydraulic Research*, 19:211–229, 1981.

[5] N. L. Coleman. Effects of suspended sediment on the open-channel velocity distribution. *Water Resources Research*, 22:1377–1384, December 1986.

[6] A. G Davies and C. Villaret. Eulerian drift induced by progressive waves above rippled and very rough beds. *J. Geophys. Res*, 104:1465–1488, January 1999.

[7] H. A. Einstein and N. Chien. Effects of heavy sediment concentration near the bed on velocity and sediment distribution. Technical report, University of California, Insitute of Engineering Research, Berkeley, California, August 1955.

[8] F. Engelund and E. Hansen. *A monograph on sediment transport in alluvial streams.* Teknisk Forlag, Copenhagen, 1972.

[9] S. M. Glenn. *A continental shelf bottom boundary layer model : the effects of waves, currents and a moveable bed.* PhD thesis, Woods Hole Oceanographic Institution / Massachusetts Institute of Technology, February 1983.

[10] S. M. Glenn and W. D. Grant. A suspended sediment stratification correction for combined wave and current flows. *J. Geophys. Res*, 92:8244–8264, July 1987.

[11] W. D. Grant and O. S. Madsen. Quantitative description of sediment transport by waves. In *Proceedings of 15th International Conference of Coastal Engineering*, pages 1093–1112. ASCE, 1976.

[12] W. D. Grant and O. S. Madsen. The continental-shelf bottom boundary layer. *Ann.Rev.Fluid.Mech.*, 18:265–305, 1986.

[13] L. N. Howard. Note on a paper of john w. miles. *Journal of Fluid Mechanics*, 10:509–512, 1961.

[14] J. A. Jimenéz and O. S. Madsen. A simple formula to estimate settling velocity of natural sediments. *Journal of Waterway, Port, Coastal and Ocean Engineering, ASCE*, 129:70–78, march, april 2003.

[15] P. K. Kundu and I. M. Cohen. *Fluid Mechanics.* Academic Press, 2ns edition, 2002.

[16] D. A. Lyn. *Turbulence and turbulent transport in sediment-laden open-channel flows.* PhD thesis, California Institute of Technology, December 1986.

[17] O. S. Madsen. Mechanics of cohesionless sediment transport in coastal waters. In *Proceedings Coastal Sediments 91*, volume 1, pages 15–27. ASCE, 1991.

[18] J. W. Miles. On the stability of heterogeneous shear flows. *Journal of Fluid Mechanics*, 10:496–508, 1961.

[19] A. S. Monin and A. M. Yaglom. *Statistical Fluid Mechanics.* MIT Press, Cambridge, Massachusetts, 1971.

[20] P. Nielsen. Coastal bottom boundary layers and sediment tranport. In Philip L-F Liu, editor, *Advanced Series on Ocean Engineering*, volume 4. World Scientific, 1992.

[21] G. N. Nomicos. *Effects of sediment load on the velocity field and friction factor of tubulent flow in an open channel.* PhD thesis, California Institute of Technology, 1956.

[22] P.R. Owen. Saltation of uniform grains in air. *J. Fluid Mech.*, 20:225, 1964.

[23] H. Schlichting. *Boundary layer theory.* McGraw-Hill, New-York, 6th edition, 1968.

[24] J. D. Smith and S. R. McLean. Spatially averaged flow over a wavy surface. *J. Geophys. Res*, 82:1735–1746, April 1977.

[25] J.D. Smith. Modeling of sediment transport on continental shelves. In Edward D. Goldberg, editor, *The Sea - Ideas and Observations on Progress in the Study of the Seas*, volume 6: Marine Modeling, chapter 13, page 539. John Wiley and Sons, New York, 1977.

[26] R. Soulsby. *Dynamics of Marine Sands.* Thomas Telford, London, 1997.

[27] R.B. Stull. *An Introduction to Boundary Layer Meteorology.* Kluwer Academic Publishers, 1988.

[28] R. Styles and S. M. Glenn. Modeling stratified wave and current bottom boundary layers on the continental shelf. *J. Geophys. Res*, 105:24,119–24,139, October 2000.

[29] P. A. Taylor and K. R. Dyer. Theoretical models of flow near the bed and their implication for sediment transport. In Edward D. Goldberg, editor, *The Sea - Ideas and Observations on Progress in the Study of the Seas*, volume 6: Marine Modeling, chapter 14, page 577. John Wiley and Sons, 1977.

[30] C. Villaret and J. H. Trowbridge. Effects of stratification by suspended sediments on turbulent shear flows. *J. Geophys. Res*, 96:10,659–10,680, June 1991.

[31] K. C. Wilson. Analysis of bed-load motion at high shear stress. *Journal of Hydraulic Engineering*, 113:97–103, 1987.

[32] K. C. Wilson. Mobile-bed friction at high shear stress. *Journal of Hydraulic Engineering*, 115(a):825–830, 1989.

[33] Chia-Shun Yih. *Fluid Mechanics, a concise introduction to the theory*, volume 54. McGRAW-HILL, 1969.